Athens Journal of Technology & Engineering

Quarterly Academic Periodical, Volume 8, Issue 2, June 2021
URL: https://www.athensjournals.gr/ajte
Email: journals@atiner.gr
e-ISSN: 2241-8237 DOI: 10.30958/ajte

Front Pages

Athens Journal of Technology & Engineering

Published by the Athens Institute for Education and Research (ATINER)

****

*

ATINER is an Athens-based World Association of Academics and Researchers based in Athens. ATINER is an independent and non-profit Association with a Mission to become a forum where Academics and Researchers from all over the world can meet in Athens, exchange ideas on their research and discuss future developments in their disciplines, as well as engage with professionals from other fields. Athens was chosen because of its long history of academic gatherings, which go back thousands of years to Plato's Academy and Aristotle's Lyceum. Both these historic places are within walking distance from ATINER's downtown offices. Since antiquity, Athens was an open city. In the words of Pericles, Athens"…is open to the world, we never expel a foreigner from learning or seeing". ("Pericles' Funeral Oration", in Thucydides, The History of the Peloponnesian War). It is ATINER's mission to revive the glory of Ancient Athens by inviting the World Academic Community to the city, to learn from each other in an environment of freedom and respect for other people's opinions and beliefs. After all, the free expression of one's opinion formed the basis for the development of democracy, and Athens was its cradle. As it turned out, the Golden Age of Athens was in fact, the Golden Age of the Western Civilization. Education and (Re)searching for the 'truth' are the pillars of any free (democratic) society. This is the reason why Education and Research are the two core words in ATINER's name.

****

The ***Athens Journal of Technology & Engineering (AJTE)*** is an Open Access quarterly double-blind peer reviewed journal and considers papers from all areas engineering (civil, electrical, mechanical, industrial, computer, transportation etc), technology, innovation, new methods of production and management, and industrial organization. Many of the papers published in this journal have been presented at the various conferences sponsored by the Engineering & Architecture Division of the Athens Institute for Education and Research (ATINER). All papers are subject to ATINER's Publication Ethical Policy and Statement.

The Athens Journal of Technology & Engineering
ISSN NUMBER: 2241-8237- DOI: 10.30958/ajte
Volume 8, Issue 2, June 2021
Download the entire issue (PDF)

Athens Journal of Technology & Engineering
Editorial and Reviewers' Board

President's Message

All ATINER's publications including its e-journals are open access without any costs (submission, processing, publishing, open access paid by authors, open access paid by readers etc.) and is independent of presentations at any of the many small events (conferences, symposiums, forums, colloquiums, courses, roundtable discussions) organized by ATINER throughout the year and entail significant costs of participating. The intellectual property rights of the submitting papers remain with the author. Before you submit, please make sure your paper meets the basic academic standards, which includes proper English. Some articles will be selected from the numerous papers that have been presented at the various annual international academic conferences organized by the different divisions and units of the Athens Institute for Education and Research. The plethora of papers presented every year will enable the editorial board of each journal to select the best, and in so doing produce a top-quality academic journal. In addition to papers presented, ATINER will encourage the independent submission of papers to be evaluated for publication.

The current issue is the second of the eighth volume of the *Athens Journal of Technology & Engineering (AJTE),* published by the Engineering & Architecture Division of ATINER.

Gregory T. Papanikos, President, ATINER.

Athens Institute for Education and Research

A World Association of Academics and Researchers

11th Annual International Conference on Civil Engineering
21-24 June 2021, Athens, Greece

The Civil Engineering Unit of ATINER is organizing its **11th Annual International Conference on Civil Engineering, 21-24 June 2020, Athens, Greece** sponsored by the Athens Journal of Technology & Engineering. The aim of the conference is to bring together academics and researchers of all areas of Civil Engineering other related areas. You may participate as stream leader, presenter of one paper, chair of a session or observer. Please submit a proposal using the form available (https://www.atiner.gr/2021/FORM-CIV.doc).

Academic Members Responsible for the Conference

- **Dr. Dimitrios Goulias**, Head, Civil Engineering Unit, ATINER and Associate Professor & Director of Undergraduate Studies Civil & Environmental Engineering Department, University of Maryland, USA.

Important Dates

- Abstract Submission: **10 May 2021**
- Acceptance of Abstract: 4 Weeks after Submission
- Submission of Paper: **24 May 2021**

Social and Educational Program

The Social Program Emphasizes the Educational Aspect of the Academic Meetings of Atiner.

- Greek Night Entertainment (This is the official dinner of the conference)
- Athens Sightseeing: Old and New-An Educational Urban Walk
- Social Dinner
- Mycenae Visit
- Exploration of the Aegean Islands
- Delphi Visit
- Ancient Corinth and Cape Sounion

Conference Fees

Conference fees vary from 400€ to 2000€
Details can be found at: https://www.atiner.gr/2019fees

9th Annual International Conference on Industrial, Systems and Design Engineering, 22-25 June 2020, Athens, Greece

The Industrial Engineering Unit of ATINER will hold its **9th Annual International Conference on Industrial, Systems and Design Engineering, 21-24 June 2021, Athens, Greece** sponsored by the Athens Journal of Technology & Engineering.The aim of the conference is to bring together academics, researchers and professionals in areas of Industrial, Systems, Design Engineering and related subjects. You may participate as stream leader, presenter of one paper, chair of a session or observer. Please submit a proposal using the form available (https://www.atiner.gr/2021/FORM-IND.doc).

Important Dates

- Abstract Submission: **10 May 2021**
- Acceptance of Abstract: 4 Weeks after Submission
- Submission of Paper: **24 May 2021**

Academic Member Responsible for the Conference

- **Dr. Theodore Trafalis**, Director, Engineering & Architecture Division, ATINER, Professor of Industrial & Systems Engineering and Director, Optimization & Intelligent Systems Laboratory, The University of Oklahoma, USA.

Social and Educational Program

The Social Program Emphasizes the Educational Aspect of the Academic Meetings of Atiner.

- Greek Night Entertainment (This is the official dinner of the conference)
- Athens Sightseeing: Old and New-An Educational Urban Walk
- Social Dinner
- Mycenae Visit
- Exploration of the Aegean Islands
- Delphi Visit
- Ancient Corinth and Cape Sounion

More information can be found here: https://www.atiner.gr/social-program

Conference Fees

Conference fees vary from 400€ to 2000€
Details can be found at: https://www.atiner.gr/2019fees

Athens Journal of Technology and Engineering - Volume 8, Issue 2, June 2021 – Pages 113-138

Liquefaction Potential Analysis in Bucharest City as a Result of the Ground Shaking during Strong Vrancea Earthquakes

By Andrei Bala[*] *& Dieter Hannich*[±]

Bucharest, the capital of Romania with about 2.5 million inhabitants, is frequently struck by intense, damaging earthquakes (2–3 events per century). The Collaborative Research Center 461 (CRC-461) entitled: "Strong Earthquakes - a Challenge of Geosciences and Civil Engineering" was established in July 1996 and ended in December 2007, but some projects continued until 2010. It was funded by the German Research Foundation and involved the University of Karlsruhe which today belongs to Karslruhe Institute of Technology. The CRC aimed strategic research in the field of strong earthquakes with regional focus on the Vrancea seismic events in Romania. Between 1995–2007 several research works were done in Romania, with the support of several Romanian research institutes and the University of Bucharest. One of the research questions was to study the occurring of liquefaction during strong earthquakes within the shallow sandy layers in Bucharest. In suitable conditions, strong earthquakes can cause, under certain geologic conditions, liquefaction and therewith ground failure as sand boils, lateral spreading, or differentiated subsidence. In the present paper we analyze the liquefaction risk for Bucharest. For this purpose, at 10 representative sites in Bucharest, Seismic Cone Penetration Tests (SCPTu) were executed. An area-wide evaluation of the liquefaction probability in Bucharest was established. The factor of safety (F_S) against liquefaction and the probability of liquefaction (P_L) were computed from the obtained test-data. For the first time, maps of the liquefaction potential index (L_i) for Bucharest were outlined. This map shows how severe the liquefaction phenomena might be during strong Vrancea earthquakes in Bucharest, amplifying the site effects.

Keywords: *hydrogeologic conditions, liquefaction probability, liquefaction hazard, Bucharest city, strong Vrancea earthquakes*

Introduction

The shallow geologic underground of Bucharest, which is represented by Quaternary sediments, is characterized by an alternation of soft cohesive and non-cohesive soil layers down to 300 m depth in the northern part. Within this sequence, several main aquifers, exist, presenting specific seasonal variations and long-time trends of the groundwater level. The particular geologic and hydrogeologic conditions existing in Bucharest raise the question if during strong Vrancea earthquakes, liquefaction can take place and if liquefaction-induced ground failure can occur. The only observation of liquefaction occurrence in

[*]Senior Research Geophysicist, National Institute for Earth Physics, Romania.
[±]Senior Geologist, Karlsruhe Institute of Technology, Germany.

Bucharest during the strong 1977 Vrancea earthquake is limited to a small area along the old riverbed of the Dambovita. Here was described sand boils aligned along fissures of several meters developed in the covering cohesive soils. This site was then investigated by standard penetration tests (SPT), followed by laboratory tests of the ejected sand and finally the factor of safety was computed (Ishihara and Perlea 1984).

Geology of Bucharest Area

The area of Bucharest is situated within the regional geological unit of the Moesian Platform, western part, which dates since the beginning of the Paleozoic era. After a sedimentary subsidence of the Carpathian foredeep during the Upper Tertiary and Quaternary, an asymmetric sedimentary basin results, Bucharest being situated at the southern margin of this southward thinning basin (Mutihac 1990). The thickness of the Tertiary sediments, reaching 8000 m near the Carpathian Arc Bend, appears reduced in the central area of Bucharest to about 500–1000 m (since Ciugudean and Martinof 2000). The Quaternary alluvial and lacustrine deposits are having in the area of Bucharest a thickness of about 200–300 m (since Liteanu 1952). Holocene loess-like sediments, recent alluvial material and anthropogenic backfill overly on the top the Quaternary deposits.

Classification of the Quaternary Deposits

A first classification on the geological and lithological description of the Quaternary deposits in the Bucharest area was made by Liteanu (1952). This classification of 7 main layers (beginning from the surface to depth) although rather old was considerably improved through the researches of Ciugudean and Martinof (2000) and Ciugudean-Toma and Stefanescu (2006), which acquired a considerable database during their work at the Metroul S.A. during the time. The classification was generally accepted in the first part of XXI century by all researchers in their studies about site conditions and dynamic properties of the sedimentary layers in and around Bucharest City (Lungu et al. 1999, Mandrescu et al. 2004, Bala et al. 2006, Bala et al. 2011).

This classification comprises the following layers (or complex sedimentary packages) with general characteristics:

Layer 1: Anthropogenic backfill and soil, with a thickness varying between 3–10 m.

Layer 2: The Upper clayey-sandy complex represents Holocene deposits of loess, sandy clays and sands. The thickness of this complex varies between 2–5 m in the "Dambovita-Colentina inter-fluvial domain", 10–16 m in the northern and southern Plaines (Baneasa-Pantelimon and Cotroceni-Vacaresti) and 3–6 m in the river meadows.

Layer 3: The Colentina gravel complex bearing the Colentina-aquifer, is a layer containing gravels and sands with varying grain size distribution. The

thickness is variable, between 1–20 m, lacking in the western part of Bucharest.

Layer 4: The Intermediate clay layer containing up to 80% hard consolidated clay and calcareous concretions with intercalated thin sand and silt lenses. The thickness of this layer varies between 0–25 m. 4 Geological and geophysical model of the quaternary layers.

Layer 5: The Mostistea sandbank, bearing the Mostistea-aquifer, is a sand layer with sands of medium to fine grain size. The thickness varies in the area of Bucharest between 1–25 m.

Layer 6: The Lacustrine complex, composed by a variation of limy marled clay and fine sands, the grain size < 0.005 mm consisting about 86%. The upper face of the complex lies at 20–50 m depth, but the thickness varies from about 60 m in the southern part of Bucharest to about 130 m in the North. The variable thickness is due to the underlying Fratesti complex which descents northward.

Layer 7: The Fratesti complex or Lower gravel complex, bearing the "Fratesti aquifer", lies discordant on Pliocene Levantine clay layers. This complex comprehends three thick (10–40 m each) sandy gravel layers (named A, B and C), separated by two marl or clay layers (each of 5–40 m thickness). This thick complex (total thickness 100–180 m), continuous present in the whole area of Bucharest, dips northward, its upper surface lying at about 75 m depth in the southern part of Bucharest and at about 190 m depth in the north (see Figure 1).

Figure 1. *Cross-Section Showing the Near-Surface Geology in Bucharest*

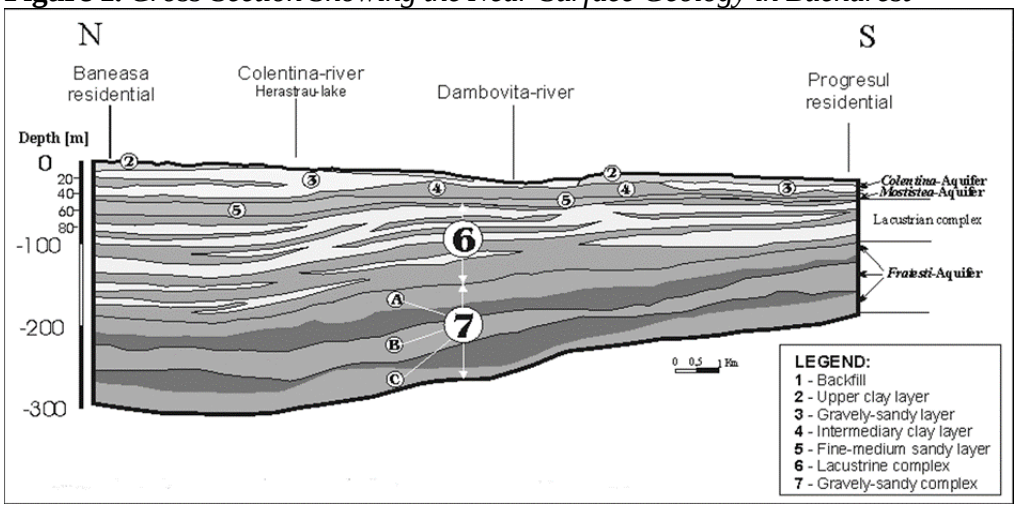

Source: after Bala et al. 2011.

Hydrogeology Characterization of Quaternary Layers

Complex hydro-geological conditions are characterizing the Quaternary underground of Bucharest. The upper-most aquifer, the Colentina-aquifer is an unconfined aquifer in direct hydraulic connection with the alluvial deposits of the two rivers crossing Bucharest, Colentina and Dambovita. Depending on the

geomorphologic units in the area of Bucharest, the phreatic groundwater level presents variable depths: a higher level, between 1 and 5 m depth in the Dambovita and Colentina meadows, between 5 and 10 m in the Dambovita-Colentina inter-fluvial domain and below 10 m in the Cotroceni-Vacaresti and Baneasa-Pantelimon Plains (after Bretotean et al. 1986). Within this aquifer the average permeability (k) lies between $1.2x10^{-4}$ and $9.7x10^{-5}$ m/s (Ciugudean and Martinof 2000).

The second, deeper aquifer, the Mostistea-aquifer presents large variations of thickness in the area of Bucharest and it is mainly a confined aquifer. The Mostistea-aquifer is connected to the mentioned Mostistea-sandbanks, composed of sands with mostly fine to medium grain size, but being also at any places in hydraulic contact with the overlying Colentina-aquifer and also especially in the southern part of Bucharest with the surface water system; so there are zones where Mostistea-aquifer is losing its confined character and it is in communication with the upper-most Colentina-aquifer. The average permeability (k) lies between $5x10^{5}$–$8.3x10^{-5}$ m/s.

The deepest Quaternary aquifer is thicker (depths of 100–300 m and thickness of 100–150 m); the Fratesti-aquifer is situated at the base of the Quaternary layers. It is a regional aquifer system with three distinguished aquifers named A, B and C, each of these having 10–40 m thick, being extended continuously in the southern part of Romania, dipping toward the Carpathians and outcropping near the Danube. The most important aquifer of this system is the layer A, being mainly used for drinking water extraction (Bretotean 2001). Due to its relative great depth, it is considered outside of the near-surface geology range and without importance for liquefaction. The permeability of the uppermost layer "A" within the Fratesti-aquifer lies at about $1.3x10^{-4}$ –$5.4x10^{-5}$ m/s (Ciugudean and Martinof 2000).

Liquefaction Occurring Conditions

The knowledge of the *local hydrogeological conditions* plays also an important role in analysing the saturation of the soil and the pore water pressure increasing and implicit liquefaction occurrence.

The depth of groundwater influences liquefaction susceptibility and plays a significant role in Bucharest (Hannich et al. 2005). It decreases significantly with increasing depth of groundwater level. Thus it is necessary to know exactly the hydrogeologic conditions, the type of aquifers (confined or unconfined), the piezometric level for each aquifer, the groundwater flow direction and the groundwater level variations in time (seasonal and long-time variations). For Bucharest the two near-surface aquifers, Colentina and Mostistea, are of interest for the evaluation of their liquefaction susceptibility. The depth of the groundwater level (Figure 2a), its seasonal variation and long-time trends (Figure 3) and the confined and unconfined character within these aquifers (Figure 2b) are deduced from long-time monitoring data. The variation of the groundwater level depth due to seasonal or extreme precipitation events, influences as well, as long-time trends can influence significantly the liquefaction susceptibility of these aquifers.

Piezometric Observations of Aquifers in Bucharest

For Bucharest there are continuous piezometric observations for the three main aquifer systems since 1973, executed in representative piezometric boreholes belonging to the National Institute for Hydrology and Water Management in Bucharest. Through recorded long-term variations, the difference between the deepest groundwater level and the highest level in the period 1973–2002 comprises 4–5 m, while seasonal variations can reach up to 2–3 m (Figure 3). These observed groundwater fluctuations in Bucharest, can lead to variations of the water saturation within a sand layer from 0–100%, with direct consequence upon the value of the shear wave velocity and the variation of the liquefaction potential (Ehret et al. 2010).

Figure 2. a) *Depth of Groundwater Level in Bucharest, Measured in January 2004 (Original Data from METROUL S.A. and INHGA, Bucharest)* b) *Confined and Unconfined Domains of the Groundwater in the "Colentina"-Aquifer in January 2004. Red Circles - 10 SCPT Sites; Pink Dots - Piezometric Boreholes*

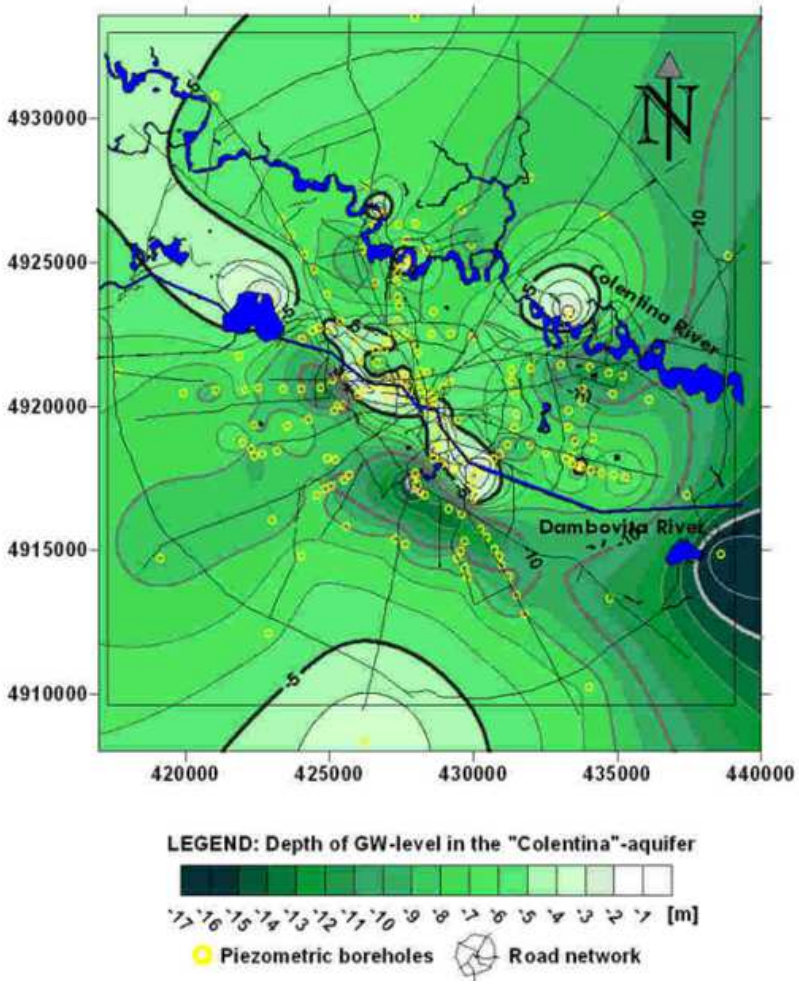

a)

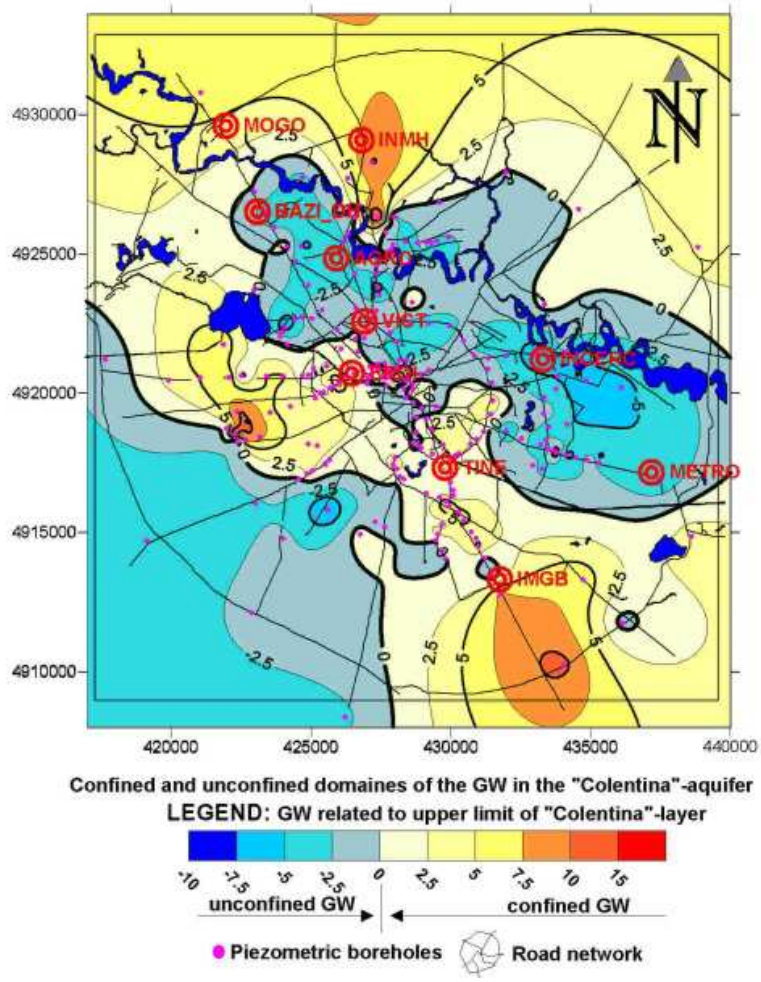

b)

Quasi-simultaneous groundwater level measurements within the Colentina-aquifer in about 230 hydrogeologic boreholes scattered over Bucharest City were beginning in 2004. In Figure 2a the depth of the groundwater level, as depths from the ground level in Bucharest in the Colentina-aquifer, is presented. Based on these data, a map is obtained describing the confined or unconfined state of the groundwater in the gravely-sandy Colentina-layer (Figure 2b). This information is necessary for the evaluation of the liquefaction potential in Bucharest.

Monitoring of groundwater level variations in the last years in some representative groundwater-boreholes within the Colentina-aquifer made possible to obtain records during extreme precipitation events. These show the speed of rise and decrease of the groundwater level in correlation with the precipitation event.

It was proved that groundwater and groundwater level changes have a very important influence on site effects. If confined aquifers exist near the surface liquefaction can take place. Under certain conditions one can benefit from the existence of liquefied layers as they attenuate the propagation of shear waves (Ehret et al. 2010).

The medium-to-fine sands of the Mostistea layer and the alluvial sands in the Dambovita meadow, fit to the easy-liquefiable area. Fluvial and alluvial environments present frequently rounded particles. For Bucharest these insights allow the acceptance that the sandy-gravely Colentina layer is liquefaction susceptible, if other influencing criteria are also fulfilled (Figure 2a). From this point of view the alluvial soils in the river meadows in Bucharest are favorable for liquefaction susceptibility.

Figure 3. *Upper Part: Annual Variations of the Groundwater in the Colentina-Aquifer during Different Years (1977, 1985, 2000, 2001) in Pipera Borehole. Lower Part: Annual Precipitations in [l/m^2] during 1977, 1985, 2001.*

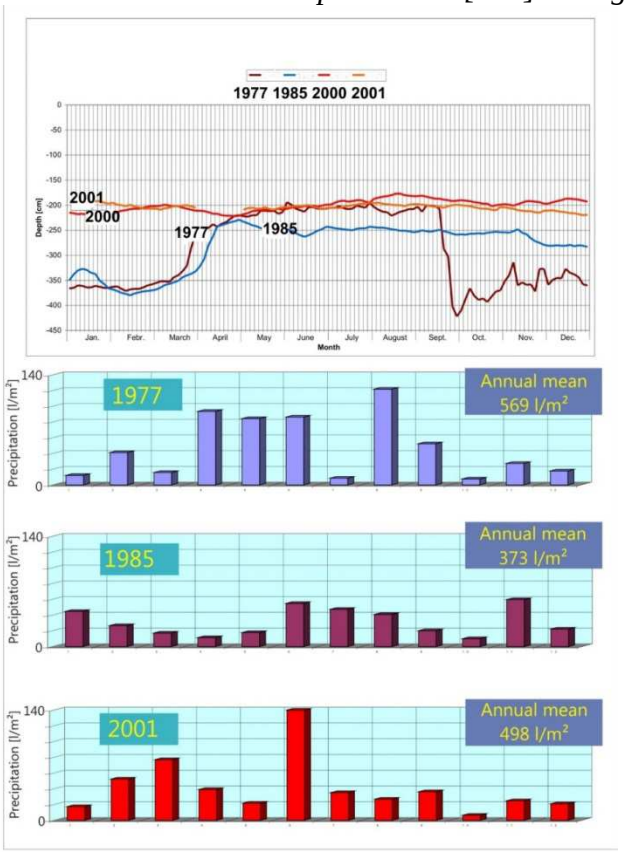

Composition of shallow Quaternary layers refers to grain size distribution, gradation and particle shape. For many years, liquefaction-related phenomena were thought to be limited to sands as finer-grained soils were considered incapable of generating the high pore water pressure associated with liquefaction. It was observed in laboratory and in the field that even non-plastic silts can liquefy (Kramer 1996). It was observed also that gravely soils are susceptible for liquefaction if undrained conditions are assured by the presence of impermeable layers above and beneath the gravely layer (Kramer 1996). Only plastic clays remain non-susceptible for liquefaction.

The medium-to-fine sands of the Mostistea layer and the alluvial sands in the Dambovita meadow, fit to the easy-liquefiable area. Fluvial and alluvial

environments present frequently rounded particles. For Bucharest these insights allow the acceptance that the sandy-gravely Colentina layer is liquefaction susceptible, if other influencing criteria are also fulfilled (Figure 2a). From this point of view the alluvial soils in the river meadows in Bucharest are favorable for liquefaction susceptibility.

Case Study in Bucharest City and Discussion

Cone Penetration Testing (CPT) Method

The analysis of the liquefaction probability, the potential of liquefaction and of ground failure at a site can be evaluated using data from *Cone Penetration Tests* (CPT). The evaluation procedure is based on empirical equations deduced by different authors (Olsen 1997, Robertson and Wride 1998, Chen and Juang 2000, Lee et al. 2003, Yuan et al. 2004). All these empirical methods follow the general stress-based approach of Seed and Idriss (1971) and require the determination of two variables, namely, the *cyclic stress ratio* (CSR) and the *cyclic resistance ratio* (CRR). Since 1971, the determination of CSR, as proposed by Seed and Idriss (1971), representing the cyclic load in simplified methods, remained unmodified.

For the determination of CRR, different simplified methods have been proposed till today. In this paper the method proposed by Olsen (1997) is applied for the determination of CSR and CRR and was already described at length by Hannich et al. (2006a) and (2007).

For Bucharest, in the determination of CSR, the characteristics of the Vrancea earthquake of 1977 were used: for Mw=7.4 and peak ground acceleration (i.e., PGA-values) at different sites in Bucharest deduced by a method proposed by Sokolov and Bonjer (2006) and Sokolov et al. (2008).

The *factor of safety* (Fs) is determined after Lee et al. (2003) as:

$$F_s = CRR / CSR_{7.5} \tag{1}$$

Probability of Liquefaction P_L

The *probability of liquefaction, P_L* can be estimated after Juang et al. (2003) by Eq. (2):

$$P_L = \frac{1}{1+\left(F_s/0.96\right)^{4.5}} \tag{2}$$

where *Fs* is the factor of safety defined by Eq. (1).

After Chen and Juang (2000), the liquefaction will occur only if the probability of liquefaction is greater than 35%.

Soil Type Index, Ic

Starting also from the CPT-data the *soil type index*, *Ic*, defined by Robertson and Wride (1998), a detailed lithological depth profile can be obtained. The index *Ic* is calculated by Eq. 3 and depends on the normalized stress-adjusted cone tip resistance (Eq. 4) and the normalized friction ratio *F* (Eq. 5):

$$I_c = \left[(3.47 - \log(q_{c1N}))^2 + (\log F + 1.22)^2\right]^{0.5} \quad (3)$$

where q_{c1N} = normalized (stress-adjusted) cone penetration resistance, defined as

$$q_{c1N} = 10\left[q_c / (\sigma'_v)^{0.5}\right], \text{ (all terms in kPa)} \quad (4)$$

F = normalized friction ratio, defined as

$$F = f_s / (q_c - \sigma_v) \times 100\% \quad (5)$$

The soil type index *Ic* helps among others to restrict the probability of liquefaction to soils with *Ic*<2.8 (Yuan et al. 2004).

Liquefaction Potential Index, Li

The *liquefaction potential index* Li is used to evaluate the ground failure risk. Its severity categories were proposed originally by Iwasaki et al. (1982) and modified by Sonmez (2003), which proposed the change of the threshold value of Fs between non-liquefiable and liquefiable layers from 1.0 to 1.2 and suggested the following equations:

$$L_i = \int_0^{20} F(z) \cdot W(z) \cdot dz \quad (6)$$

$F(z) = 1 - F_s$ *for* $F_s < 0.95$

$F(z) = 2*10^6*EXP(-18.427*F_s)$ *for* $0.95<F_s<1.2$

$F(z) = 0$ *for* $F_s>1.2$

$W(z)= 10 -0.5*z$ *for* $\leq z \leq 20$ *m*

$W(z)= 0$ *for* $z \geq 20$*m.*

z = depth

To interpret the obtained values of *Li* (Eq. 6), a classification is used in Table 1, after several studies.

Li et al. (2006) have assumed threshold probability of 0.35 as the border between liquefaction/no liquefaction. They also suggested that LPI=5 can still be used as a lower bound of failure cases below which no liquefaction-induced ground failure is expected whereas LPI = 13 is used as boundary for high and very high liquefaction risk.

Table 1. *Liquefaction Potential Index L_i Classification Index*

Liquefaction potential index L_i			**Liquefaction potential category**
Iwasaki (1982)	**Lee et al. (2003)**	**Li et al. (2006)**	
0	0	0	Non-liquefiable (based on $F_s < 1.2$)***
$0 < L_i < 2$	$0 < L_i < 2$	$0 < L_i < 2$	Low
$2 < L_i < 5$	$2 < L_i < 8$*	$2 < L_i < 5$	Moderate
$5 < L_i < 15$	$8 < L_i < 16$**	$5 < L_i < 13$	High
$15 > L_i$	$16 > L_i$	$13 > L_i$	Very high

*for CRR calculated after Olsen (1997) this value is 8 (Lee et al. 2003).
**for CRR calculated after Olsen (1997) this value is 16 (Lee et al. 2003).
***modified by Sonmez (2003).

The liquefaction potential index proposed by Lee et al. (2003) is used to evaluate the severity of the liquefaction induced ground failure.

SCPTu-Measurements in Bucharest

The first systematic research of seismic site effects take place between 1997–2007, within the Collaborative Research Centre (CRC-461) performed by the University of Karlsruhe, Germany in collaboration with several research institutes from Bucharest, Romania.

Seismic Cone Penetration Tests (SCPTu) were executed in Bucharest at 10 representative sites, located in the river meadow of the Dâmbovița River, in the inter-fluvial domain and in the Northern and Southern Plains (see Figure 2b). In Bucharest it was possible to reach depths of 35 m. Through the continuously recorded cone (tip resistance and the sleeve friction) it was possible to get detailed lithological profiles, soil type index profiles and the factor of safety over the depth using empirical methods. These data are used to calculate the liquefaction potential index and the liquefaction severity index, over a 20 m-depth interval. Based on these indicators the contour maps of the liquefaction potential and of the severity of liquefaction were outlined for Bucharest City.

Seismic Cone Penetration Tests (SCPTu) were carried out in Bucharest in order to determine missing data on shear wave velocities for the near-surface area (depths 0–35 m). At the same time important geotechnical data on the tip resistance and the sleeve friction are obtained, which should enable the probability of the occurrence of soil liquefaction using empirical methods. The SCPTu measurements were carried out at 10 selected locations in Bucharest (Figure 2b). The principle of the measurements as well as the mathematical principles and formulas that are required for the evaluation of the CPT data are described in the paper (Hannich et al. 2006b).

The results of the shear wave velocities determined by SCPTu are given in Table 2 for layers 2–6 in Bucharest.

Table 2. *Results of the Shear Wave Velocities Determined through Seismic Cone Penetration Tests (SCPTu) in Bucharest for the Near-Surface Depths (0–35 m)*

Layer no./ Location	**2.Upper Clay layer**	**3.Colentina aquifer**	**4.Intermediate Clay layer**	**5.Mostiștea aquifer**	**6.Lacustrine layer**
	Shearwave velocity Vs (m/s)				
BAZI	291	194	295	308	307
AGRO	332	296	320	-	-
VICT	282	252	303	-	-
INCERC	295	311	320	-	-
IMGB	223	275	-	-	-
INMH	236	-	283	434	-
METRO	296	292	261	320	355
MOGO	272	244	294	363	-
TINE	167	256	361	-	-
EROI	230	209	253	301	336
Average	278	266	300	345	333

Source: after Hannich and Hötzl (2008).

Liquefaction Potential in Bucharest City

In this paper the calculations were outlined for the 1977-Vrancea earthquake of magnitude Mw=7.4, which supposed to generate the PGA computed values which are presented in the Table 3 for each site.

Starting from the magnitude of 7.4 of the 1977 Vrancea-earthquake and the deduced PGA-values (Sokolov and Bonjer 2006, Sokolov et al. 2008) at the ten SCPTu-sites in Bucharest, the factor of safety (*Fs)*, the probability of liquefaction (*Pl*), the liquefaction potential index (*Li*) as well as the liquefaction severity index (Ls) were calculated. Table 3 contains the summarized results for Bucharest during the 1977 earthquake. It can be seen, that the highest liquefaction potential category ("High") and the highest liquefaction severity class ("Moderate") were obtained for the TINE and EROI sites, in the Tineretului Park. This result agrees with the observed and induced (man-made) liquefaction phenomena which were observed in 2015 and described in the Annex1 of the present paper.

In Table 3 (column 3) the shearwave velocities are obtained by Bala et al. (2011) as $\boldsymbol{V_{S\text{-}30}}$ computed in the specific sites. In column 5 the values of peak ground acceleration (PGA) are computed according to Sokolov and Bonjer (2006) for an earthquake with the same magnitude as the event from 04.03.1977.

Table 3. *Liquefaction Risk Analysis for Bucharest City*

No.	Name	V_{S-30} Share-wave velocity [m/s]	Water Level GW [m]	Deduced PGA [m/s²]*	L_s	Liquefaction severity class*	L_i	Liquefaction potential category**
1	TINE	237	-1.8	2.6	**38.89**	Moderate	**13.23**	**High**
				4.0	**45.25**	Moderate	**18.76**	**Very high**
2	EROI	287	-4.2	2.5	**17.72**	Moderate-low	**6.22**	**High**
				4.0	**33.38**	Low-moderate	**9.83**	**High**
3	BAZI	267	-5	3.6	**22**	Low	**7.5**	**High**
			-8.5		**27.9**	Low	**16.5**	**Very high**
4	MOGO	281	-7.5	3.5	14.56	Low	1.91	Low-Moderate
5	VICT	290	-6	3.0	16.2	Low	1.62	Low
6	AGRO	311	-7.5	3.0	3.9	Very Low	0.64	Low
				4.5	20.77	Low	3.53	Moderate
7	IMGB	251	-8.5	2.7	2.82	Very low	0.15	Low
8	INMH	264	-10	3.0	1.19	Very low	0.09	Non-liquefaction
9	METRO	303	-8.5	2.5	0.99	Very low	0.18	Low
10	INCERC	305	-11.5	2.5	0	Non-liqu.	0	Non-liquefaction
				4.0	7.06	Very low	0.32	Low

* Liquefaction severity classification after Sonmez and Gokceoglu (2005).
** Liquefaction potential category after Sonmez (2003).

We discuss first the obtained results for three sites, at the locations in which the liquefaction potential index have high values (Table 3): TINE (Figure 4a); EROI (Figure 4b) and BAZI (Figure 4c).

In Figure 4a it can be observed, that at TINE for a PGA-value of 2.6 m/s² and for a depth interval of 12 m (between 6–18 m depth) the probability of liquefaction is over 35%, partly even 60%. For this site the calculations were performed also for a PGA-value of 4.0 m/s², showing an increase of the probability of liquefaction for the same depth interval over 80%. This shows the scale of the influence of PGA upon the liquefaction evaluation.

Not far from the values computed at TINE are the next values computed in Figure 4b for the site EROI. The evaluation was performed for a PGA-value of 4 m/s² and presents a probability over 80% for a depth interval above the ground water.

In Figure 4c the calculation results at BAZI location are presented. The evaluation was performed for a PGA-value of 3.6 m/s² and presents a probability over 80% for a depth interval of 6 m (between 7 m and 13 m). For this site, calculations for a 3.5 m higher groundwater level were performed also, showing an increase of the probability up to nearly 100% and also an increase over 60% for a deeper depth interval.

Figure 4. a) *Liquefaction Evaluation at the TINE Location for PGA=2.6 m/s^2* b) *Liquefaction Evaluation at the EROI Location for PGA=4.0 m/s^2* c) *Liquefaction Evaluation at the BAZI Location PGA=3.6 m/s^2*.

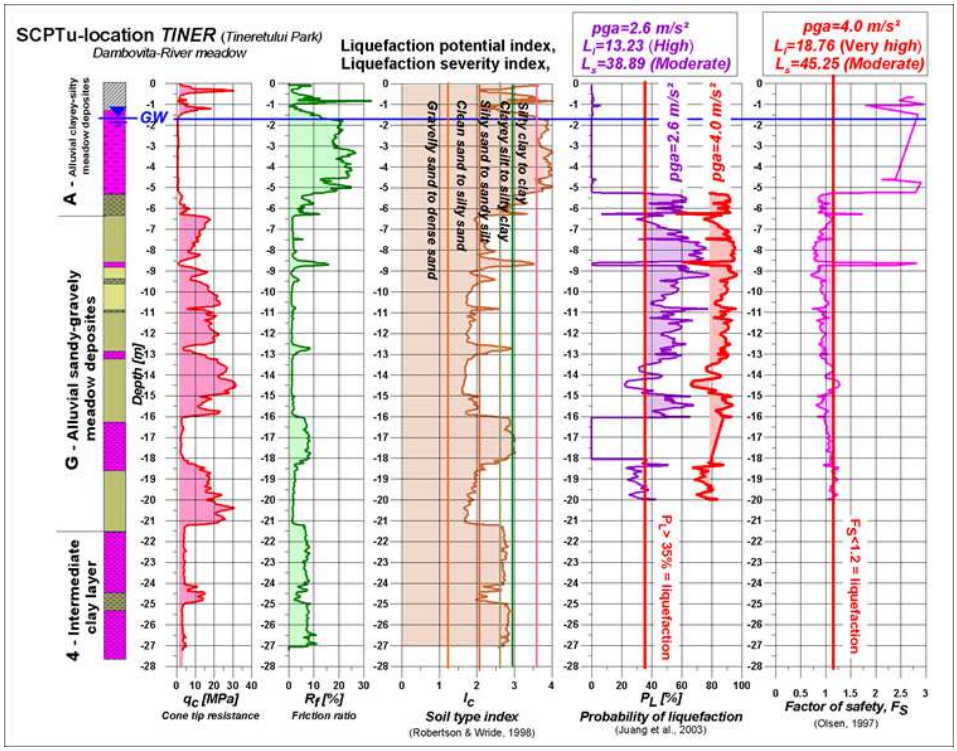

a)

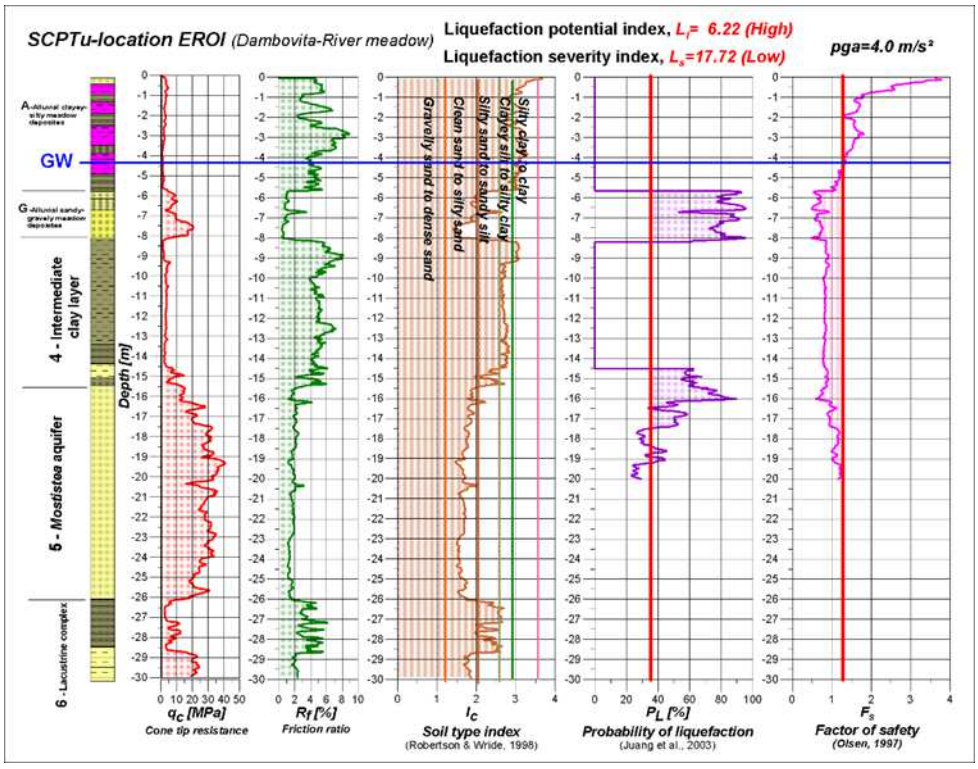

b)

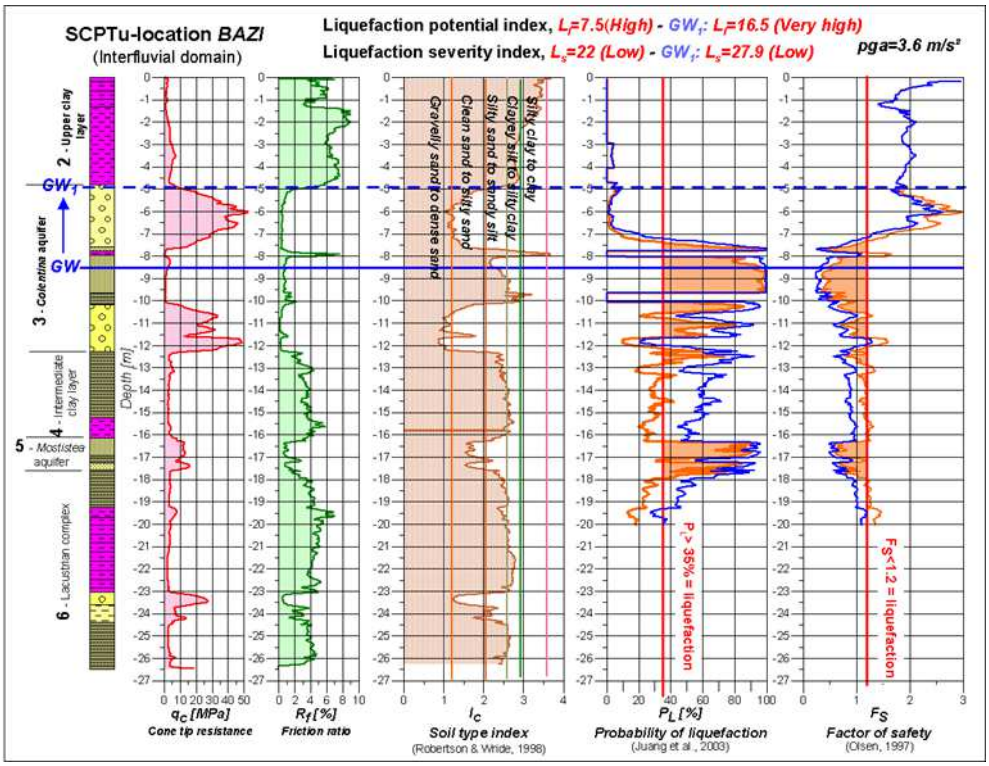

c)

The Influence of the Local PGA-Value

The local PGA-value recorded in a site, influences directly the factor of safety Fs through the CSR-value. To observe the scale of this influence, for the TINE site and the BAZI site the liquefaction probability was calculated for PGA-values of 2.5 m/s² and of 4.0 m/s² (Figure 4a and Figure 4b). At the location TINE (Figure 4a) the liquefaction probability increase very strong for a higher PGA-value, the liquefaction potential became "very high", but the liquefaction severity remains "moderate". In Figure 4b it can be seen, that for 2.5 m/s² the probability is lower than 35%, but for 4.0 m/s² the probability became greater than 60% and even 80%, but only for thin soil layers. The liquefaction potential became from "non-liquefiable" to "low" and the liquefaction severity became from "non-liquefiable" to "very low". The liquefaction severity increases only a little, also due to the great thickness (about 6 m) of the covering clay layer. It can be said, that for a stronger earthquake than the 1977 one, at greater PGA-values, liquefaction effects can appear also at some new sites that until now were considered as "non-liquefiable".

Analysis of the Influence of Groundwater Level Variations for Liquefaction in Bucharest

Seasonal groundwater level variations and groundwater level variations due to extreme precipitation events must be taken into account as a main time-variable influencing factor for liquefaction in Bucharest. The extend of the groundwater level variations within the upper-most aquifer, the Colentina aquifer was studied by continuous level-records during the research period of the CRC-461 project. To emphasize the scale of the influence of groundwater level variations, the

liquefaction probability and the other liquefaction indices were calculated for different groundwater level. In Figure 4c these differences are presented for the case of the BAZI location. It can be seen, that for a 3 m higher groundwater level, the probability of liquefaction increase for the whole depth interval of 12 m, but especially for the depth interval between 13–16 m, where the probability was below 35%, it is now greater than 50%. The liquefaction potential became from "high" to "very high", but the liquefaction severity remains "moderate", mainly due to the great thickness (about 5 m) of the covering clay layer at this site.

Further it can be shown, that changes of groundwater level influence the ground response significantly and cannot be neglected for site effect analyses (Ehret et al. 2007).

The Influence of Shear-Wave Seismic Velocities

In Table 1 all the relevant information about the SCPTu measurements perfomed in Bucharest in 10 sites are given after Hannich and Hötzl (2008).

The shallow seismic velocity structure of the uppermost subsurface is the first step in estimating the amplification of earthquake-induced ground motion and for Bucharest it was presented by Von Steht et al. (2008) using classical methods like seismic refraction.

Extensive information about shear-wave seismic velocities are presented by Bala et al. (2011) for the whole Bucharest City and employing several seismic methods adapted to the work in a big city.

Hannich and Orlowsky (2014) presented shear-wave seismic velocities obtained by MULTI-OFFSET VERTICAL SEISMIC PROFILING (MOVSP) measurements and obtained the V_S characteristic values for the 7 principal Quaternary layers.

Figure 5. *Shear-Wave Velocity Evaluation by SCPT at the TINE Location*

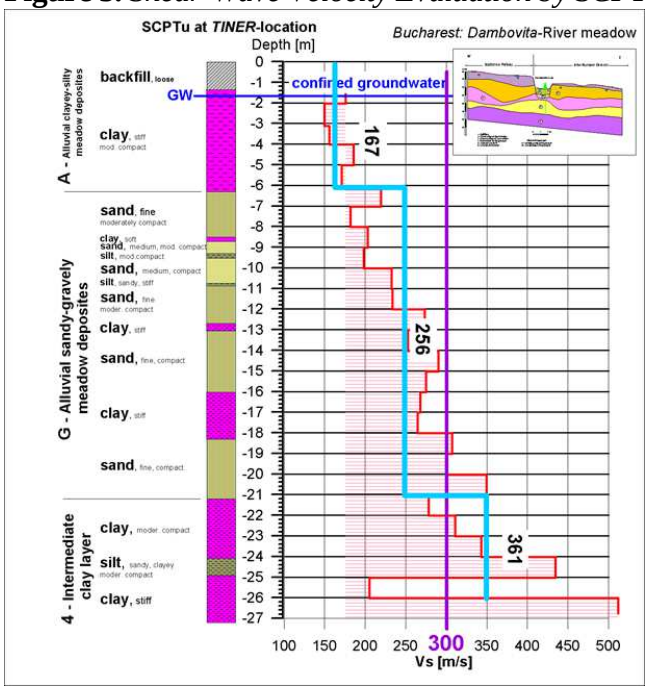

Characteristic for liquefaction prone areas are reduced shear-wave velocities of the near-surface geologic formations. The SCPT-method enabled the detailed determination of the shear-wave velocity at the different locations. As an example, in Figure 5 the variation of the shear-wave velocity until a depth of 27 m at the TINE location (Tineretului Park) is presented. Reduced shear-wave velocities of about 167 m/s were determined here for the first 6 m depth although the value in the Table 3 is about 237 m/s, being computed until a depth of 30 m.

In complete contrast with the first 3 sites presented in Figure 4, in Figure 6 the liquefaction evaluation with low and very low values of liquefaction potential index is presented for the sites INMH; METRO; INCERC which are placed outside the river meadow area and to the north-east of the interfluvial domain. For values of PGA in the 2.5–4 m/s^2, the values of liquefaction potential index is close to 0, showing the lack of possibility of occurring liquefaction. The existence of ground water table at depth around 10 m is playing a key role along with the composition of the shallow layers in the area. In Figure 6c the liquefaction evaluation for the INCERC location is presented. For a PGA-value of 2.5 m/s² estimated here from the ground motion records of the 1977 earthquake, the liquefaction evaluations using CPT-data, show a probability under 35%, that means under that conditions no liquefaction will take place.

Figure 6. *Liquefaction Evaluation with low Values of Liquefaction Potential Index at:* a) *INMH for PGA=3 m/s^2* b) *METRO for PGA=2.5 m/s^2* c) *INCERC PGA$_1$= 2.5 and PGA$_2$=4.0 m/s^2*

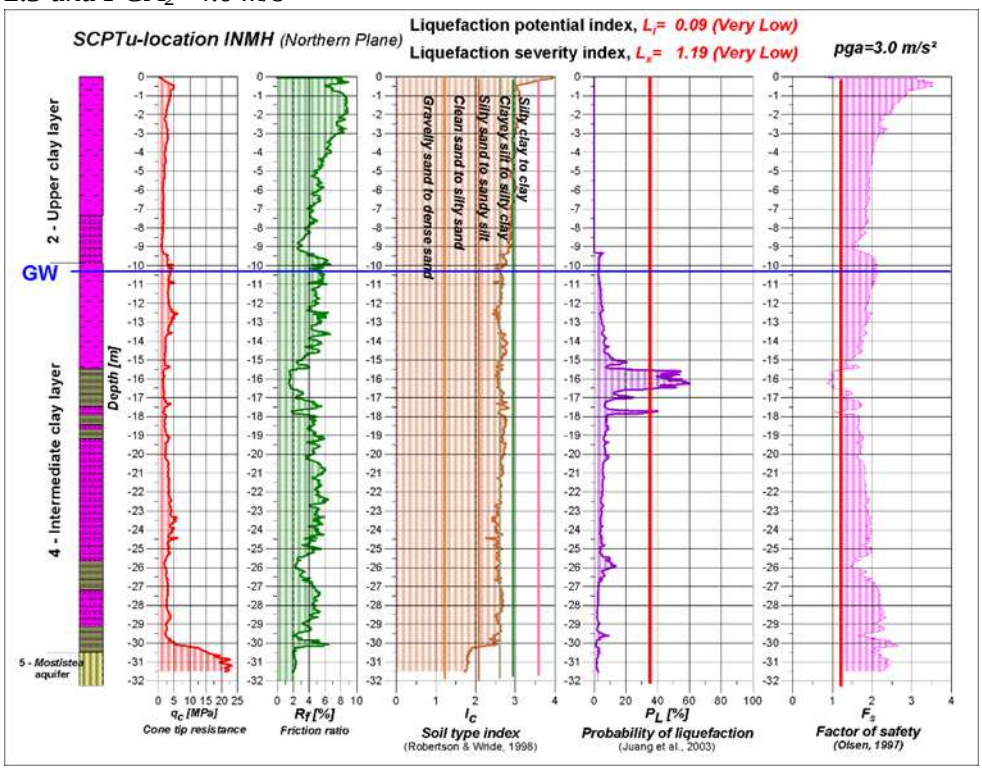

a)

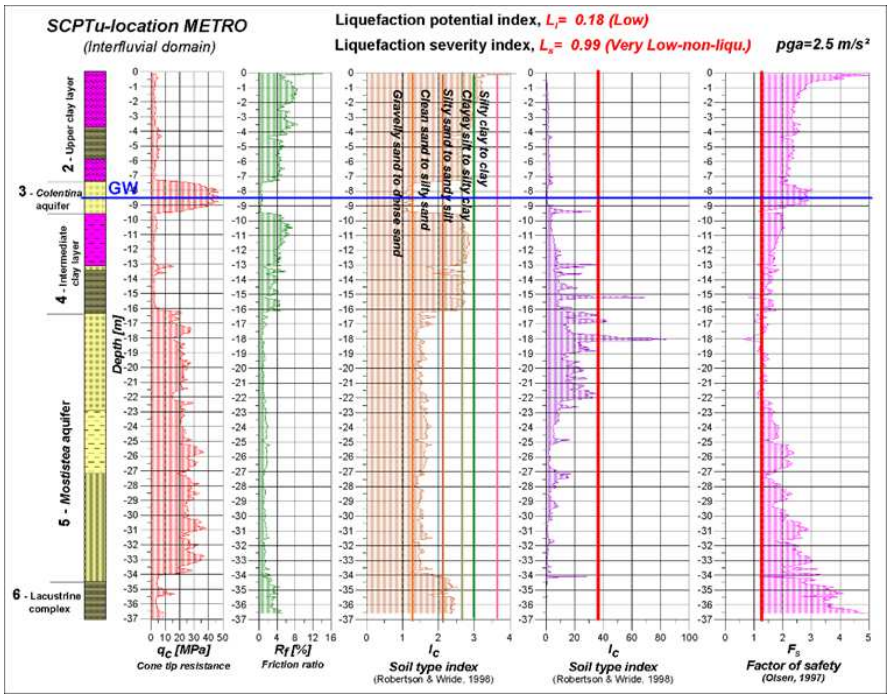

b)

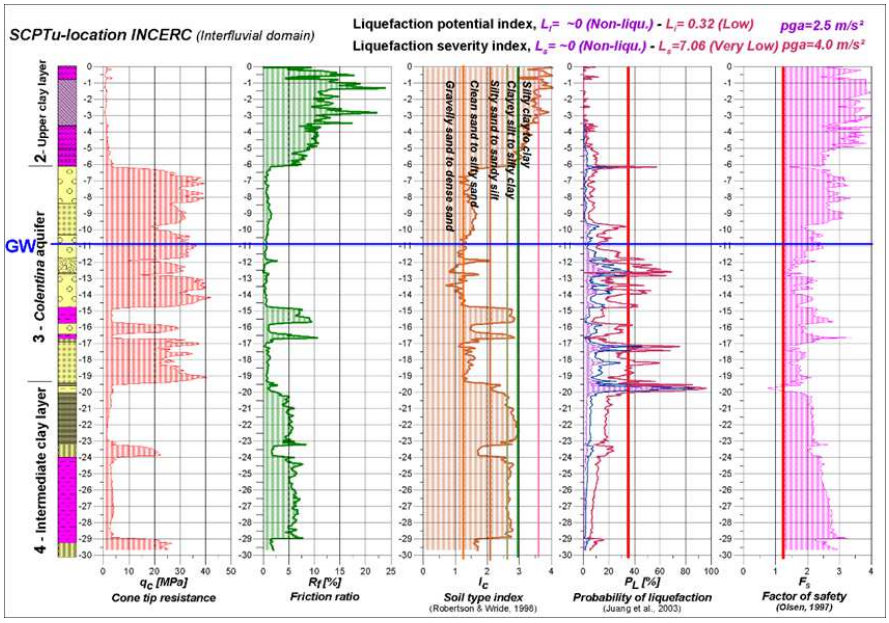

c)

It is worth to note that all 3 locations presented in Figure 6 are located to the north-west of Bucharest, outside the meadow area of Colentina River.

As for the liquefaction evaluation in Figure 6 we can observe that for these wells we have water table at the deepest level, between 8.5 and 10.5 m. For the last site at INCERC (Figure 6c): one for a site acceleration of 2.5 m/s^2 – and liquefaction potential index as well as probability of liquefaction are close to 0. For PGA_2= 4.0 m/s^2 – both parameters are still very low.

Discussion of the Liquefaction Potential for Bucharest City

Based on the SCPTu-data and the liquefaction potential index Li, as well as on the liquefaction severity index Ls, maps for Bucharest were prepared, showing the areas with higher risk to liquefaction process during strong earthquakes like the 1977 one.

The map for the liquefaction potential index Li for Bucharest is presented in Figure 7, by interpolation of the Li-values obtained at the ten SCPTu-locations and additional 4 phantom locations with adopted values for Li. The analysis was performed taking into account the magnitude of this 1977 Vrancea earthquake (Mw=7.4) and a PGA distribution deduced by Sokolov and Bonjer (2006) for Bucharest central area.

It can be observed that a larger area with low potential (Li > 2) extends SE-NW, comprising the Dambovita river meadow and the eastern part of the Colentina river meadow. Within this larger area, two local areas – one in the Tineretului Park and the other in the Eroilor Park – around the locations TINE and EROI, areas with "high" potential (Li > 8) were contoured. Around the BAZI and the AGRO locations, an area with a moderate potential index (Li > 5) was outlined.

Figure 7. *Contour Map of the Liquefaction Potential Index Li for Bucharest City, Computed for Evaluated PGA-Values Corresponding to 1977 Earthquake (Table 1) and a Return Period of 475 Years*

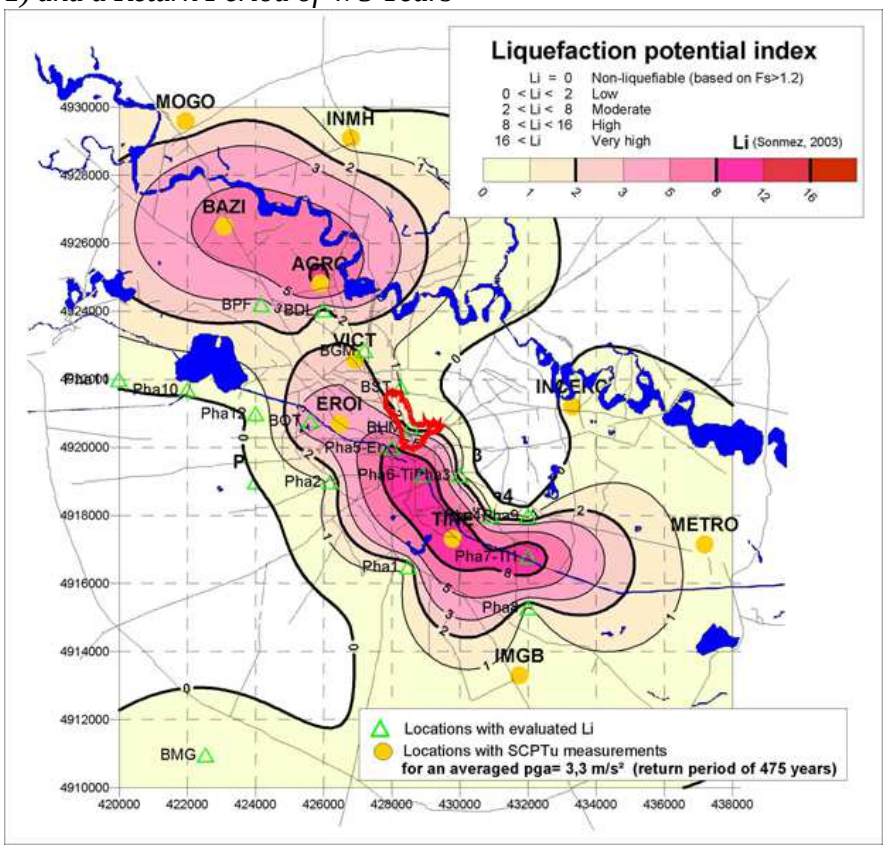

We have produced here a liquefaction potential map for an average of PGA=3.3 m/s^2, with a return period of 475 years. However other probabilistic maps, displaying the liquefaction potential for the shaking expected in a 100-year time window accounting for all earthquakes and the likelihoods of each occurring can be performed as well.

Conclusions

The liquefaction probability was calculated for each of the 10 SCPTu locations on the basis of the CPT data (tip resistance and sleeve friction) using empirical methods. Simplified procedures, originally proposed by Seed and Idriss (1971) is still one of the most frequently used, being based on stress calculations, namely as the ratio between the cyclic stress ratio (CSR) and the cyclic resistance ratio (CRR). The method has been revised and updated and a number of similar methods have been adapted for the calculation of CRR during the years. The Olsen (1997) method is used in the present study because it was believed to be most appropriate for the raw data and conditions available in Bucharest.

Calculations were carried out on each SCPTu location but with different input data, depending on the site.

1. On each locations the basic data used as input consisted in the actual shearwave velocity computed in the same location as well as the ground motion acceleration computed in place for an Vrancea earthquake with magnitude Mw ≥ 7.4 (as for the great earthquake from 04.03.1977).
2. Some calculations are made with different groundwater levels, which document the influence of the groundwater fluctuations on the occurrence of liquefaction, like for location Bazi (Figure 4c). It can be seen that at a higher GW level, the liquefaction probability is significantly higher than for the lower level of groundwater. Also for the lower range, the liquefaction is significant, clearly above the limit value of 35%.
3. The influence of elevated PGA levels, i.e. events of larger magnitudes, are documented for an increased likelihood of liquefaction. At the site INCERC (Figure 6c) there are used two levels of maximum acceleration: PGA_1=2.5 m/s^2 and PGA_2=4.0 m/s^2. For the latter value a greater risk of liquefaction can be seen in the graphics.
4. The importance of the exact knowledge of the groundwater levels in a region, especially in urban areas, in connection with a correct classification of the liquefaction potential and the seismic hazards mapping is pointed out. At the same time, historical high and low levels of the groundwater must be known in order to correctly assess the liquefaction risk.

In the present paper it was stressed that groundwater level changes influence the ground response strongly and cannot be neglected for site effect analyses, the same effect was noted by previous works (Ehret et al. 2010), which were using other methods.

In the presence of confined aquifers, liquefaction can take place in the subsurface. This results in attenuation of shear wave propagation and can reduce

duration and amplitude of ground shaking and ground water level changes, even sezonal variations, should be considered for seismic microzonation studies.

The main goals of this research direction could be achieved if additional measurements during moderate to strong Vrancea earthquakes can be adopted for an overall assessment. The developed groundwater flow model is functional and enables the answer to a main problem of being able to forecast groundwater levels for future times and at certain locations in Bucharest. However additional, denser data on anthropogenic influences in the city center area and additional continuous groundwater level measurement data in the urban area are required. The question of the influence of different groundwater levels and thus different degrees of water saturation within the sand layers on the shear wave velocity could be only partially answered by the SCPTu measurements, but further laboratory investigations by means of resonant column tests will provide additional data.

The map of liquefaction potential index was computed for all Bucharest area and we can see 3 locations with great liquefaction index at TINE and EROI, as well as at BAZI locations. The locations at EROI are very sensitive to liquefaction, due to the present geotechnical parameters and actually an incident has happened during the construction stage at the underground station Eroilor in 2015, exactly in the same area. The whole incident is described in Annex 1.

After our observations from Annex 1 a new study demonstrates the effects of the same incident. The study of Gheorghe et al. (2019) reached to the same conclusions as ours (presented in Annex 1): the construction of the metro station in the Eroilor area (TINE location) posed a threat to the structures aboveground, due to the geotechnical conditions and annual ground movement recorded prior to the incident of the metro in December 2015. Future similar events might still occur in the case of underground constructions in Bucharest.

Two of the locations, where a high potential index was computed in Table 3, are also mentioned in a recent paper that is presenting the vertical displacements map of Bucharest, obtained using Sentinel-1 data, trends at city scale. The 2 locations TINE and EROI in the present study have been put into evidence by Radutu et al. (2020) as 2 zones, situated just near the Dâmbovița river, with measurable subsidence areas, which make them unfit for constructions.

The question of the influence of magnitude, frequency content and duration of the Vrancea earthquakes on changes in pore water pressure in the Colentina sand and gravel layer remain a task for the future, that must be pursued as it was demonstrated a clear link between our measurements and seismic hazard in a high populated area as Bucharest City.

References

Bala A, Raileanu V, Zihan I, Ciugudean V, Grecu B (2006) Physical and dynamic properties of the shallow sedimentary rocks in the Bucharest Metropolitan Area. *Romanian Reports in Physics* 58(2): 221–250.

Bala A, Hannich D, Ritter JRR, Ciugudean-Toma V (2011) Geological and Geophysical Model of the Quaternary Layers based on in situ measurements in Bucharest, Romania. *Romanian Reports in Physics* 63(1): 250–274.

Bretotean M, Reich C, Baldovin M (1986) Problems of groundwater abstraction optimization from shallow and medium deep aquifers in the city area of Bucharest (in Romanian). *Studii si Cercetari – Hidrologie (Bucuresti)* 53: 127–142.

Bretotean M (2001) *Phreatic level variations in Bucharest between 1973-2001* (in Romanian). Internal Report. Bucharest: National Institute for Meteorology and Hydrology.

Chen CJ, Juang CH (2000) Calibration of SPT- and CPT-based liquefaction evaluation methods. In PW Mayne, R Hryciw (eds.), *Innovations and Applications in Geotechnical Site Characterization*, 49–64. Geotechnical Special Publication 97.

Ciugudean V, Martinof D (2000) *Geological, geomorphological and hydrogeological conditions in the city area of Bucharest*. Internal Report. Bucharest: S.C. Metroul S.A.

Ciugudean-Toma V, Stefanescu I (2000) Engineering geology of the Bucharest city area, Romania. In *Proceedings of IAEG -2006 Engineering Geology for Tomorrow's Cities*. Paper no. 235.

Ehret D, Hannich D, Schmitt S, Huber G (2007) Numerical modelling of side effects – Influences of groundwater level changes. In *Proceedings of the 1st IASME/WSEAS International Conference on Geology and Seismology (GES'07).* Portoroz, Slovenia, May 15–17.

Ehret D, Rohn R, Hannich D, Grandas C, Huber G (2010) Numerical modelling of seismic site effects incorporating non-linearity and groundwater level changes. *Journal of Earth Science* 21(6): 931–940.

Gheorghe M, Armaș I, Dumitru P, Călin A, Bădescu O, Necșoiu M, (2019) Monitoring subway construction using Sentinel-1 data: a case study in Bucharest, Romania. *International Journal of Remote Sensing* 41(7): 2644–2663.

Hannich D, Hötzl H (2008) Teilprojekt B7: Hyrogeologie und Standorteffekte bei Erdbeben in Bukarest Arbeitsbericht Phase IV (2005–2007), Sonderforschungsbereich 461. (Subproject B7: hyrogeology and standard effects on earthquakes in Bucharest Work report phase IV (2005–2007), collaborative research center 461). *Starkbeben: Von geowissenshaftlichen Grundlagen zu IngenieurmaBnahmen, Geologisches Institut, Abt. Hydrogeologie, Universitätsverlag Karlsruhe.*

Hannich D, Orlowsky D (2014) Shear-wave velocities of the quaternary layers, determined by multi-offset vertical seismic profiling (MOVSP) in Bucharest, Romania. *Romanian Reports in Physics* 66(4): 1207–1225.

Hannich D, Hötzl H, Ehret D, Bretotean M, Danchiv A, Ciugudean V (2005) The impact of hydrogeology on earthquake ground motion in soft soils. In *Proceedings of the International Conference 250th Anniversary of the 1755 Lisbon Earthquake*, 358–361.

Hannich D, Hötzl H, Cudmani R (2006a) The influence of groundwater on damage caused by earthquakes – An overview (in German). *Grundwasser* 11(4): 286–294.

Hannich D, Huber G, Ehret D, Hötzl H, Balan S, Bala A, et al. (2006b) SCPTu-Techniques used for shallow geologic/hydrogeologic site characterization in Bucharest, Romania. In *ESG 2006 – Third International Symposium on the Effects of Surface Geology on Seismic Motion* 1, 981–992.

Hannich D, Hötzl H, Ehret D, Huber G, Danchiv A, Bretotean M (2007) Liquefaction probability in Bucharest and influencing factors. In *Proceedings of the International Symposium on Strong Vrancea Earthquakes and Risk Mitigation*, 205–221. Bucharest, Romania.

Ishihara K, Perlea V (1984) Liquefaction-associated ground damage during the Vrancea earthquake of March 4, 1977. *Soils and Foundations*, 24(1): 90–112.

Iwasaki T, Arakawa T, Tokida K (1982) Simplified procedures for assessing soil liquefaction during earthquakes. In *Proceedings of the Conference on Soil Dynamics and Earthquake Engineering*, 925–939. Southampton, UK.

Juang CH, Yuan H, Lee DH, Lin PS (2003) Simplified CPT-based method for evaluating liquefaction potential of soils. *Journal of Geotechnical and Geoenvironmental Engineering* 129(1): 66–80.

Kramer SL (1996) *Geotechnical earthquake engineering*. Upper Saddle River, NJ: Prentice Hall.

Lee D-H, Ku C-S, Yuan H (2003) A study of the liquefaction risk potential at Yuanlin, Taiwan. *Engineering Geology* 71(1–2): 97–117.

Li DK, Juang CH, Andrus RD (2006) Liquefaction potential index: a critical assessment using probability concept. *Journal of GeoEn*gineering 1(1): 11–24.

Liteanu E (1952) Geology of Bucharest city area. In *Com. Geol. St. Tehn. Econ, series E,* no. I. Bucharest (in Romanian).

Lungu D, Aldea A, Moldoveanu T, Ciugudean V, Stefanica M (1999) Near-surface geology and dynamic properties of soil layers in Bucharest. In F Wenzel, D Lungu, O Novak (eds.), *Vrancea Earthquakes: Tectonics, Hazard and Risk Mitigation,* 137–148. Dordrecht: Kluwer Academic Publishers.

Mandrescu N, Radulian M, Marmureanu Gh (2004) Site conditions and predominant period on seismic motion in the Bucharest urban area. *Revue Roumaine de Geophysique* 48: 37–48.

Mutihac V (1990) *Geologic structure of Romania* (in Romanian). Bucharest: Edit. Tehnică.

Olsen RS (1997) Cyclic liquefaction based on the cone penetration test. In TL Youd, IM Idriss (eds.), *Proceedings of the NCEER Workshop of Evaluation of Liquefaction Resistance of Soils*, 225–276. Buffalo, NY: State University of New York at Buffalo.

Radutu A, Venvik G, Ghibus T, Gogu CR (2020) Sentinel-1 data for underground processes recognition in Bucharest City, Romania. *Remote Sensing* 12(24): 4054.

Robertson P, Wride C (1998) Evaluating cyclic liquefaction potential using the cone penetration test. *Canadian Geotechnical Journal* 35(Jan): 442–459.

Seed HB, Idriss IM. (1971) Simplified procedure for evaluating soil liquefaction potential. *Journal of the Soil Mechanics and Foundations Division* 97(9): 1249–1273.

Sokolov V, Bonjer K-P (2006) Modeling of distribution of ground motion parameters during strong Vrancea (Romania) earthquakes. In *Proceedings of First European Conference on Earthquake Engineering and Seismology*, paper no. 363. Geneva, Switzerland, 3-8 September 2006.

Sokolov V, Bonjer K-P, Wenzel F, Grecu B, Radulian M (2008) Ground-motion prediction equations for the intermediate depth Vrancea (Romania) earthquakes. *Bulletin of Earthquake Engineering* 6(3): 367–388.

Sonmez H (2003) Modification to the liquefaction potential index and liquefaction susceptibility mapping for a liquefaction-prone area (Inegol-Turkey). *Environmental Geology* 44(7): 862–871.

Sonmez H, Gokceoglu C (2005) A liquefaction severity index suggested for engineering practice. *Environmental Geology* 48(1): 81–91.

Von Steht M, Jaskolla M, Ritter JRR (2008) Near surface shear wave velocity in Bucharest, Romania. *Natural Hazards and Earth System Sciences* 8(6): 1299–1307.

Yuan H, Yang SH, Andrus RD, Juang CH (2004) Liquefaction-induced ground failure: a study of the Chi-Chi earthquake cases. *Engineering Geology* 71(1–2): 141–155.

Annex 1

In the end of the present paper we should brought into discussion a serious incident that occurred in 2015 on the Line 5 (in construction at that time) of the underground in Bucharest, incident that unfortunately proved that the conditions of the shallow layers and the groundwater level are distributed as we presented and the occurrence of a liquefaction along the Dambovița river is a serious threat for the all inhabitants in the area.

The two Tunnel Boring Machine (TBM)s, the giant equipment that digs the subway tunnels on the underground line 5 to Drumul Taberei zone, arrived at the entrance to "Eroilor 2" station, and on Friday 11.11.2015 at noon the first TBM named "Sf. Varvara", broke the molded wall of the future station. A little later about 500 cubic meters of water, gravel and sand poured into the station (which is at 22 m depth), leaving behind a "gap" under the concrete slab under the Bv. Eroilor Sanitari. When the TBM came out at the end of the tunnel, it broke that molded wall and a lot of water and alluviums entered the station, according to sources from the construction site.

This mass has practically moved from the areas where the collapse is seen on the surface and left a gap in which the plaque of the road collapse with 30–40 cm from surface.

Figure 8. *Schematic Set of the Area of the Incident*

Source: https://monitorizari.hotnews.ro/stiri-infrastructura_articole-20665433-intamplat-metrou-surpat-pamantul-eroilor-acolo-unde-sapa-cartitele-magistrala-5.htm.

According to other sources close to the situation, the large amount of water that collected and caused other alluvium also came from a depletion well (water

drainage well) that was damaged when the TBM machine entered the station, and the water entered the groundwater and the soil in the area softened. After the incident, when the first settlements appeared under the road, the builder filled the gap with almost 70 cubic meters of concrete, but the compaction phenomenon continued and another 120 cubic meters of concrete were poured. Eventually, the settlement stagnated. For safety reasons, however, the authorities opted to evacuate some 14 persons from the two nearby buildings.

Figure 9. *Photo after the Incident with Collapse of the Road and the 2 Affected Buildings across the Road*

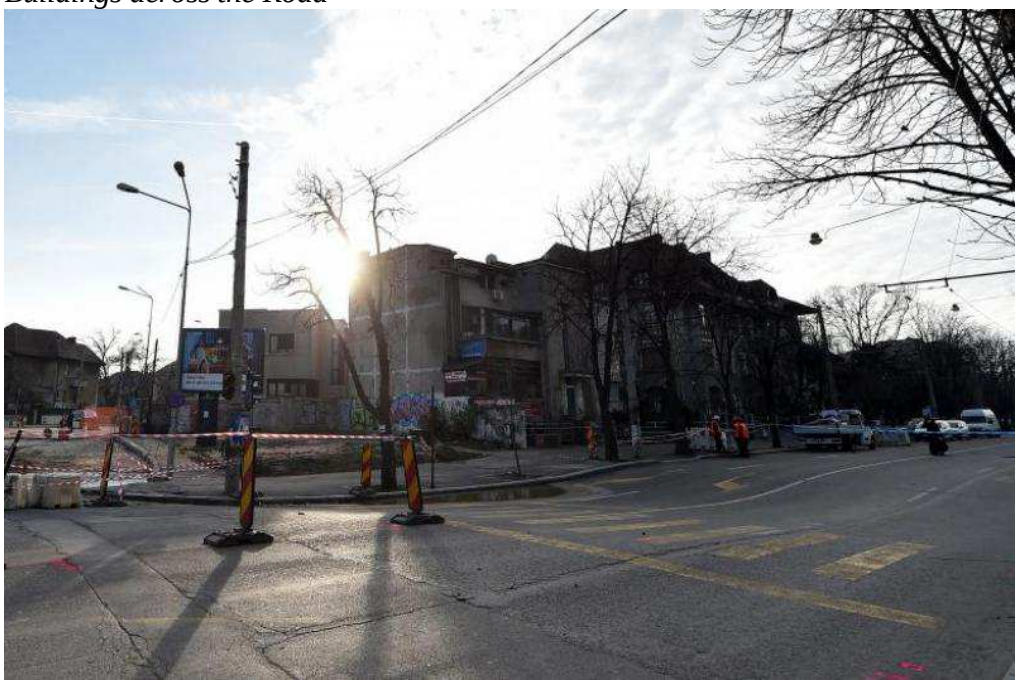

Source: Agerpres.

That was almost all we have found about the incident from the media of that time.

In our rough interpretation the 500 cubic meters of water and alluvium could not be replaced completely by only 200 cubic meters of concrete that was put under the road in an effort of stabilizing the ground. The situation has much in common with the liquefaction phenomenon presented above and it involves a great quantity of water mixed with silt and gravel which acted as a thick liquid and pour into the underground station by the hole in the molded wall that was dug by the TBM.

No earthquake was involved in the incident, but the TBM in its movement created a lot of ground-shaking of the underground, enough to mobilize the mass of water and alluviums and to make it move to the underground station at Eroilor 2.

The situation was serious enough so that the constructor took some immediate measures in order to stabilize the ground, close the traffic and emptied 2 buildings which were in a danger of collapsing. Although the promises of the constructors

were to rebuild the area in a couple of months, it took more than a year before the traffic was opened at surface and the construction of line 5 was resumed.

But the situation of the two constructions just across the street was not good, as they were still uninhabitable.

Eventually both of them were refitted after more than one and a half year after the incident.

This incident was presented as it involves the same material and conditions as a real liquefaction and acted in the same way and it took place in the underground station named Eroilor (Figure 9), which is the exact spot in which our paper predicted a high probability of a liquefaction to occur (see Figure 4b and Figure 8 – zone EROI).

After we have proposed this incident on the M-5 subway line, as a proof of existence of geotechnical conditions able to determine an induced liquefaction of the terrain, we have new scientific proofs recorded and interpreted by (Gheorghe et al. 2019). They have used a medium-resolution SAR imagery for monitoring subsidence due to tunneling which was used before to detect fine movements of the terrain along subway lines.

In the case of the M-5 subway belt, processing two data stacks each containing more than 160 Sentinel-1 images, revealed movement patterns associated with underground construction works, consisting of cumulative subsidence values of up to 20 mm with an average yearly velocity of up to 8 mm/year (Gheorghe et al. 2019) prior and near the moment of the technical incident at Eroilor stations described in Annex 1.

The subsidence values of −40 mm on top of the metro station reported by the authorities immediately after the event could not be detected due to technical problems, but after that there are recorded proofs that the terrain in the area begin to raise very slow and it was not gaining the initial values.

Athens Journal of Technology and Engineering - Volume 8, Issue 2, June 2021 – Pages 139-168

Design of a Four-Seat, General Aviation Electric Aircraft

By Priya Chouhan[*] & Nikos J. Mourtos[+]

Financial and environmental considerations continue to encourage aircraft manufacturers to consider alternate forms of aircraft propulsion. On the financial end, it is the continued rise in aviation fuel prices, as a result of an increasing demand for air travel, and the depletion of fossil fuel resources; on the environmental end, it is concerns related to air pollution and global warming. New aircraft designs are being proposed using electrical and hybrid propulsion systems, as a way of tackling both the financial and environmental challenges associated with the continued use of fossil fuels. While battery capabilities are evolving rapidly, the current state-of-the-art offers an energy density of ~ 250 Wh/kg. This is sufficient for small, general aviation electric airplanes, with a modest range no more than 200 km. This paper explores the possibility of a medium range (750 km) electric, four-seat, FAR-23 certifiable general aviation aircraft, assuming an energy density of 1500 Wh/kg, projected to be available in 2025. It presents the conceptual and preliminary design of such an aircraft, which includes weight and performance sizing, fuselage design, wing and high-lift system design, empennage design, landing gear design, weight and balance, stability and control analysis, drag polar estimation, environmental impact and final specifications. The results indicate that such an aircraft is indeed feasible, promising greener general aviation fleets around the world.

Keywords: *general aviation aircraft, electric aircraft, aircraft design*

Introduction

The main source of energy in aviation today is fossil fuels. As our energy consumption increases exponentially, it leads to a corresponding rise in the demand for these fuels, which will persist in the next few decades. This increased demand causes an increase in fuel prices, which in turn increases the operating cost for airlines, business flying, and general aviation. More importantly, the increasing use of fossil fuels in aviation results in increasing CO_2 emissions, as well as increasing noise levels around airports. There are, of course, other ways to produce energy for airplanes, without using fossil fuels. Many of these are currently being explored but they are not, at the moment, close to their full potential (Riddell 2004). Electric aircraft offer lower emissions, lower noise levels during taxing, takeoff and landing, lower operating costs, and improved overall efficiency. This paper explores the possibility of an electric four-seater aircraft, as an alternative to conventional gasoline-powered aircraft.

[*]Research Assistant, Department of Aerospace Engineering, San Jose State University, USA.
[+]Professor & Chair, Department of Aerospace Engineering, San Jose State University, USA.

The paper presents the preliminary design of a four-passenger, electric, general aviation aircraft, with a range of 750 km, a cruise speed of 270 km/hr at a cruising altitude of 3,000 m, a takeoff field length of 760 m and a landing field of 600 m. The main challenge currently associated with electric aircraft is the low specific energy density of the batteries, which results in prohibitive levels of battery weight for typical power requirements. This paper examines possible design solutions that would meet the mission specification of a general aviation aircraft, as described above.

Comparative Study of General Aviation Electric Aircraft

This section presents a review and comparison of electric general aviation aircraft with a similar mission specification.

Bye Aerospace eFlyer 4

The eFlyer (Figure 1) was developed from the smaller two seat Bye Aerospace aircraft and is made of composite materials. It features a cantilever low wing with a fixed landing gear, a single engine tractor configuration, with four-seats enclosed under a bubble canopy. The low wing configuration offers greater fuselage volume for passengers, makes it easier to refuel, and easier to retract the landing gear inside the wing. A single electric motor capable of producing 105 kW (141 hp) is powered by ten batteries, which provide an endurance of four hours.

Figure 1. *Bye Aerospace eFlyer 4 (Bye Aerospace 2020)*

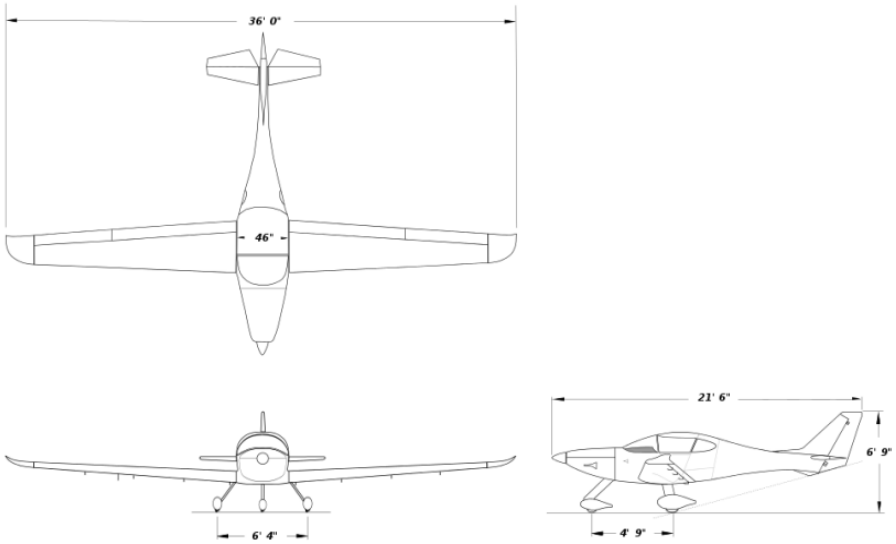

Pipistrel Panthera

The Pipistrel Panthera (Figure 2) is a lightweight, all-composite, highly efficient, four-seat aircraft, which is currently under development. The Panthera electro features a cantilever low wing arrangement, similar to eFlyer 4. The four-seater aircraft is powered by a Siemens 200 kW electric motor and is intended to achieve a 400 km range with a cruise speed of 218 km/hr. The T-tail configuration offers a simple design, low empennage weight, better tail efficiencies, while at the same time reducing the interference from the wake of the wing and the propeller slipstream.

Figure 2. *Panthera Electro (Panthera 2020)*

Yuneec International E430

Yuneec E430 (Figure 3) is a two-seater electric aircraft with a cruise speed of 100 km/hr, designed for commercial production. It has a V-tail and a high wing made of composites with a high aspect ratio. The high wing makes loading and unloading easier, provides better visibility towards the ground and good ground clearance. The aircraft is powered by 3 to 5 packs of Yuneec OEM lithium polymer rechargeable batteries, which provide 2.5 hours endurance. The batteries can be recharged in 3 to 4 hours from a 220-volt outlet.

Figure 3. *Yuneec E430 (Yuneek 2020)*

Pipistrel Taurus Electro G2

The Taurus Electro G2 (Figure 4) is a two-seat glider with a range of 600 km. It features a low wing configuration with a T-tail and has replaced the old gasoline-powered engine with a high-performance electric power train and Li-Po batteries.

Figure 4. *Taurus Electro G2 (Taurus Electro 2020)*

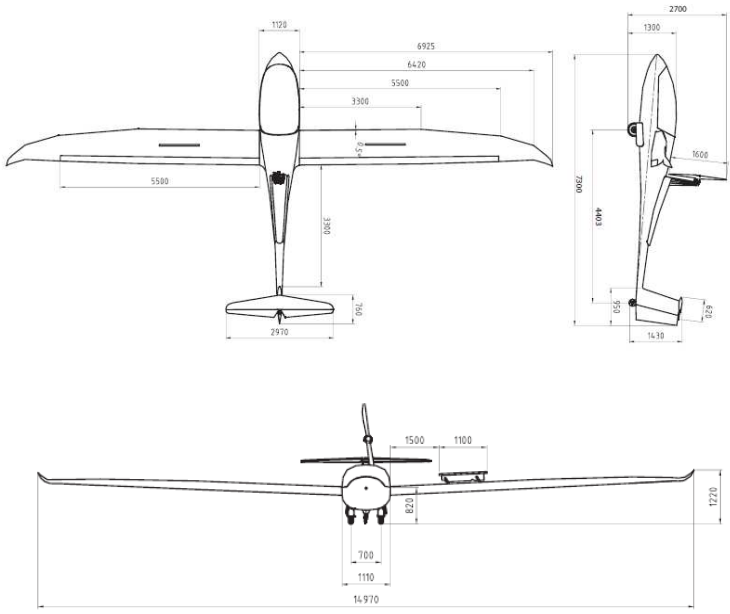

Airbus Vahana

The Airbus Vahana (Figure 5) is an electric-powered eight propeller VTOL personal air vehicle prototype by Airbus. It is a self-piloted vehicle with a capacity of two passengers for a range of 100 km cruising at 140 miles/hr. It uses the distributed electric propulsion (DEP) concept on eVTOL aircraft. DEP allows for quickly changing the speed of each propeller independently to compensate for gusty winds, keeping the aircraft stable during flight.

Figure 5. *Airbus Vahana (Airbus Vahana 2020)*

Preliminary Sizing

The preliminary sizing of the proposed aircraft consists of weight sizing and performance sizing, as described below (Roskam 1985a).

Weight Sizing

The method below estimates the mission takeoff weight (W_{TO}), the empty weight (W_E), and the battery weight (W_{BAT}) of the airplane for the mission specification given in the introduction.

Figure 6 shows a regression plot of takeoff versus empty weight for the airplanes listed in Table 1.

Table 1. *Takeoff and Empty Weight of Similar Electric Airplanes*

Aircraft	**Takeoff Weight (W_{TO}) lbs**	**Empty Weight (W_E) lbs**
Pipistrel Taurus Electro G2 (Wikipedia)	1,212	674
Lange Antares 23E (Wikipedia)	1,873	1,124
Extra 330 LE (Wikipedia)	2,094	1,455
Sunflyer 4 (Bye Aerospace)	2,700	1,900
Airbus Vahana (Airbus)	1,797	1,532
Pipistrel Panthera (Wikipedia)	2,645	1,764
Silent 2 Electro (Alisport Swiss)	6,482	4,321
Electrolight 2 (Siegler 2011)	6,805	4,062
NASA Scuba Stingray (Banke 2015)	3,195	1,438

Figure 6. *Regression Plot of Takeoff versus Empty Weight for the Airplanes in Table 1*

The line in Figure 6 is described by:

$$y = 0.9652x + 0.3143 \quad (1)$$

while the relationship between takeoff weight and empty weight is given by:

$$\text{Log } W_{TO} = A + B \log W_E \quad (2)$$

A comparison of equations (1) and (2) gives the regression coefficients A and B for the relationship between takeoff and empty weight of electric, general aviation aircraft: A = 0.3143 and B = 0.9652. The mission weights of the airplane are now calculated as follows.

Payload Weight

Using an average weight of 175 lbs per passenger plus 30 lbs of baggage (Roskam 1985a) the payload weight is W_{PL} = 4 x (175 + 30) = 820 lbs.

Battery Weight

Hepperle (2012) gives the following empirical formula for the range of electric aircraft:

$$R = E^* * \eta * \left(\frac{1}{g}\right) * \left(\frac{L}{D}\right) * \left(\frac{W_{BAT}}{W_{TO}}\right) \quad (3)$$

Thus, aircraft range depends on lift-to-drag ratio, specific energy density of the battery, total system efficiency, and takeoff weight. Table 2 shows theoretical values of specific energy predicted for the near future (Hepperle 2012).

Table 2. *Specific Energy Density for Various Types of Batteries*

Battery	**Theoretical Value**	**Expected in the next 5-10 years**
Li-Ion	390 Wh/kg	250 Wh/kg
Zn-air	1,090 Wh/kg	400-500 Wh/kg
Li-S	2,570 Wh/kg	500-1,250 Wh/kg
Li-O_2	3,500 Wh/kg	800-1,750 Wh/kg

Using the data in Table 2, a Li-O_2 battery with an energy density of 1500 Wh/kg is used in the proposed design. The battery-powered propulsion system offers the highest efficiency compared to conventional turboprop, turbofan and fuel cell systems (Abdel-Hafez 2012). The takeoff weight for the mission is calculated from equation (4) and the weight breakdown is shown in Table 3.

$$W_{TO} = W_E + W_{PL} + W_{BAT} \quad (4)$$

Table 3. *Summary of Mission Weights*

Take-off weight W_{TO} (lbs)	3,980
Payload weight W_{PL} (lbs)	820
Operating empty weight, W_E (lbs)	2,523
Battery Weight, W_{Bat} (lbs)	637

Takeoff Weight Sensitivities

Take-off weight sensitivities are obtained using the regression coefficients A = 0.3143 and B = 0.9652 calculated above and coefficients C and D calculated below (Roskam 1985a):

$$W_E = CW_{TO} - D \tag{5}$$

For fully electric aircraft C = 1 and

$$D = W_{PL} + W_{BAT} = 1457\ lbs \tag{6}$$

The equations below describe various sensitivities.

Takeoff weight with respect to payload:

$$\frac{\delta W_{TO}}{\delta W_{PL}} = \frac{B*W_{TO}}{D-C(1-B)*W_{TO}} \tag{7}$$

Takeoff weight with respect to empty weight:

$$\frac{\delta W_{TO}}{\delta W_E} = \frac{B*W_{TO}}{inv.Log10\left[\frac{Log_{10}W_{TO}-A}{B}\right]} \tag{8}$$

Range with respect to takeoff weight:

$$\frac{\delta R}{\delta W_{TO}} = -E^* * \eta_{tot} * (\mathrm{L/D}) * (1/\mathrm{g}) * \left(\frac{\mathrm{W_{BAT}}}{\mathrm{W_{TO}^2}}\right) \tag{9}$$

Range with respect to the lift-to-drag ratio:

$$\frac{\delta R}{\delta(L/D)} = \left(1 - f_s - f_p\right) * E^* * \eta_{tot} * (1/\mathrm{g}) \tag{10}$$

Range with respect to battery energy density:

$$\frac{\delta R}{\delta E^*} = \left(1 - f_s - f_p\right) * (L/D) * \eta_{tot} * (1/\mathrm{g}) \tag{11}$$

The sensitivities calculated from the equations above are shown in Table 4 and plotted in Figures 7, 8 and 9.

Table 4. *Takeoff Weight and Range Sensitivities*

Sensitivity Parameters	Sensitivity Values
$\delta W_{TO}/\delta W_{PL}$	2.92 lbs/lb
$\delta W_{TO}/\delta W_{E}$	1.515 lbs/lb
$\delta R/\delta W_{TO}$	-0.188 km/lb
$\delta R/\delta (L/D)$	74 km
$\delta R/\delta E^{*}$	0.50 km/Wh/kg

Figure 7. *Takeoff Weight vs. Payload Weight*

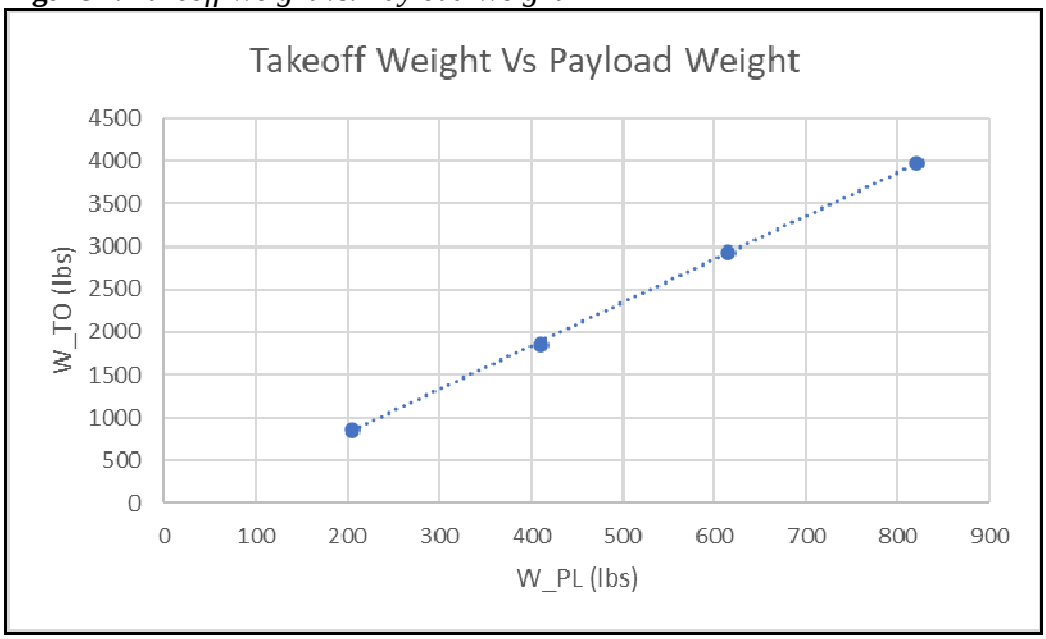

Figure 8. *Range vs. Specific Energy Density*

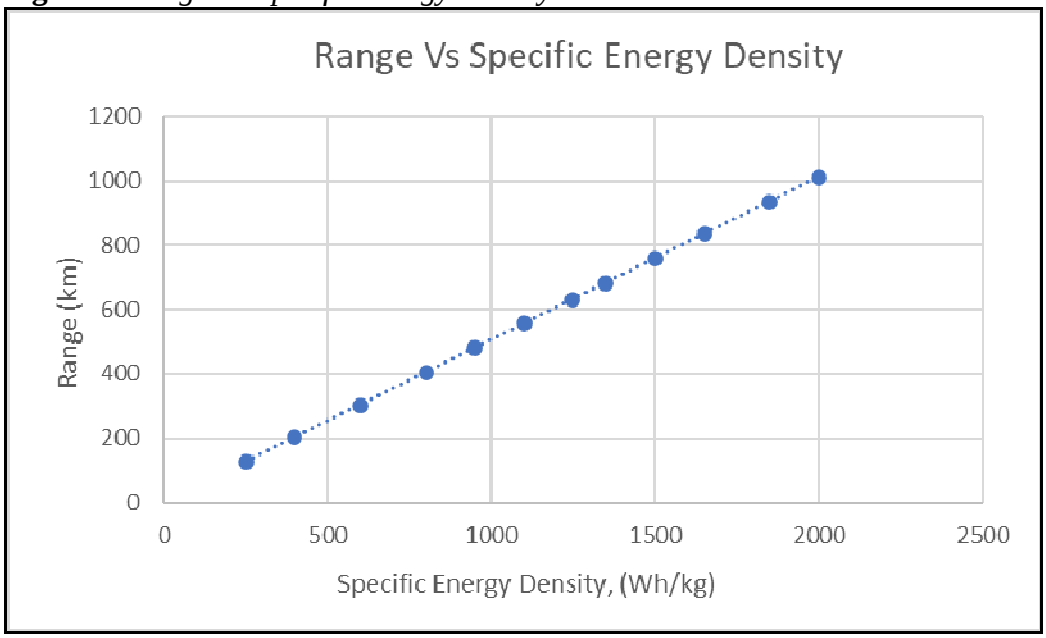

Figure 9. *Range vs. Lift-to-Drag Ratio*

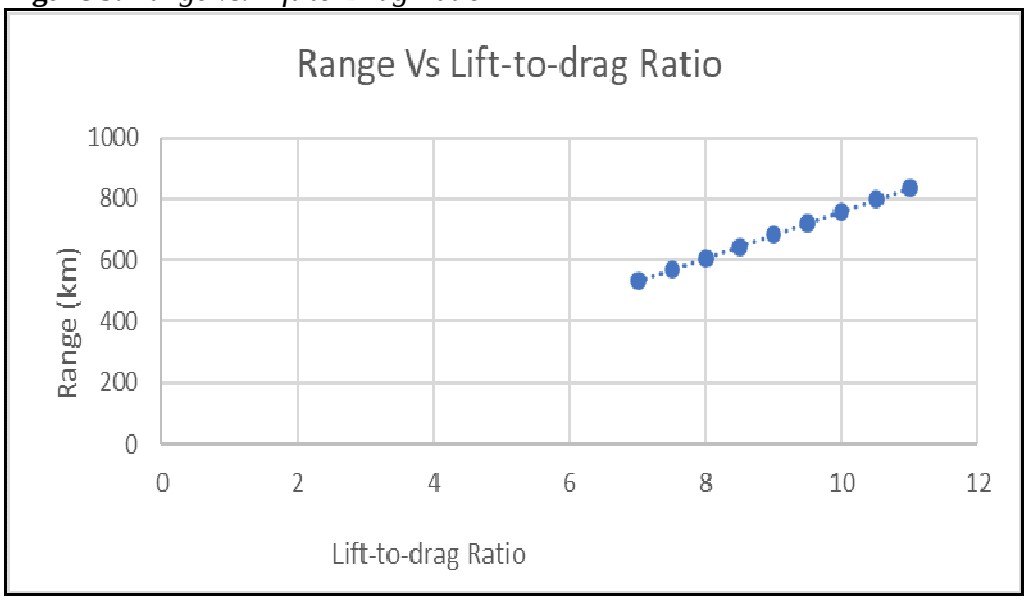

As expected, range depends strongly on the lift-to-drag ratio but also on the specific energy density of the batteries. This is because the takeoff weight of electric aircraft tends to be higher than conventional aircraft due to the weight of the batteries. Hence, improving battery energy density is paramount in helping increase the range of electric aircraft.

Performance Sizing

The proposed aircraft has a takeoff weight less than 6,000 lbs, hence it falls under the FAR-23 certification regulations. A performance constraint analysis is used to determine the design point of the aircraft, namely the combination of wing area and power required to meet all the mission and FAR 23 requirements. Each requirement is plotted as a relationship between wing loading (W/S) and power loading (W/P), as shown in Figure 11. To meet takeoff and landing requirements an assumption must be made about the maximum lift coefficient of the aircraft in each of the two configurations. The matching graph of the aircraft is presented in Figures 11 and 12.

Stall Speed Requirement

The stall speed requirement is set at 60 knots and relates to wing loading, density altitude and maximum lift coefficient as shown in equation (12). Single-engine airplanes have a range of maximum lift coefficients between 1.3 and 1.9 (Roskam 1985a). A density altitude of 10,000 ft is assumed (0.0056 lb/ft^3).

$$V_{stall} = \left(2 * \frac{W/S}{\rho * C_{Lmax}}\right)^{\frac{1}{2}} \quad (12)$$

Takeoff Distance Requirement

The takeoff distance requirement is $S_{TO} = 2500\ ft$.

Takeoff distance relates to wing loading, power loading, density ratio and maximum lift coefficient as shown in equation (13), using the takeoff parameter defined in equation (14).

$$S_{TO} = 8.134\ TOP_{23} + 0.0149\ TOP_{23}^2 \quad (13)$$

$$S_{TOG} \infty \left((W/S)_{TO} * \frac{(W/P)_{TO}}{\sigma * C_{Lmax}}\right) = TOP_{23} \quad (14)$$

The density ratio at 10,000 feet is: $\sigma = 0.7386$
while the takeoff parameter is (Roskam, part I, 1985):

$$TOP_{23} = 220\ \frac{lbs^2}{ft^2 * hp} \quad (15)$$

Hence, the takeoff distance requirement may be expressed as:

$$\left(\frac{W}{S}\right)_{TO} * \frac{\left(\frac{W}{P}\right)_{TO}}{C_{LMAX_{TO}}} < 162\ \frac{lbs^2}{ft^2 * hp} \quad (16)$$

Landing Distance Requirement

The landing distance requirement is $S_L = 2000\ ft$ at sea level.

Landing weight is heavier for electric aircraft since battery weight stays the same throughout the flight unlike the reduction in fuel weight in conventional aircraft. Hence:

$$W_L/W_{TO} = 1 \quad (17)$$

The landing distance relates to stall speed by:

$$S_L = 0.5136 * V_{SL}^2 \quad (18)$$

Relating stall speed to wing loading and maximum lift coefficient yields:

$$\frac{2 * (W/S)_L}{0.002049 * C_{Lmax_L}} = (V_S * 1.688)^2 \quad (19)$$

from which we get the relationship for the wing loading as a function of the maximum lift coefficient in the landing configuration.

$$\left(\frac{W}{S}\right)_L = \left(\frac{W}{S}\right)_{TO} = 11.36 * C_{Lmax_L} \quad (20)$$

Drag Polar Estimation

To size the aircraft according to climbing requirements, it is necessary to estimate first the drag polars (Roskam 1985a). The drag coefficient is given by:

$$C_D = C_{D0} + \frac{C_L^2}{\pi * A * e} \quad (21)$$

The low speed drag coefficient can be expressed as a function of the equivalent parasite drag area:

$$C_{D0} = f/S \quad (22)$$

The equivalent parasite area is estimated from similar aircraft using the takeoff weight as follows:

$$Log_{10} f = a + b * \log_{10} S_{wet} \quad (23)$$
where a = −2.0458 and b = 1.00

$$Log_{10} S_{wet} = c + d * \log_{10} W_{TO} \quad (24)$$
where c = 1.0892 and d = 0.5147

From which we get: $S_{wet} = 875\ ft^2\ and\ f = 7.9$ (25)

Assuming an aspect ratio A = 10 and an Oswald efficiency factor e = 0.85 for the clean configuration, the drag polars are shown in Table 5.

Table 5. *Drag Polars for the Proposed Aircraft*

Flight Condition	Zero-Lift Drag Coefficient (C_{D0})	Oswald Efficiency Factor (e)	Drag Polar
Clean	0	0.85	$0.0407 + 0.0374C_L{}^2$
Takeoff flaps	0.0165	0.80	$0.0572 + 0.0397C_L{}^2$
Landing flaps	0.0615	0.75	$0.1022 + 0.0424C_L{}^2$
Landing gear	0.0215	no effect	$0.1237 + 0.0424C_L{}^2$

Climb Requirements

The rate of climb in fpm is expressed as (Roskam 1985a):

$$RC = dh/dt = 33{,}000 * RCP \quad (26)$$

where the rate-of-climb parameter is given by:

$$RCP = \frac{\eta_p}{W/P} - \frac{(W/S)^{1/2}}{19*\sigma^{1/2}*C_L^{3/2}/C_D} \quad (27)$$

The airplane must meet the climb requirements under FAR 23.65 and FAR 23.77, as listed below.

FAR 23.65
The minimum rate of climb at sea level must be at least: $RC = 300$ fpm
This gives a rate-of-climb parameter: $RCP = 0.0091$ hp/lbs

Using the drag polar for the clean aircraft from Table 5 we get the following relationship between wing loading and power loading:

$$208/(2.3 + (W/S)^{1/2}) = W/P \quad (28)$$

The minimum climb gradient for land planes is 1:12. Using:

$$CGRP = 18.97 * \eta_p * \frac{\sigma^{1/2}}{(W/P)*(W/S)^{1/2}} = \frac{\{CGR+(L/D)^{-1}\}}{C_L^{1/2}} \quad (29)$$

we get the relationship between wing loading and power loading:

$$(W/P) * (W/S)^{1/2} = 110.3 \quad (30)$$

FAR 23.77
The climb gradient must be at least: $CGR = 1/30 = 0.0333$
from which we get:

$$(W/P) * (W/S)^{1/2} = 113 \quad (31)$$

Cruise Speed Requirement

The cruise speed for propeller-driven aircraft is calculated at 70% to 80% of total power. At this power setting, the profile drag is higher than the induced drag, which is approximately:

$$C_{D_i} = 0.1C_{D_0} \quad (32)$$

Cruise speed is proportional to the power index, defined as:

$$V_{cr} \infty I_p = \left(\frac{W/S}{\sigma*(W/P)}\right)^{1/3} \quad (33)$$

For a cruise speed of 150 knots (172 mph) the power index is $I_p = 1.0$ (Roskam 1985a). Hence equation (33) yields:

$$\left(\frac{W/S}{\sigma*(W/P)}\right)^{1/3} = 1 \qquad (34)$$

It is now possible to determine the best combination of wing loading and power loading by plotting all requirements in the matching graph, as shown in Figure 10 and assuming appropriate values for the maximum lift coefficients. A clean version of this graph is reproduced in Figure 11. Table 6 summarizes the results from these studies.

Figure 10. *Matching Graph for the Proposed Aircraft*

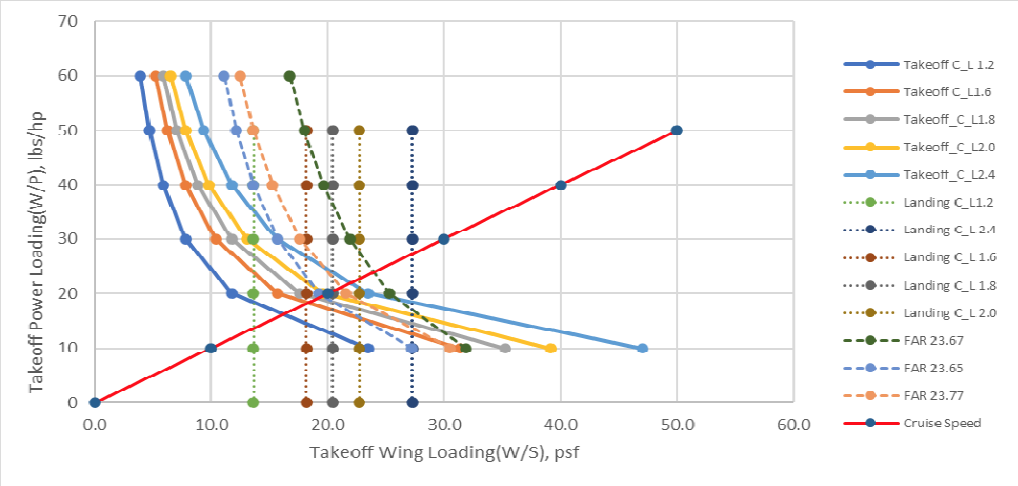

Figure 11. *Matching Graph Including only the Three Critical Requirements, which Define the Design Point*

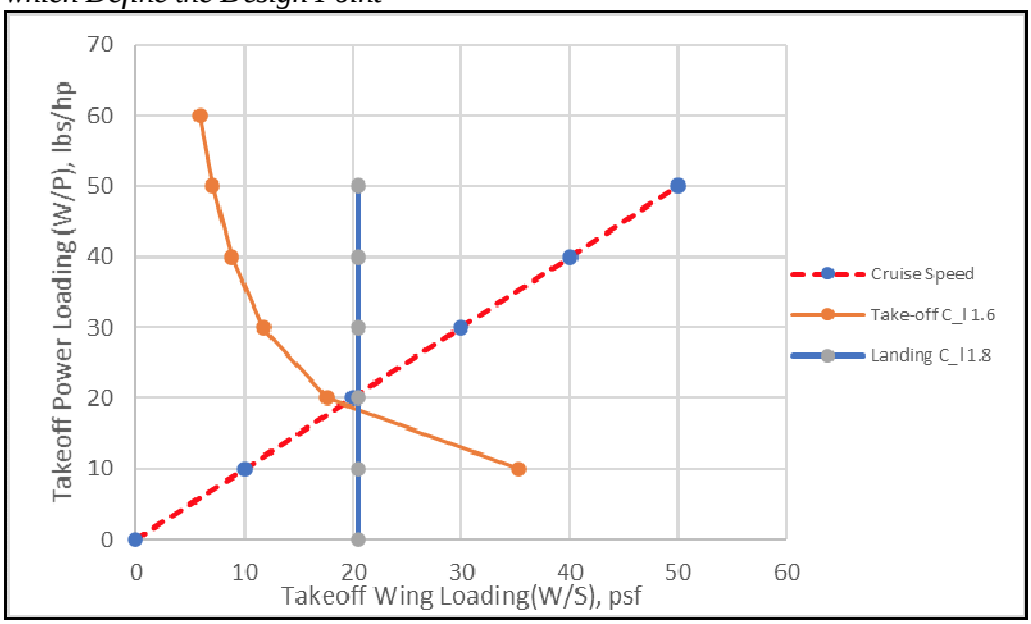

The design point shown in Figure 11 results in a wing loading of 20.5 psf and a power loading of 20 lbs/hp. The various design parameters that correspond to these values are summarized in Table 6.

Table 6. *Design Parameters*

Maximum lift coefficient, C_{Lmax}	Clean	1.5
	Takeoff	1.6
	Landing	1.8
Aspect ratio		10
Wing loading, W/S		20.5 psf
Takeoff power loading, $(W/P)_{TO}$		20 lbs/hp
Wing area, S		194 ft^2
Take-off power, P_{TO}		199 hp

Preliminary Design

The following subsections present the preliminary design of the proposed aircraft (Roskam 1985b).

Configuration

The proposed configuration is shown in Figure 12. It features a low, cantilever wing with zero sweep for better aerodynamic performance at low speeds. The T-tail was chosen to increase the effective aspect ratio of the vertical stabilizer, while keeping the horizontal stabilizer outside the wing wake. Finally, a conventional tricycle landing gear offers fewer parts, lower weight, lower cost, is easier to design, and most importantly, provides for good ground stability.

Figure 12. *Proposed Aircraft Configuration*

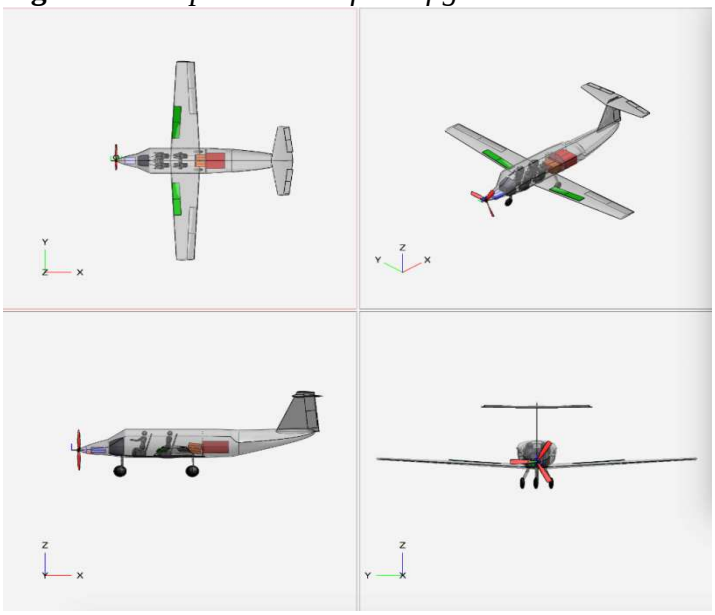

Propulsion System

The electric engine chosen is a Siemens brushless motor-SP 260D. It features a double winding motor with a 95% efficiency at 2500 rpm and is lightweight. Energy density, safety, cost, reliability and maintainability were all considered in the selection of rechargeable, lithium-air batteries with an energy density of 1,500 Wh/kg, expected to be available in 2025 (Hepperle 2012).

The propulsion system is integrated in the fuselage with the electric motor placed at the front and the batteries placed in the wing as well as in the aft fuselage section. The propeller diameter is obtained from equation (35) (Raymer 2012):

$$D_p = \left(4 * P_{max} * n_p * P_{bl}\right)^{1/2} = 5.50 \text{ ft} \qquad (35)$$

Fuselage Design

Fuselage design parameters were calculated using the definitions and aerodynamic considerations in Roskam (1985b) and are shown in Table 7. An isometric view of the fuselage is shown in Figure 13 prepared using the methods and examples in Roskam (1986).

Table 7. *Fuselage Design Parameters*

Fuselage Parameters	**Dimension**
Length (l_f)	29.40 ft
Inner diameter (d_f)	4.5 ft
Fineness ratio (l_f/d_f)	6.53 ft
Rear fuselage angle (θ_{fc})	5 deg
Cabin length	10.4 ft
Nose length	5 ft
Tail cone length	14 ft

Figure 13. *Isometric View of Fuselage*

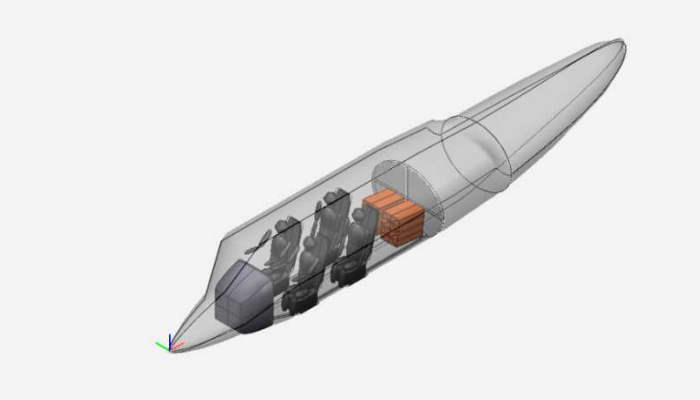

Wing and Lateral Control Surface Design

A NASA LS-0417/13 airfoil is selected because of its superior aerodynamic characteristics (McGhee et al. 1979). From the design wing loading of 20.5 psf, the wing area is:

$$S = W_{TO}/(W/S) = 194\ ft^2 \quad (36)$$

while the wingspan is found from:

$$b = \sqrt{A * S} = 44\ ft \quad (37)$$

The root, tip, and mean aerodynamic chords are found as follows:

$$c_r = 2S/(b * (1 + \lambda_w) \quad (38)$$

$$c_t = \lambda_w * c_r \quad (39)$$

$$\bar{c} = \left(\frac{2}{3}\right) * c_r * \frac{1+\lambda_w+\lambda_w^2}{1+\lambda_w} \quad (40)$$

while the spanwise location of mean aerodynamic chord is given by:

$$\bar{y} = \left(\frac{b}{6}\right) * \frac{1+2\lambda_w}{1+\lambda_w} \quad (41)$$

The wing design parameters are summarized in Table 8.

Table 8. *Wing Design Parameters*

Wing area (S)	194 ft^2
Aspect ratio (A)	10
Wingspan (b)	44 ft
Sweep angle (Λ)	0 deg
Airfoil thickness at the wing centerline $(t/c)_r$	0.14
Airfoil thickness at the wing tip $(t/c)_t$	0.12
Taper ratio (λ)	0.50
Dihedral (Γ)	7 deg
Root chord (c_r)	5.87 ft
Tip chord (c_t)	2.90 ft
Mean aerodynamic chord ($\bar{c}$)	4.57 ft
Spanwise location of mac ($\bar{y}$)	9.75 ft
Wing Aerodynamic Center, (χ_{ac})	1.14 ft
Aileron Chord Ratio (c_a/c)	0.25
Aileron Span Ratio (b_a/b)	0.60

Empennage, Directional and Longitudinal Control Surface Design

The main objective of the horizontal stabilizer is to counter the pitching moments produced by the wing. This must be accomplished, of course, with the smallest possible empennage area. The location of the empennage amounts to estimating the necessary moment arms x_v *and* x_h, as defined in Roskam (Figure 8.1, 1985b). For the proposed aircraft we find:

$$x_v = 13.5\ ft; \qquad x_h = 11.5\ ft \tag{42}$$

Using the tail volume coefficients, we can now calculate the required area for the horizontal and vertical stabilizers.

$$V_h = x_h * (S_h/(S * \bar{c})) \tag{43a}$$

$$V_v = x_v * (S_v/(S * b)) \tag{43b}$$

$$\text{Assuming} \qquad V_h = 0.50 \ and \ V_v = 0.04 \tag{43c}$$

$$\text{we find} S_h = 46.25\ ft^2 \ and \ S_v = 26\ ft^2 \tag{44}$$

The most important design parameters of the empennage are shown in Table 9.

Table 9. *Empennage Design Parameters*

Design Parameters	Horizontal Stabilizer	Vertical Stabilizer
Aspect Ratio	5	1.6
Taper Ratio	0.5	0.4
Wingspan	15.20 ft	6.44 ft
Root Chord	4.05 ft	5.76 ft
Tip Chord	2.02 ft	2.3 ft
Mean Aerodynamic Chord	3.15 ft	4.27 ft
Sweep	10°	15°
Airfoil	NACA 0012	NACA 0012
Dihedral	0°	90°
Incidence	0°	0°

Figure 14. *Isometric View of the Empennage with respect to the Wing*

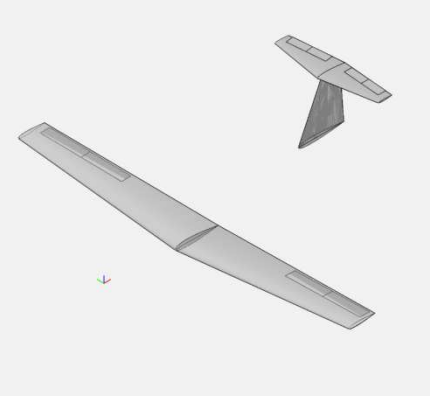

Landing Gear Design & Weight and Balance Analysis

To size the landing gear, the center of gravity must first be determined through a weight and balance analysis. Since the weight of the landing gear itself must be included in the weight and balance analysis, an iteration is required to finalize the size and disposition of the landing gear as well as the center of gravity location of the aircraft.

Weight and Balance Analysis

The initial center of gravity location is determined through a Class-I weight fraction analysis of the major subgroups of the aircraft, using the takeoff weight (Roskam 1985b). Each component weight is expressed as a fraction of the takeoff weight (W_{TO}) or the empty weight (W_E), as shown in Table 10.

Table 10. *Component Weight Fractions for Similar Airplanes and the Proposed Aircraft*

Type	Cessna 210	Beech J-35	Cessna 210 J	Proposed Electric Aircraft
Wing Group /W_{TO}	0.09	0.131	0.099	0.106
Emp. Group /W_{TO}	0.024	0.02	0.025	0.023
Fuselage Group /W_{TO}	0.109	0.069	0.12	0.099
Landing Gear /W_{TO}	0.071	0.071	0.056	0.066
Fixed equip. /W_{TO}	0.199	0.201	0.171	0.190
W_E /W_{TO}	0.094	0.115	0.099	0.103

Using the average weight fractions from Table 10, the Class-I component weights are obtained as shown in the second column of Table 11. The mission weights from weight sizing are included in the third column. The sum of the weights in the first column yields an empty weight of 2342 lbs, which is slightly lower than the value estimated in weight sizing (2535 lbs). The difference is due to round-off errors in the weight fractions used. This difference is redistributed among all the components in proportion to their weights.

Table 11. *Subgroup Component Weight Summary for the Proposed Aircraft*

Component	Class-I Estimation (lbs)	Adjustments	Class-I Weight (lbs)
Wing	425	35	460
Empennage	92	8	99
Fuselage	395	33	428
Landing Gear	263	22	285
Powerplant	758	63	821
Fixed Equip.	409	34	443
Empty Weight	2342	195	2535
Payload			820
Battery Weight			637
Takeoff Weight			3980

The location of the center of gravity for each of the major airplane components is calculated using the geometric definitions in Roskam (Table 10.2, 1985b) (see Table 12).

Table 12. *Center of Gravity Location of Major Aircraft Components*

Component	Length (ft)	cg location w.r.t. component length	cg location w.r.t. component leading edge/nose (ft)	cg location w.r.t. aircraft nose (ft)
Fuselage	29.4	$0.39 * l_f$	11.466	11.466
Wing	4.57	$0.40 * c_w$	1.828	11.758
Vertical Stabilizer	4.27	$0.30 * c_v$	1.281	26.411
Horizontal Stabilizer	2.56	$0.30 * c_h$	0.768	27.608
Empty Weight	29.4	$0.45 * l_f$	13.23	13.23

Landing Gear Design

The maximum static load per strut is calculated from the following equations:

Nose wheel strut: $P_n = W_{TO} * \frac{l_m}{(l_m + l_n)} = 1053\ lbs$ (45)

Main wheel strut: $P_m = W_{TO} * \frac{l_n}{l_m + l_n} * \frac{1}{n_s} = 1465\ lbs$ (46)

where, $l_m = 2.7\ ft\ and\ l_n = 7.5\ ft$

where the geometry for the static load on the tricycle gear is defined in Roskam (Figure 9.2a, 1985b). Here $n_s = 2$, as there are two main gear struts. One nose gear strut is used based on the maximum static load calculation. The gear ratios are determined as follows:

$n_s * \frac{P_m}{W_{TO}} = 0.74,$ Main gear tire: $D_t * b_t = 16.5 * 6\ inches$ (47)

$\frac{P_n}{W_{TO}} = 0.26,$ Nose gear tire: $D_t * b_t = 14 * 5\ inches$ (48)

The general arrangement of the landing gear is determined using two geometric, tip-over criteria:

Longitudinal tip-over criterion

The main landing gear must be behind the aft center of gravity location and the angle between this location and the main landing gear should be 15 degrees as shown in Figure 15.

Figure 15. *Longitudinal Tip-Over Criterion for the Proposed Aircraft*

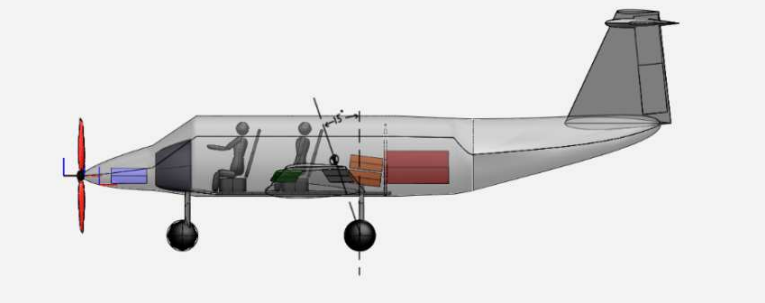

Lateral tip-over criterion

The lateral tip-over criterion (Figure 16) requires that $\psi \leq 55^0$.

Figure 16. *Lateral Tip-Over Criterion (Roskam 1985b)*

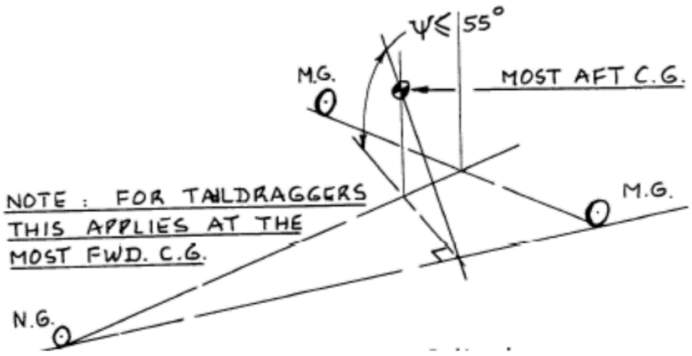

Longitudinal ground clearance criterion

The longitudinal ground clearance criterion requires that the angle defined by the ground contact of the main landing gear and the fuselage tail is greater than the airplane liftoff angle (typically 15^0). As shown in Figure 17, the proposed configuration clearly exceeds this value.

Figure 17. *Longitudinal Ground Clearance Criterion*

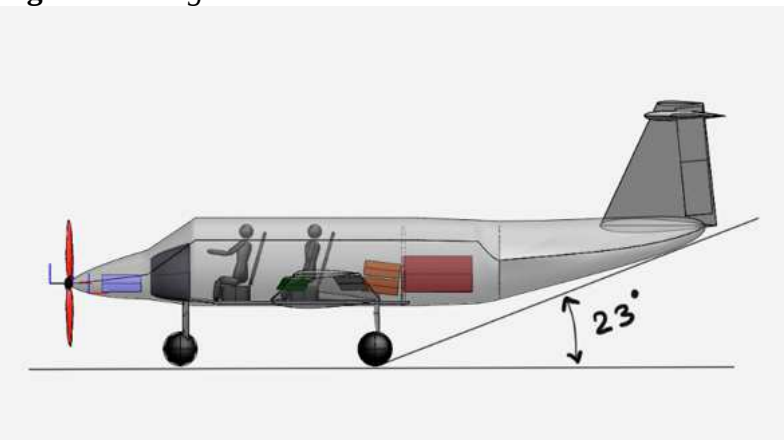

Lateral ground clearance criterion

The lateral ground clearance criterion requires that the angle defined by the ground contact of the main gear and the lowest parts of the wing is at least 5^0 with tires and struts deflated. Figure 18 shows that the proposed configuration exceeds this value.

Figure 18. *Lateral Ground Clearance Criterion*

As mentioned earlier, an iterative process is required to determine the disposition of the landing gear, as we need to estimate first the center of gravity location of the airplane, which must include the weight of the landing gear itself. As a result of this process, the main landing gear was moved 1.5 ft forward to meet the two geometric criteria mentioned above. A CAD model of the proposed aircraft configuration is shown in Figure 19.

Figure 19. *Center of Gravity Excursion Diagram*

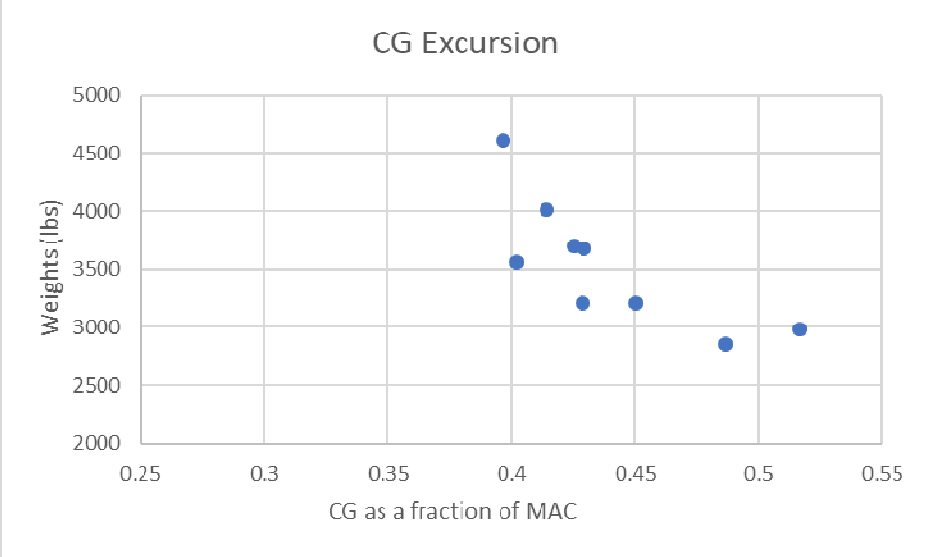

Weight and Balance Analysis

Table 13 shows the component weight breakdown and the center of gravity coordinates of each component, using the final disposition of the landing gear (Roskam 1985c).

Table 13. *Component Weights and Center of Gravity Coordinates*

Airplane Component	**Weight** (lbs)	x (ft)	$W*x$ $(ft*lbs)$	z (ft)	$W*z$ $(ft*lbs)$
Wing	460	11.76	5408.68	5	2300
Empennage	99	27.01	2673.94	16.4	1623.6
Fuselage	428	11.47	4907.45	6.5	2782
Nose landing gear	57	5.88	335.16	1.5	85.5
Main landing gear	228	14.70	3351.60	2.5	570
Powerplant	800	4.41	3528	6	4800
Fixed equipment	443	11.47	5079.44	6.5	2879.5
Empty weight	2535	13.23	33538.05	7.38	18708.3
Front row passengers:	350	10	3500	6.5	2275
Rear row passengers:	350	12	4200	6.5	2275
Luggage	120	15	1800	6	720
Batteries	620	11.758	7289.96	5.2	3224
Takeoff Weight					3872

Center of Gravity Location for Various Loading Scenarios

Table 14 and Figure 20 show respectively the center of gravity locations and excursion diagram for different loading scenarios.

Table 14. *Final Center of Gravity Location for Different Loading Scenarios*

Loading scenarios	**CG locations from nose (ft)**	**Weight(lbs)**
Empty Weight	13.23	2535
Empty Weight + Front Row passengers	12.84	2885
Empty Weight + Rear row passengers	13.08	2885
Empty Weight + Passengers	12.75	3235
Empty weight + Baggage	13.31	2655
Empty Weight + Passengers + Baggage	12.83	3355
Empty Weight + Passengers + Baggage + Batteries	12.65	3872

The center of gravity travel is $0.13\ \bar{c}$, well within the acceptable range for single engine propeller-driven aircraft: $0.06\ \bar{c}\ and\ 0.27\ \bar{c}$ (Roskam 1985b). The

most forward and most aft center of gravity locations are 12.64 ft and 13.31 ft respectively from the fuselage nose. The stability and control analysis carried below may require additional iterations to obtain the final center of gravity location of the airplane.

Figure 20. *Longitudinal Stability χ-Plot*

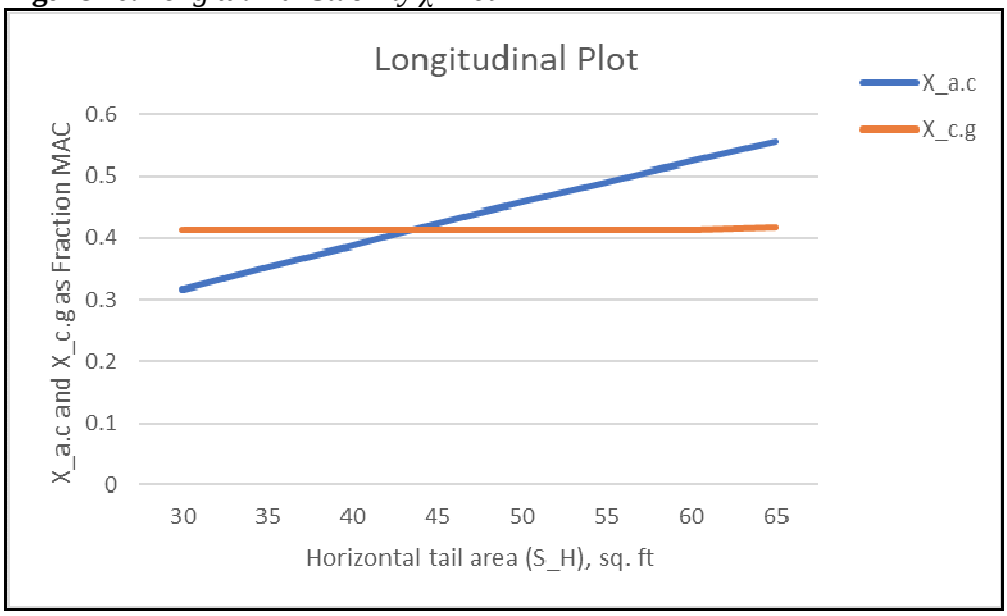

In Figure 20, the horizontal stabilizer area corresponding to the minimum static margin of 5% is 50.50 ft^2, while the horizontal stabilizer area obtained through the tail volume coefficient method was 46.25 ft^2.The difference is within the allowed margins of error for Class-I preliminary design. Hence, the proposed configuration is longitudinally statically stable, and no iteration is required.

Stability and Control Analysis

The static longitudinal and directional stability of the proposed configuration is established through a Class I stability and control analysis. The longitudinal and directional χ-plots will determine any changes needed in the horizontal and vertical tail areas.

Static Longitudinal Stability

The two lines in Figure 20 represent respectively the rates at which the center of gravity and the aerodynamic center move as we change the horizontal tail area. The aft center of gravity location was obtained earlier in the weight and balance analysis. The weight of the empennage is known (100 lbs). The horizontal tail weight is 49.95 lbs for a planform area of 46.25 ft^2. Assuming that the weight of the horizontal stabilizer is independent of surface area, the location of the aerodynamic center is found from equation (49). The longitudinal stability parameters are summarized in Table 15.

$$\bar{X}_{ac_A} = \frac{X_{ac_{wf}} + \left\{C_{L_{\alpha_h}} * \left(1 - \frac{d\varepsilon_h}{d\alpha}\right) * \left(\frac{S_h}{S}\right) * \bar{X}_{ac_h}\right\}}{1 + \frac{C_{L_{\alpha_h}} * \left(1 - \frac{d\varepsilon_h}{d\alpha}\right) * \left(\frac{S_h}{S}\right)}{C_{L_{\alpha_{wf}}}}} \quad (49)$$

Table 15. *Static Longitudinal Stability Parameters*

Parameters	Values
$x_{ac_{wf}}$	0.091
$C_{L_{\alpha_{wf}}}$	0.095 per deg
$C_{L_{\alpha_h}}$	0.069 per deg
$d\varepsilon_h/d\alpha$	0.4
x_{ac_h}	3.61

In Figure 21 the x_{ac} and the x_{cg} are plotted as functions of the horizontal tail area, which varies from 0 to 60 ft^2. The aircraft needs to be inherently stable with a static margin of 5%, hence:

$$\frac{dC_m}{dC_L} = \bar{x}_{cg} - \bar{x}_{ac} = -0.05 \quad (50)$$

Figure 21. *Directional Stability χ-Plot*

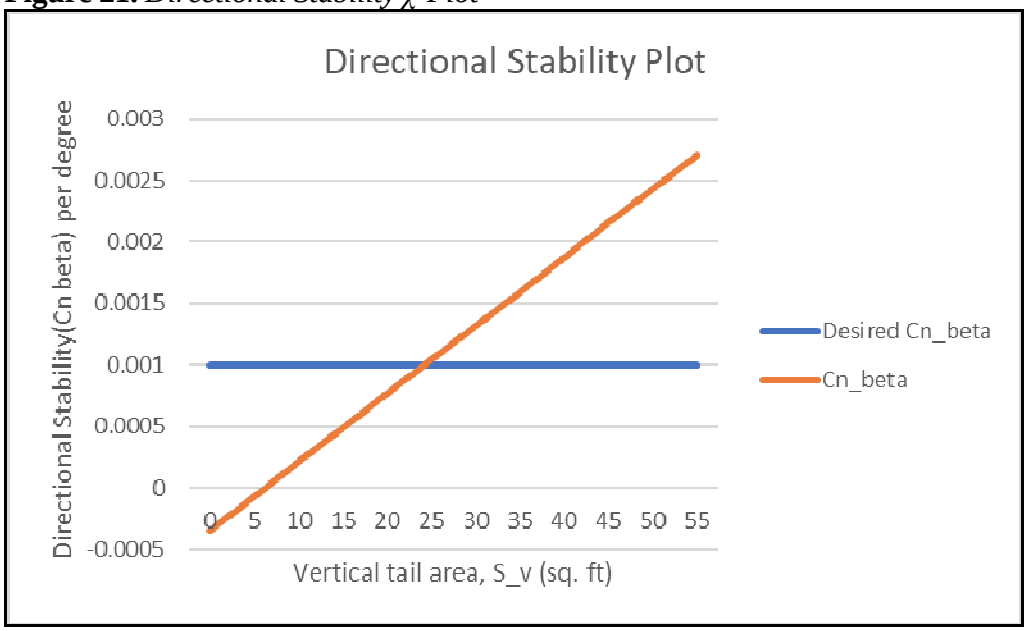

The proposed design is directionally stable with a vertical tail area of 25.2 ft^2 obtained from Figure 21 at C_n = 0.001. The value obtained from the tail volume coefficient method was 26 ft^2. The difference between the two values is 3%, which falls within the acceptable limits of accuracy for a Class I preliminary design.

Directional Stability

The static directional stability is determined using a directional χ-plot with the side slip moment coefficient plotted as a function of vertical tail area. The $C_{n\beta}$ leg of the χ-plot follows from equation (51):

$$C_{n_\beta} = C_{n_{\beta_{wf}}} + C_{L_{\alpha_v}} * \frac{S_v}{S} * \frac{X_v}{b} \quad (51)$$

The wing-fuselage contribution $C_{n_{\beta_{wf}}}$ is calculated from equation (52):

$$C_{n_{\beta_{wf}}} = -K_n * K_{Rl} * S_{fs} * (l_f/Sb) \quad (52)$$

The static directional stability parameters are shown in Table 16.

Table 16. *Static Directional Stability Parameters*

Parameters	Values
$C_{n_{\beta_{wf}}}$	-0.000341 per deg
$C_{L_{\alpha_v}}$	0.035 per deg
K_n	0.0011
K_{Rl}	1.5

The directional χ-plot of the aircraft is shown in Figure 22.

Drag Polars

The drag polars were estimated in the performance sizing. The objective of this section is to recalculate these drag polars using the actual geometric characteristics of the airplane.

Airplane Total Wetted Area

The wetted area for the wing, horizontal and vertical tail can be calculated from:

$$S_{wet_{plf}} = 2 * S_{ex_{plf}} * 1 + \frac{0.25(t/c)_r * 1 + \lambda_l}{1+\lambda} \quad (53)$$

while the wetted area of the fuselage can be calculated from:

$$S_{wetted_{fuse}} = \pi * D_f * l_f * \left(1 - \frac{2}{\lambda_f}\right)^{\frac{2}{3}} * (1 + \frac{1}{\lambda^2_f}) \quad (54)$$

Table 17 shows the wetted areas of the main aircraft components calculated from equations (53) and (54).

Table 17. *Wetted Area of Main Aircraft Components*

Component	**Wetted Area (ft^2)**
Wing (S_{wet_w})	406.18
Vertical stabilizer (S_{wet_v})	53.56
Horizontal stabilizer (S_{wet_h})	96.28
Fuselage (S_{wet_f})	437.93
Total (S_{wet})	963.00

Airplane Zero-Lift Drag

Using the total wetted area from Table 19 in Figure 5.20 of Roskam (1987) the equivalent parasite area of the airplane is:

$$f = 9ft^2 \quad (55)$$

from which we can calculate the zero-lift drag coefficient:

$$C_{D_0} = f/S = 0.046 \quad (56)$$

Low Speed Drag Increments

Using the drag increments due to flaps and the landing gear for the takeoff and landing configurations from Table 5, the revised drag polars for various flight configurations are shown in Table 18 and plotted in Figure 22. Table 19 compares the lift-to-drag ratios assumed in preliminary sizing with those calculated through the actual drag polars of the aircraft. The difference in values is within 5%, hence resizing of the aircraft is not necessary.

Table 18. *Airplane Drag Polars*

Flight Condition	**C_D**
Clean	$0.0460 + 0.0374C_L^2$
Takeoff flaps	$0.0625 + 0.0397C_L^2$
Landing flaps	$0.1075 + 0.0424C_L^2$
Landing gear	$0.1290 + 0.0424C_L^2$

Table 19. *Comparison of the Lift-to-Drag Ratios from Preliminary Sizing (Assumed) and Preliminary Design (Calculated)*

Flight Condition	**L/D (preliminary sizing)**	**L/D (preliminary design)**	**Difference**
Cruise	11.72	11.50	2%
Takeoff	10.0	9.70	3%
Landing	7.50	7.35	2%

Figure 22. *Drag Polars for Cruise, Takeoff and Landing Configurations*

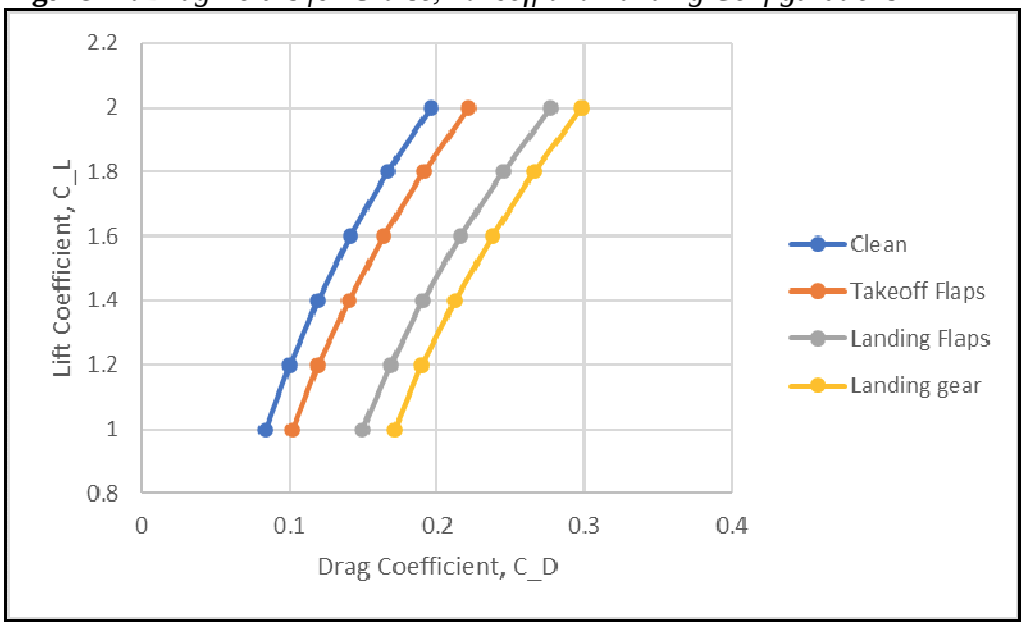

Environmental and Safety Considerations

The environmental issue associated with the proposed design is the use of lithium-O_2 batteries in electric design. Even though the electric aircraft requires no fuel and produces less noise than conventional aircraft, it is clearly not a zero-emission aircraft. The process associated with the production of these batteries emits air pollutants that affect air quality and health. Moreover, the lifetime of these batteries is still short and induces battery waste containing toxic or corrosive materials such as lithium. This hazardous waste could pose additional threats to health and the environment if improperly disposed. Rechargeable batteries will address to a large extent the disposal issue.

Conclusions

The paper demonstrated that a fully electric, four passenger, FAR-23 certifiable, general aviation airplane with a 750 km range is feasible, assuming an energy density of 1500 Wh/kg. Clearly, it will take significant improvements in battery technology to allow for such an aircraft. Nevertheless, as research continues to push the limits of this technology, it is not unlikely to have these batteries available as early as 2025.

References

Abdel-Hafez A (2012) Power generation and distribution system for a more electric aircraft-a review. In R Agarwal (ed.), *Recent Advances in Aircraft Technology*, 289-308. In Tech.

Airbus. Airbus Vahana. Retrieved from: https://www.airbus.com/innovation/zero-emission/urban-air-mobility/vahana.html. [Accessed 1 September 2020]

Alisport Swiss. Silent Electro 2. Retrieved from: http://www.alisport.com/?product=silent-2-electro-2. [Accessed 28 September 2020]

Banke J (2015) *Students electrify NASA with future airplane designs*. National Aeronautics and Space Administration – NASA.

Bye Aerospace. Retrieved from: https://byeaerospace.com. [Accessed 5 October 2020]

Bye Aerospace. eFlyer4. Wikipedia. Retrieved from: https://en.wikipedia.org/wiki/Bye_ Aerospace _eFlyer_4#Specifications_(eFlyer_4). [Accessed 28 September 2020]

Extra EA-300. Wikipedia. Retrieved from: https://en.wikipedia.org/wiki/Extra_EA-300. [Accessed 28 September 2020]

Hepperle M (2012) *Electric flight-potential and limitations*. NATO/OTAN, STO-MP-AVT-209.

Lange Antares. Retrieved from: https://en.wikipedia.org/wiki/Lange_Antares. [Accessed 28 September 2020]

McGhee RJ, Beasley WD, Whitcomb RT (1979) *NASA low and medium speed airfoil development*. NASA TM 78709.

Panthera. Retrieved from: Pipistrel-USA. <https://www.pipistrel-usa.com/panthera/. [Accessed 27 August 2020]

Pipistrel Taurus. Wikipedia. Retrieved from: https://en.wikipedia.org/wiki/Pipistrel _Taurus#Specifications_(Taurus_M). [Accessed 28 September 2020]

Raymer DP (1992) *Aircraft design: a conceptual approach*. Washington, District of Columbia: AIAA Education Series.

Riddell A, Ronson S, Counts G, Spenser K (2004) *Towards sustainable energy: the current fossil fuel problem and the prospects of geothermal and nuclear power*. California, USA: Stanford University.

Roskam J (1985a) *Aircraft design part I: preliminary sizing of airplanes*. Lawrence, Kansas, USA: DARcorporation.

Roskam J (1985b) *Airplane design part II: preliminary configuration design and integration of the propulsion system*. Lawrence, Kansas, USA: DARcorporation.

Roskam J (1985c) *Airplane design, part V: component weight estimation*. Lawrence, Kansas, USA: DARcorporation.

Roskam J (1986) *Airplane design, part III: layout design of cockpit, fuselage, wing and empennage: cutaways and inboard profiles*. Lawrence, Kansas, USA: DARcorporation.

Roskam J (1987) *Airplane design, part VI: preliminary calculation of aerodynamic, thrust and power characteristics.* , Lawrence, Kansas, USA: DARcorporation.

Sigler D (2011) *Going vintage electrically*. Sustainable Skies. Retrieved from: http://sustainableskies.org/going-vintage-electrically/. [Accessed 28 September 2010]

Sun Flyer. Bye Aerospace. Retrieved from: https://byeaerospace.com/sun-flyer/. [Accessed 24 August 2020]

Taurus Electro. Pipistrel-USA. Retrieved from: https://www.pipistrel-aircraft.com/aircraft/electric-flight/taurus-electro/. [Accessed 1 September 2020]

Yuneek E430. Retrieved from: http://commercial.yuneec.com/about-us. [Accessed 5 October 2020]

Yuneek International E430. Wikipedia. Retrieved from: http://commercial.yuneec.com/about-us. [Accessed 5 October 2020]

Athens Journal of Technology and Engineering - Volume 8, Issue 2, June 2021 – Pages 169-180

Numerical Uncertainty in Parallel Processing Using Computational Fluid Dynamics as Example

By Mark Lin[*] & Periklis Papadopoulos[±]

Computational methods such as Computational Fluid Dynamics (CFD) traditionally yield a single output – a single number that is much like the result one would get if one were to perform a theoretical hand calculation. However, this paper will show that computation methods have inherent uncertainty which can also be reported statistically. In numerical computation, because many factors affect the data collected, the data can be quoted in terms of standard deviations (error bars) along with a mean value to make data comparison meaningful. In cases where two data sets are obscured by uncertainty, the two data sets are said to be indistinguishable. A sample CFD problem pertaining to external aerodynamics is copied and ran on 29 identical computers in a university computer lab. The expectation is that all 29 runs should return exactly the same result; unfortunately, in a few cases the result turns out to be different. This is attributed to the parallelization scheme which partitions the mesh to run in parallel on multiple cores of the computer. The distribution of the computational load is hardware-driven depending on the available resource of each computer at the time. Things, such as load-balancing among multiple Central Processing Unit (CPU) cores using Message Passing Interface (MPI) are transparent to the user. Software algorithm such as METIS or JOSTLE is used to automatically divide up the load between different processors. As such, the user has no control over the outcome of the CFD calculation even when the same problem is computed. Because of this, numerical uncertainty arises from parallel (multicore) computing. One way to resolve this issue is to compute problems using a single core, without mesh repartitioning. However, as this paper demonstrates even this is not straight forward.

Keywords: *numerical uncertainty, parallelization, load-balancing, automotive aerodynamics*

Introduction

If you will, imagine punching in 2 plus 2 on a calculator a million times and expect a different answer than 4 each time. Taking it one step further, what if a software program is ran over and over on a computer? Lastly, what if this process is repeated for many days, weeks even? Would one expect a different result? The answer should be no, right? This is important because it describes the basic operation of a numerical solver, for example CFD, to arrive at a single solution (Eça and Hoekstra 2014).

[*]Graduate Student, San Jose State University, USA.
[±]Professor, San Jose State University, USA.

The motivation for this study is that previously, when one computer is not available in the lab (for example, another student is logged on), the author would get on another computer to run his CFD code. Overtime, he has observed that even when the same code is running the result would not replicate sometimes (Beckwith et al. 1993). This troubles him. Before we start let's be mindful that the computers are identical, and likely purchased in a batch order from the same manufacturer Dell.

The Problem

The situation that is being described here is exactly how a CFD code functions. It is a computer program with many lines of code, run over-and-over again, for many days. A CFD code computes the solution to five coupled, partial differential equations (the Navier-Stokes Equations). While solving a partial differential equation on the computer is a complicated task according to Hennig et al. (2015), the exact lines of computer instruction sent to the hardware should be the same even when the physical hardware is different (although with the same specifications).

This paper addresses the result inconsistency across a set of identical computers. The precise problem that is investigated in this paper is to take the same CFD code, copy it onto a bunch of identical computers (Figure 1), run it for exactly the same amount of time (i.e., iterations) and report the finding. If the result turns out to be different, comment on how to proceed in that situation.

Figure 1. *The Group of Computers that are Used in this Study*

One assumption in this study is that because the CFD software is a commercial software (ANSYS Fluent), due to its proprietary nature ANSYS Technical Support cannot comment on the repeatability of the source code. They can only provide consultation and it is up to the authors to research the root cause. Furthermore,

numerical uncertainty as it relates to computation problems encompasses a wide body of research into areas such as mathematical formulation of a physical problem (Cruse and Rizzo 1968), numerical solution methods (Press et al. 2007), and computer programming and processors (Landau et al. 2008). While CFD is used as an example in this study, the problem this paper examines has to do specifically with computer programming and processors.

The case that's to be used to illustrate is a simple fluent simulation from a study presented at the 2nd ATINER Mechanical Engineering Conference (Lin and Papadopoulos 2018). The simulation is a rear wing assembly from a racecar model in angled flow (yaw). An example of the output after four days of computation is shown in Figure 2. The metrics that are used for comparison are the resultant downforce and the resultant drag force from ANSYS's CFD-Post module.

Figure 2. *Sample Output from the CFD Run (7.5° Sideslip Angle, 15000 Iterations)*

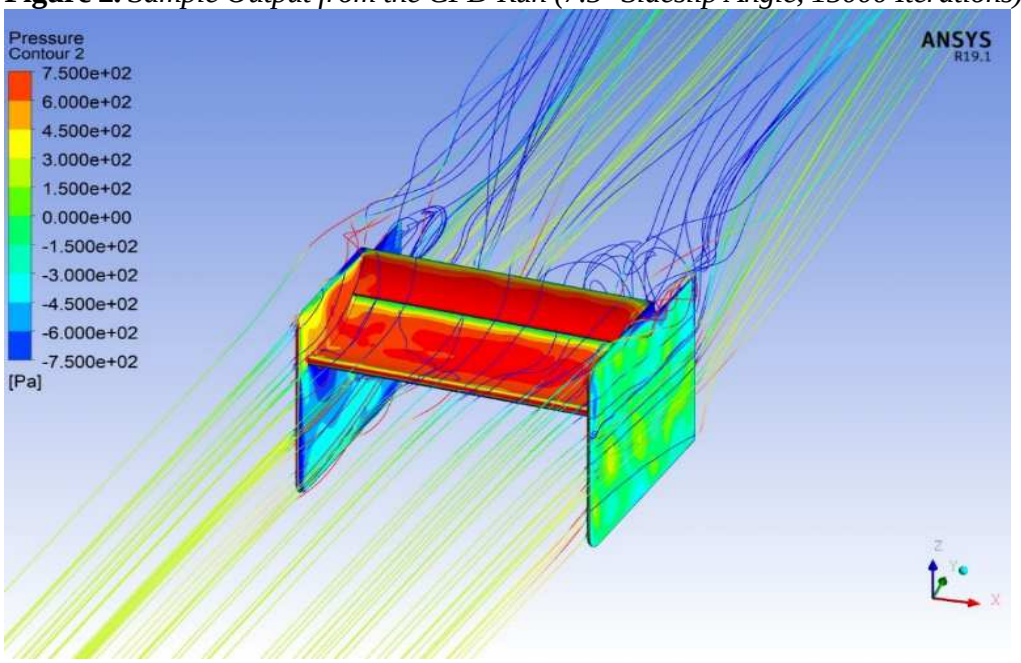

Approach

In this study, 29 computers at San Jose State University's Engineering 164 computer lab (a.k.a. ENG164) are used. Every computer has exactly the same specifications as shown in Figure 3. Each computer has an Intel Core i7 processor with 8 cores (i.e., 4 physical cores and 4 virtual cores) that can be used for parallel computing (López Azaña 2015). The computers also have 16 GB of RAM and 1TB of hard drive. Among the 29 computers, there is one exception: computer no. E164-30. While this computer looks the same as the others, it turns out that it has a different processor: an Intel Core i5 processor with only 4 cores. However, as the result shows it behaves the same as the other 28 computers.

Figure 3. *Specifications of Computers in ENG164 Lab*

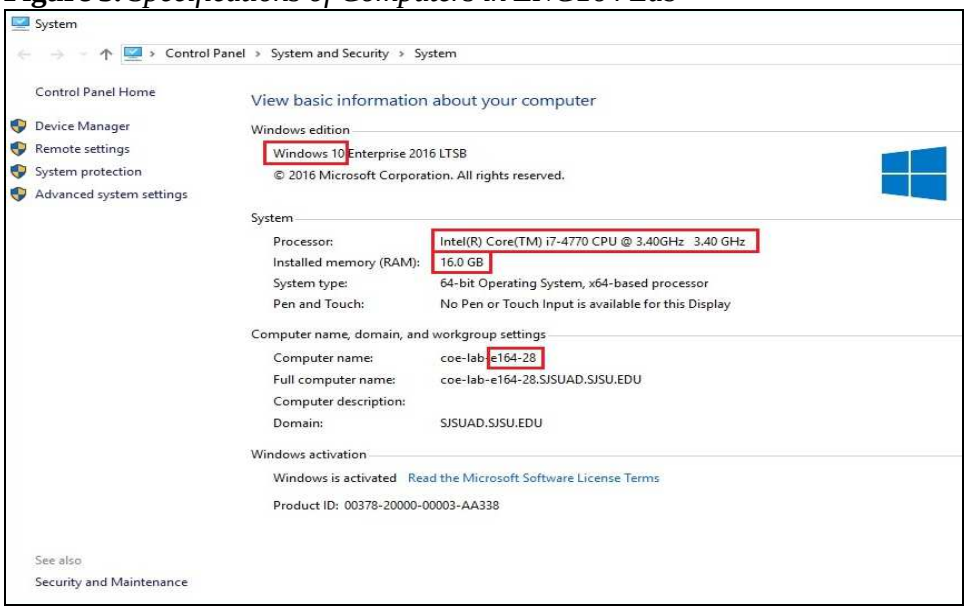

The CFD program in this study is a commercial software ANSYS Fluent (release 19.1 to 2019 R3) that is installed on every computer (ANSYS Manual 2014). Each copy of Fluent solver is ran in double-precision, parallel processing, utilizing 6 out of 8 cores as shown in Figure 4. For the exception case E164-30, only 3 cores were used. From this ANSYS Fluent solver description, it is argued that all software is identical on every computer to calculate the CFD problem. On average, each computer takes about 4 days to finish running 15000 iterations. In Fluent the residual checking option is turned off so that every computer can run to exactly 15000 iterations without terminating even if the convergence criteria is met earlier.

Figure 4. *The Same ANSYS Fluent Solver Setup on Every Computer*

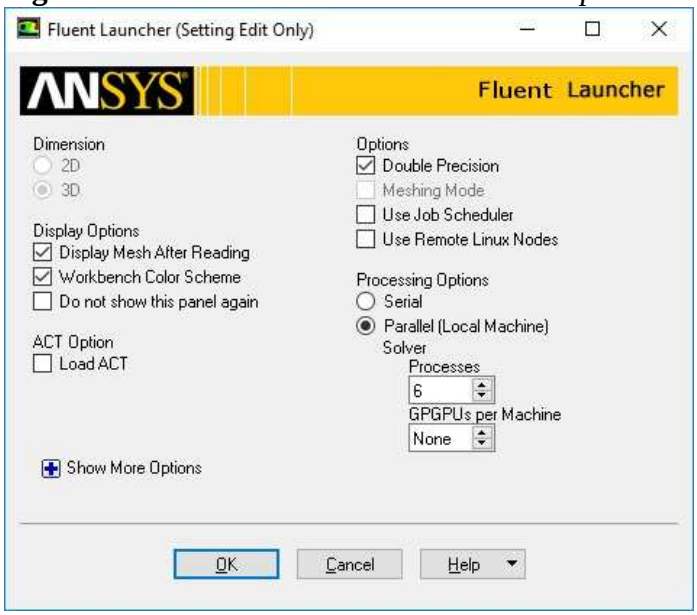

Within ANSYS Fluent, the case that is setup to run is a simple two-airfoil rear wing from a racecar model. The geometry is simple, and it is rotated 7.5° with respect to the enclosure. The freestream is also rotated 7.5° so that it is coming in head-on to the leading edge of the airfoils. The rear wing assembly is placed in the mid-height of the enclosure so there is no ground effect, and the only boundary layer is on the wing itself. This set of boundary conditions is chosen because we want to simulate as many non-symmetric 3D boundary conditions as possible. The solver that is used is the Transition SST turbulence model, with a CFL number of 0.5. This is a convenient simulation to run because it has been performed previously. The same code is simply copied from an external hard drive onto every computer so no further changes to the code are made to run on each computer.

Multicore (Parallel) Computation Results

As shown in Table 1, 25 out of 29 results are identical but 4 of them are different. Initially this result causes much headache. The computers are identical running the same code so there really is no reason for this behavior. While some may argue that the difference is small, less than 1%, but the important question is why are not they exactly the same?

Table 1. *Summary of Multicore Results from 29 Computers in ENG164 Computer Lab*

Computer	Downforce (Fz)	Drag Force (Fy)	Drag Force (Fx)	Combined Drag Force
E164-01	-560.705	198.408	35.0799	201.4853
E164-02	-560.705	198.408	35.0799	201.4853
E164-03	-560.705	198.408	35.0799	201.4853
E164-04	-560.705	198.408	35.0799	201.4853
E164-05	-560.705	198.408	35.0799	201.4853
E164-06	-560.705	198.408	35.0799	201.4853
E164-07	-560.705	198.408	35.0799	201.4853
E164-08	-560.705	198.408	35.0799	201.4853
E164-09	-560.705	198.408	35.0799	201.4853
E164-10	-560.705	198.408	35.0799	201.4853
E164-11	-560.705	198.408	35.0799	201.4853
E164-12	-560.705	198.408	35.0799	201.4853
E164-13	-560.705	198.408	35.0799	201.4853
E164-14	-560.705	198.408	35.0799	201.4853
E164-15	-560.705	198.408	35.0799	201.4853
E164-16	-560.705	198.408	35.0799	201.4853
E164-17	-560.706	198.408	35.0808	201.4855
E164-18	-560.705	198.408	35.0799	201.4853
E164-19	-560.705	198.408	35.0799	201.4853
E164-20	-560.705	198.408	35.0799	201.4853
E164-21	-560.705	198.408	35.0799	201.4853

E164-22	-560.19	198.714	34.9482	201.7638
E164-23	-560.705	198.408	35.0799	201.4853
E164-24	-560.705	198.408	35.0799	201.4853
E164-25	Computer removed from **ENG164**			
E164-26	-560.705	198.408	35.0799	201.4853
E164-27	-560.705	198.408	35.0799	201.4853
E164-28	-560.705	198.408	35.0799	201.4853
E164-29	-560.706	198.409	35.0796	201.4863
E164-30	-560.97	198.941	35.249	202.0396

As it turns out, the use of parallel computing with multiple CPU cores running simultaneously has an effect on the consistency of result. Walshaw and Cross (2007) explained that when in parallel computing the mesh is partitioned into different blocks. Each block is sent to a different core (CPU) and the load between each block is distributed and balanced. The CPU load on each core is distributed differently depending on the available RAM size, the hard drive space, and the other Windows processes that are running. This part of the computing process is done automatically and is entirely transparent to the user so we have no control over how the blocks are divided up. Software algorithm such as JOSTLE or METIS (this is used by ANSYS) is used to perform this task. An illustration of this redistribution process is shown in Figure 5. This parallelization difference is further confirmed by Mishra and Aggarwal in 2011, in their paper "ParTool: A Feedback-Directed Parallelizer", presented at the 9th International Symposium on Advanced Parallel Processing Technologies (Mishra and Aggarwal 2001). This fact has been confirmed by ANSYS Application Support that parallel computing would most likely not lead to the same result (Kishore A, personal communication, July 29, 2019 to May 28, 2020).

Figure 5. *Example Graphs that are Mapped onto Two Different Processor Configurations*

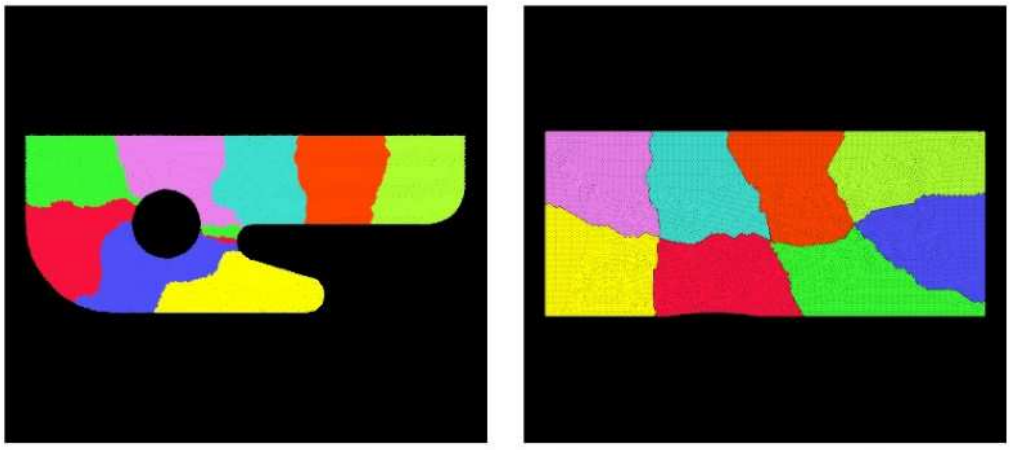

(a) mapping onto a 1D array (b) mapping onto a 2D array

Source: Walshaw and Cross 2007.

Single-Core Computation Results

While ongoing discussion has been focused on parallel computing utilizing the multicores of an Intel Core™ i7-4770 processor, it has been explained to us why when using parallel computing, the result may be different. Next, the study is switched to utilizing single-core processing to make the comparison fair (Maity et al. 2013). This is not an easy decision to make because the code will take longer to run in the single-core mode. The processing time is more than 10 days to complete. In addition, we have to ensure the runs will not be interrupted during the 10-day period, either by students or by Windows update. The single-core results are shown in Table 2.

Table 2. *Summary of Single-Core Results from 29 Computers in ENG164 Computer Lab*

Computer	Downforce (Fz)	Drag Force (Fy)	Drag Force (Fx)	Combined Drag Force
E164-01	-559.807	199.02	44.4015	203.915
E164-02	-559.807	199.02	44.4015	203.915
E164-03	-559.807	199.02	44.4015	203.915
E164-04	-559.807	199.02	44.4015	203.915
E164-05	-559.807	199.02	44.4015	203.915
E164-06	-559.807	199.02	44.4015	203.915
E164-07	-559.807	199.02	44.4015	203.915
E164-08	-559.807	199.02	44.4015	203.915
E164-09	-559.807	199.02	44.4015	203.915
E164-10	-559.807	199.02	44.4015	203.915
E164-11	-559.807	199.02	44.4015	203.915
E164-12	-559.807	199.02	44.4015	203.915
E164-13	-559.807	199.02	44.4015	203.915
E164-14	-559.807	199.02	44.4015	203.915
E164-15	-559.807	199.02	44.4015	203.915
E164-16	-559.807	199.02	44.4015	203.915
E164-17	-559.807	199.02	44.4015	203.915
E164-18	-559.807	199.02	44.4015	203.915
E164-19	-559.807	199.02	44.4015	203.915
E164-20	-559.807	199.02	44.4015	203.915
E164-21	-559.807	199.02	44.4015	203.915
E164-22	-559.807	199.02	44.4015	203.915
E164-23	-559.807	199.02	44.4015	203.915
E164-24	-559.807	199.02	44.4015	203.915
E164-25	Computer removed from **ENG164**			
E164-26	-559.807	199.02	44.4015	203.915
E164-27	-559.807	199.02	44.4015	203.915
E164-28	-559.807	199.02	44.4015	203.915
E164-29	-559.807	199.02	44.4015	203.915
E164-30	-559.807	199.02	44.4015	203.915

A careful note must be said about how this single-core result is achieved: it is through much trial and tribulation. Therefore one should not expect, and normally

would not achieve, consistent result such as this even if one were to run in single-core mode without the care and control that is exercised in this academic study.

From this result there are three important things to note: first is that all the results are identical, which is what we set out to prove. However, in order to get to this stage there are many details unsaid in this statement. After numerous 10-day runs on 29 computers, we have learned that it is important to look at the residuals. If the residuals are not the same at the end of the run (at 15000 iterations), the integral results of downforce and drag force would not be the same. Secondly, if the solving process starts off at a different starting point, meaning with a different set of initial conditions, no matter how close they are to begin with, the result will never be the same no matter how long the case runs (Alayil 2016). A sample of the initial value is shown in Figure 6. This taught us that the current problem is not so much about convergence as it is about number crunching. Once the residual values start to deviate as the iteration progresses, the difference would start to propagate from one residual value to the next. One note about the initialization scheme is that there are two types available in ANSYS: hybrid initialization and standard initialization. For this study hybrid initialization is used. Hybrid initialization requires some guessing on Fluent's part by solving the Euler equation on a coarse mesh and use that as the initial guess, as oppose to standard initialization where the user has to specify all the initial parameters which leads to a longer solve time.

In ANSYS the residual is written as

$$a_p \phi_p = \sum_{nb} a_{nb} \phi_{nb} + b \tag{1}$$

$$R^{\phi} = \| \sum_{nb} a_{nb} \phi_{nb} + b - a_p \phi_p \| \tag{2}$$

a_p is the center coefficient, a_{nb} is the influence coefficient for the neighboring cell, and b is the contribution of the source term. The residual is the higher order Taylor Series terms that are left out when the conservation equation is discretized. This discretization error is tracked iteration-to-iteration, and it's the change in residuals that's plotted. Typically, we want the change in residuals to be smaller than three orders of magnitude from the start. Therefore, to have all 29 computers produce the same result, one needs to first make sure that their residuals are the same. The trick to solve this problem is to check the residuals during the 15000 iterations to see when they start to deviate.

Figure 6. *Sample Initialization and Residuals from Fluent Solver*

```
/***Include Solver Example***/
-Case will be initialized with constant pressure
   iter     scalar-0
   1    1.000000e+00
   2    1.463416e-03
   3    2.631864e-04
   4    8.668557e-05
   5    2.347466e-05
   6    7.955006e-06
   7    2.599028e-06
   8    9.270428e-07
   9    3.401770e-07
   10   1.448375e-07
Hybrid initialization is done.
  iter  continuity     x-velocity     y-velocity     z-velocity     energy         k              omega          intermit
        retheta        cl-1           cd-1           surf-mon-2     surf-mon-1     time/iter
 Reversed flow on 3 faces (2.4% area) of pressure-outlet 6.
    1   1.0000e+00     1.0000e+00     1.0000e+00     1.0000e+00     1.0000e+00     8.0242e-01     4.4196e-01     5.4988e-04
        1.1375e+02     1.2150e+01     1.5784e+00     1.1985e+01     -3.8831e+02    345:48:37      14999
    2   8.3024e-01     8.7096e-01     8.7202e-01     7.4272e-01     8.2991e-01     6.7417e-01     4.1124e-01     3.2043e-03
        9.5692e-01     1.5757e+01     1.2060e+01     1.1981e+01     -3.6751e+02    372:27:01      14998
    .
    .
    .
14999   6.8973e-03     2.9161e-04     2.0077e-03     3.1864e-03     6.8967e-03     6.0816e-04     1.4815e-04     4.5492e-07
        1.5752e-05     3.2611e+02     7.2449e+01     1.4839e+01     1.0764e+02     0:01:05        1
15000   6.8688e-03     2.9147e-04     2.0052e-03     3.1852e-03     6.8681e-03     6.0817e-04     1.5489e-04     4.5793e-07
        1.5808e-05     3.2614e+02     7.2297e+01     1.4839e+01     1.0761e+02     0:00:00        0
   Writing "| gzip -2cf > SolutionMonitor.gz"...
   Writing temporary file C:\\Users\\010815~1\\AppData\\Local\\Temp\\flntgz-152043002 ...
Done.
/****End Solver Example***/
```

The third important thing is that during the solving process, the run cannot be interrupted and restarted, otherwise the residuals would also start to deviate. This is attributed to a coding error in the interrupt/resume routine in Fluent as shown in Figure 7. Note that the last four residual values that are highlighted in yellow: once the program is stopped and restarted again, these four values would flip in order. Prior to realizing this, it has been a common practice for people to pause the solution, examine the result, and restart again. However as we've shown here, doing this would distort the residuals field. Result will never be the same again so all runs have to be completed in one-shot without stopping.

Obeying these do-not-do rules, what works eventually is to initialize the program just once for all 29 computers, run to completion without stopping, examine the last iteration residuals, and plot the integral results for all 29 computers. As previously noted, there are too many details in a commercial CFD program that could cause the results to differ, which has been faithfully demonstrated in this study. As this study shows, the result does not have to be different - one just needs to be extremely careful to eliminate all the possibilities.

Figure 7. *Example of the Solver Process that is Interrupted and then Restarted Again*

```
/***Example of Solver Interruption***/
  iter  continuity   x-velocity   y-velocity   z-velocity   energy       k            omega        intermit
        retheta      cl-1         cd-1         surf-mon-2   surf-mon-1   time/iter
    17  1.2174e-01   2.7499e-02   6.1869e-02   1.0322e-01   1.2131e-01   2.8837e-02   4.9984e-02   4.0734e-03
        1.0671e-02   5.9466e+01   1.0792e+02   1.1864e+01   -3.3634e+02  282:45:05    14983
    18  1.2337e-01   2.6605e-02   5.5318e-02   9.1153e-02   1.2291e-01   2.6485e-02   4.5585e-02   3.9282e-03
        9.5939e-03   6.1226e+01   1.1132e+02   1.1851e+01   -3.3802e+02  280:17:15    14982
 Reversed flow on 1 face (0.5% area) of pressure-outlet 6.
    19  1.2550e-01   2.5063e-02   5.2885e-02   8.7777e-02   1.2505e-01   2.4458e-02   4.1788e-02   3.7698e-03
        8.7626e-03   6.2778e+01   1.1437e+02   1.1837e+01   -3.4098e+02  279:08:44    14981
Writing "| gzip -2cf > FFF-30.1-1.cas.gz"...
Writing temporary file C:\\Users\\010815~1\\AppData\\Local\\Temp\\flntgz-300645 ...
/***Interrupt Solver***/

/***Restart Solver***/
  iter  continuity   x-velocity   y-velocity   z-velocity   energy       k            omega        intermit
        retheta      cl-1         cd-1         surf-mon-2   surf-mon-1   time/iter
    19  1.2550e-01   2.5063e-02   5.2885e-02   8.7777e-02   1.2505e-01   2.4458e-02   4.1788e-02   3.7698e-03
        8.7626e-03   -3.4098e+02  1.1837e+01   1.1437e+02   6.2778e+01   0:00:00      14981
 Reversed flow on 1 face (0.5% area) of pressure-outlet 6.
Writing "| gzip -2cf > status.txt.gz"...
Writing temporary file C:\\Users\\010815~1\\AppData\\Local\\Temp\\flntgz-268602 ...
Done.
    20  1.2639e-01   2.3437e-02   5.0661e-02   8.4820e-02   1.2595e-01   2.2697e-02   3.8489e-02   3.6125e-03
        8.0446e-03   -3.4385e+02  1.1823e+01   1.1711e+02   6.4131e+01   349:32:00    14980
 Reversed flow on 1 face (0.5% area) of pressure-outlet 6.
    21  1.2619e-01   2.1551e-02   4.8649e-02   8.2233e-02   1.2579e-01   2.1150e-02   3.5593e-02   3.4831e-03
        7.4447e-03   -3.4935e+02  1.1809e+01   1.1954e+02   6.5273e+01   345:20:57    14979
/****End Interrupt Example***/
```

Discussion

Now that data has been shown and conclusion drawn that not all CFD runs produce exactly the same result (unless extreme caution is exercised), it is time to offer an alternative way of looking at CFD data, namely to see it as a statistical distribution rather than as a precise number. In statistics, the result is typically quoted as an average with an error bar (Huff 1993). This makes comparison of two distributions possible by saying whether one is better than the other when it's outside of data uncertainty; or conversely, by saying whether two datasets are indistinguishable when the mean value is overlapping within the error bars. In the multicore computation case here, the mean value (μ) from 29 runs is 560.696 N and the standard deviation (σ) is 0.109 N. Hence, if a normal distribution is assumed then the result can be quoted as $\mu \pm 3\sigma$ to encompass 99.7% of the population (Devore 1991). For this dataset (n=29), the downforce would be 560.696 ± 0.327 N and the drag force would be 201.514 ± 0.342 N.

When a computer is utilizing multiple cores, it is performing parallel computing: the program is broken into smaller blocks, sent to different processors, and all are running at the same time. In that case the instructions are not executed sequentially but in parallel, and the intermediate results are passed back-and-forth between the different CPU's. Parallelization uses Message Passing Interface (MPI) to pass information in a distributed memory environment which is the de-facto standard in HPC systems (Fagg et al. 2001). Fluent offers three MPI choices: PCMPI, Microsoft MPI, and Intel MPI which adds another variable to data consistency (Sharcnet 2019). In practical computing, parallel processing utilizing

multiple cores is still the norm and offers significant advantage in shorter solve time (Ali and Khan 2012). Therefore, acknowledging that the result will be different due to these inherent uncertainties, the use of statistical averaging and data distribution is warranted (Oliver et al. 2014).

Conclusions

This study has taken two years to complete because of the long solve time and the availability of 29 identical computers in a university engineering lab setting. The data shows that while most of the time the computational result is exactly the same, but occasionally the result would differ. We are happy to report we can finally achieve the same result on all 29 computers. This time by having access to 29 identical computers in the ENG164 computer lab during COVID-19 lockdown, a definitive view of how computational results could vary has been demonstrated.

It has been shown that the same CFD code, running on identical computers, and using the same solver, while most of the time would yield the same result, but once-in-a-while the result would not repeat. This is the main conclusion from this paper. Since it has been demonstrated that this can happen, the idea of quantifying a statistical error is not unreasonable. It is now possible to calculate an average and a standard deviation for computational results. Therefore, when reporting computational results from a parametric study where a design parameter is varied, in addition to doing a curve fit through the data points one should also show error bars on the data set. This would make comparison of different designs more meaningful and allow real trends to be seen outside of numerical uncertainty.

Acknowledgments

The authors would like to thank Prof. N. Mourtos of San Jose State University for granting access to ENG164 lab that provides the 29 computers that are used in this study. The authors would also like to thank ANSYS Corporation for providing the Fluent license that is used in this research, and the consultation with ANSYS technical support staff.

References

Alayil R (2016) *Why does the CFD Results change with different initialization techniques?* ResearchGate Discussion Board.

Ali J, Khan RZ (2012) Performance analysis of matrix multiplication algorithms using MPI. *International Journal of Computer Science and Information Technologies* 3(1): 3103–3106.

ANSYS Inc. (2014) *Introduction to ANSYS fluent, 15.0 release*. Training Manual, 1st Edition, Inventory #000575.

Beckwith T, Marangoni R, Lienhard J (1993) *Mechanical measurements*. 5th Edition. Reading, Massachusetts: Addison-Wesley Publishing Company.

Cruse TA, Rizzo FJ (1968) A direct formulation and numerical solution of the general transient elastodynamic problem. *Journal of Mathematical Analysis and Applications* 22(1): 244–259.

Devore J (1991) *Probability and statistics for engineering and the sciences*. 8th Edition. Boston, Massachusetts: Brooks/Cole Publishing Company.

Eça L, Hoekstra M (2014) A procedure for the estimation of the numerical uncertainty of cfd calculations based on grid refinement studies. *Journal of Computational Physics* 262C(Apr): 104–130.

Fagg GE, Bukovsky A, Dongarra J (2001) HARNESS and fault tolerant MPI. *Parallel Computing* 27(11): 1479–1495.

Hennig P, Osborne MA, Girolami M (2015) Probabilistic numerics and uncertainty in computations. *Proceedings of the Royal Society A* 471(2179).

Huff D (1993) *How to lie with statistics*. New York: W. W. Norton & Company, Inc.

Landau RH, Paez MJ, Bordeianu CC (2008) *A survey of computational physics. Chapter 14 high-performance and parallel computing hardware, and programming for it*, 352–389. Princeton, New Jersey: Princeton University Press.

Lin M, Papadopoulos P (2018) Application of computer aided design tools in CFD for computational geometry preparation. In *ATINER Conference Paper Proceedings Series* (Athens, Greece, 24–28 July 2018).

López Azaña D (2015) *Differences between physical CPU vs logical CPU vs Core vs Thread vs Socket*. Retrieved from: https://www.daniloaz.com/en/differences-between-physical-cpu-vs-logical-cpu-vs-core-vs-thread-vs-socket/. [Accessed 6 October 2020]

Maity S, Bonthu SR, Sasmal K, Warrior H (2013) Role of parallel computing in numerical weather forecasting models. In *IJCA Special Issue on International Conference on Computing, Communication and Sensor Network* 4(Mar): 22–27.

Mishra V, Aggarwal SK (2011) ParTool: a feedback-directed parallelizer. *Advanced Parallel Processing Technologies* 6965(2011): 157–171.

Oliver TA, Malaya N, Ulerich R, Moser RD (2014) Estimating uncertainties in statistics computed from direct numerical simulation. *Physics of Fluids* 26(3).

Press WH, Teukolsky SA, Vetterling WT, Flannery BP (2007) *Numerical recipes: the art of scientific computing*. 3rd Edition. New York: Cambridge University Press.

Sharcnet (2019) *Starting parallel ANSYS fluent on a windows system using command line options*. Sharcnet.

Walshaw C, Cross M (2007) JOSTLE: parallel multilevel graph-partitioning software - An overview. *Mesh Partitioning Techniques and Domain Decomposition Techniques*, 10.4203/csets.17.2.

Athens Journal of Technology and Engineering - Volume 8, Issue 2, June 2021 – Pages 181-198

The D-Learning Alternative during COVID-19 Crisis: A Preliminary Evaluation based on Kirkpatrick's Model

By Jalal Ismaili[*] & El Houcine Ouazzani Ibrahimi[±]

The COVID-19 pandemic has placed schools around the world under unprecedented challenges where saving students' lives is placed ahead of education as a priority. Within these conditions of distress and uncertainty, education authorities had no choice but to move traditional classes into online ones to ensure the sustainability of studies. The abrupt inevitable decision has been a first for most if not all teachers and students who are invited to cope with a totally new teaching/learning model without necessarily having prior experience in Distance Learning in terms of apparatus or techniques. This study comes as an in-progress appraisal of the D-learning scenarios proposed by Moulay Ismail University (MIU) in Meknes, Morocco, based on a two-level evaluation model (Reaction and Learning) proposed by Daniel Kirkpatrick. It is a real-time evaluation of a learning strategy that has long been considered optional for some students, to become, rather, a plan A constituent for many education departments around the world. The study investigates areas of success and failure from the students' perspective via 4 sub-indicators: accessibility, autonomy, retention and psychological impact. The study concludes that the figures can be more reassuring about the D-learning experience in MIU once issues related to connectivity and communication are redressed.

Keywords: *d-learning, e-learning, pandemic, COVID-19, Kirkpatrick's model, information and communication technology*

Background

Following the Moroccan government's decision of complete lockdown to prevent any uncontrolled spread of COVID-19, the ministry of education took measures to ensure the continuity of studies by, for instance, placing at the disposal of universities access to TV and radio channels to broadcast lectures and courses on multiple topics for different areas of knowledge. By the same token, universities tried to be more autonomous by setting up their own D-learning platforms and social media channels, recording their authentic video podcasts and sharing access to prestigious library databases. As the confinement is going to last longer than expected in many parts of the globe, governments are calling their citizens to cope with the virus and the new mode of living. So far, uncertainty prevails for teachers, students and decision-makers on whether the students will be able to resume their studies at schools as normal as they did before the pandemic.

[*]Assistant Professor, The Higher Institute of Technology, Moulay Ismail University, Morocco.
[±]Professor, Laboratory of Discourse, Creativity, Society and Religions, Faculty of Letters and Humanities Sais, Sidi Mohamed Ben Abdellah University, Morocco.

D-learning will probably continue to serve as a plan B for many schools around the globe, especially those challenged by large size classes where social distancing is highly required. So far, the official bulletins and communications issued by the government (Minister of National Education 2021, MapNews 2021) tend to promote an assuring discourse that has not been empirically verified. Because it is of paramount importance to retrieve feedback from students to evaluate the effectiveness of the experience and pinpoint areas of imperfection that hinder the attainment of optimal results, this study comes to provide a preliminary concise evaluation of the D-learning model adopted by The MIU affiliate Higher Institute of Technology. The school that hosts students from divergent communities and social milieus (urban communities, suburban towns and remote villages …) should serve as a typical case study that fully satisfies the criteria of representation and randomness. The institute takes advantage of the university's digital resources and apparatus whose added value is yet to be proven during these peculiar conditions. The evaluation examines the process's *Accessibility* (students' ability to access the resources placed at their disposal to maintain the continuity of studies), *Autonomy* (the students' ability to process/digest the course material provided by the faculty), *Retention* (the student's ability to provide pertinent feedback and perform well during exams) and *Psychological impact* (the student's ability to cope with the conditions that characterise the D-learning model)

The paper is divided into 6 sections and organised as follows: The first section discusses the significance of Information and Communication Technology (ICT) before the pandemic, followed by a review of ICT programs in Morocco. The related work section is dedicated to the state of the art relative to D-learning before and during the pandemic in Morocco. The practical part starts with a briefing about the methodology, and results. Finally, comes the implications and interpretations section and conclusion.

E-Learning and D-Learning in Morocco: GENIE Programme

The ministry of national education in Morocco celebrates the programme of Generalisation of Information and Communication Technologies in Education (GENIE) as the most elaborate collaborative ICT programme in the country. In order to approximate the global ever-evolving research in Information and Communication Technology for Education (ICTE), the Moroccan ministry of education launched the Generalisation of ICT in Education Programme (GENIE) in 2006 to establish a nationwide strategy that systematises the abrupt occasional initiatives by teachers and voluntary associations whose effectiveness remained, for a while, questionable and more intuitive.

In its initial version, GENIE was granted a period of three years with three principal axes; infrastructure, training and digital resources:

> **Infrastructure**: setting up multimedia environments with internet connection for students in partnership with international hardware and software companies. Each Regional Academy of Education and Training (RAET)

places at the disposal of affiliated teachers 2 multimedia rooms for professional training.

Training: It was based on a waterfall approach. At the central unit in Rabat, a group of "Master Trainers" is selected and trained by experts. These Master Trainers will undertake the mission of coaching 4 regional coaches from each of the 16 RAETs. These 4 coaches would, in return, give training to 2 or 3 school staff who should eventually transfer the training to their co-workers.

Digital resources: also called content development aims at providing digital resources and establishing a national laboratory of digital resources and a national ICTE web portal.

GENIE II (2009-2013) was particularly characterised by the introduction of a fourth axis to be added to infrastructure, training and digital resources; that is of usage development. The new mission sets a number of priority objectives such as the acquisition of digital resources, launching an ICTE web portal, organising sensitisation campaigns and sharing workshops. It also investigates and tracks what the end users do with ICT (Ennda 2010). Although the pace of realisation has tangibly improved, the programme fell short again of achieving 100% of the target goals.

Within the Strategic Vision of Reform 2015/2030 launched by the Supreme Council for Education, Training and Scientific Research (SCETSR), particularly in the sixth lever, the council calls for the equipment of educational institutions with the necessary infrastructure, equipment, didactic material… and digital libraries... It also calls for the equipment of classrooms with audio-visual aids and ICTs. The vision has lifted the ban on GENIE and freed it from any fixed-term plans. Starting from 2016, the programme has for the first time opened up on Open-Source programmes thanks to the National Laboratory of Digital Resources (NLDR) and the Morocco-Korean Centre of ICTE Training (MKCT) by means of several projects.

Programme Evaluation: Donald Kirkpatrick's Four Levels of Evaluation

In 1959, Donald Kirkpatrick proposed 4 basic levels of evaluation published in the Training and Development Journal to make up a reference mark for most, if not all, subsequent models of evaluation (Kirkpatrick 2009).When launched for the first time, it made part of a project on evaluating a supervisory training programme, yet the model's simplicity, effectiveness and comprehensiveness required in any evaluation process makes it a good fit for a wide range of study fields including medicine, higher education, vocational education in enterprises, blended learning, ICT, etc. (Moldovan 2016, Tamkin et al. 2002). Because of the ever-evolving research on evaluation, Kirkpatrick had to consistently adapt or update the levels' guidelines, while the four levels (reaction/learning/ behaviour/ evaluation) remained unchangeable. The levels are also referred to as steps or even taxonomy as each one leads to a more elaborate level that is "more difficult and

time-consuming, but ... also provides more valuable information" (Kirkpatrick and Kirkpatrick 2006).

1. Reaction: Kirkpatrick also calls it a "measure of customer satisfaction" (Kirkpatrick 1996). A customer according to him is anyone who takes part of the training course whether they paid for it or not, whether it was voluntary or forced by an organisation. Although the model was conceived about 60 years ago, Kirkpatrick adopts a bottom-up approach to the evaluation process as he believes that the positive reactions of trainees are important for trainers and for those who make public programs.
2. Learning: This step measures the effectiveness of learning process and the impact it made on the learners at one of these levels: knowledge, skills or attitudes. Certain programs target enhancing one of these competencies such as languages or engineering, while others can incorporate integrative approaches to enhance two or even three such as motivation and communication courses. The evaluator, there- fore, must determine clearly their objectives to remain on a safe side.
3. Behaviour: This step is referred to as transfer of training. It examines whether the training has impacted the learner's behaviour at work or school as intended by the institution after attending a particular training. Kirkpatrick, as stated earlier in this chapter, draws attention to the fact that institutions that carry out evaluation are likely to skip behaviour and results evaluation; nevertheless, some institutes bypass the first two levels to address particularly behaviour evaluation from the very beginning. He disapprovingly does not recommend the procedure and even calls it a "serious mistake" because a programme's failure to deliver at the level of behaviour does not impulsively mean that it failed to deliver at the level of reaction and learning.
4. Results: This step examines the final results and the effects of the training on learners and institution as well. Optimal results should, for instance, reveal an increase of profit, better quality products, better graduation rates, cost reduction, reinforcement of desirable practices and values, lower drop-out rates, etc. "It is important to recognise that results like these are the reason for having some training programmes. Therefore, the final objectives of the training programme need to be stated in these terms" (Kirkpatrick 2009).

Related Work

Academic research on D-learning during the COVID-19 pandemic is still in progress in many parts of the world. It will certainly take time to conduct a thorough appraisal of this unprecedented experience. Meanwhile, a number of research papers have tried to share perspectives from different parts of the world

In a study entitled "Influence of COVID-19 confinement on students' performance in higher education" Gonzalez et al. (2020) analyse the effects of

COVID-19 confinement on the autonomous learning performance of students in higher education at Universidad Autónoma de Madrid (Spain). They compare the differences in assessments before and during the pandemic by dividing students into two groups; a control group from previous years and an experimental group that was interrupted because of the confinement. According to the study, there is a significant positive effect of the COVID-19 confinement on the students' performance.

In a paper entitled "Global impact of COVID-19 on education systems: the emergency remote teaching at Sultan Qaboos University", Osman (2020) highlights the impact of COVID-19 pandemic on the education system in the Sultanate of Oman. The paper provides an analytical description of the Emergency Remote Teaching Plan in higher education and how the experience has changed the teaching and learning landscape.

In a paper entitled "Innovations in teacher education at the time of COVID-19: an Australian perspective" Scull et al. (2020) address the Australian response to the emerging COVID-19 challenges to the education sector and details how the Australian university implemented a number of innovative solutions to move online. The conversion incorporates synchronous and asynchronous learning opportunities. The paper tries to investigate the factors that contributed to fostering high levels of interaction of pre-service teachers, particularly by means of interviews with professors. Scull et al. provide a number of cues and key lessons that "might benefit others looking for ways to provide high-quality teacher education programmes during and after the COVID-19 pandemic."

As for the Moroccan context, Oubibi and Wei (2017) argue that e-learning and Massive Open Online Courses (MOOCs), as popular forms of D-learning, are becoming an option no more; they rather represent an imminent conversion towards the undisputed digitalised future of the university. According to them, universities are facing substantial financial and technical imperatives that make e-learning, via blended learning model and (MOOCs), a tempting solution for the university and for the students in China and Morocco. The study also highlights the disparity of readiness for change between Morocco and China in favour of the latter due to investments in ICT placed at the disposal of Chinese universities, teachers and students. In an effort to contribute to promoting D-Learning in Moroccan universities, Riyami et al. (2016) propose a pedagogical plan using MOOC for teacher training. It is a chart of international MOOCs available for university professors which identifies trainings customised to the beneficiaries' areas of expertise and levels. The study also proposes a management plan to motivate teachers during the training.

Bouziane (2019) conducted an exhaustive synthetic survey of master and doctoral theses in which he investigated success and failure experiences relative to ICT in education in Morocco. The study affirms that online learning, in particular, is not given the attention it is worth by decision makers, which proved to be indeed a strategic pitfall during the Corona pandemic. Bouziane checked the level of Morocco's e-readiness to integrate into the information society based on a Harvard e-readiness assessment framework (Bouziane, 2019). He concluded that, apart from networked economy, the other indicators of network access, networked

society and network policy scored a satisfactory level of preparedness. Whereas indicators and sub-indicators of relevance to the Moroccan university scored lower than average. In another study conducted by Elaasri and Bouziane (2019), they evaluate seven online courses in a digital working space of Hassan II university using Quality Matters rubrics. They concluded that the courses fell short of delivering satisfactory results as far as the quality standards are concerned

The World Economic Forum (2020) showcased the surge of demand for D-learning technologies, particularly online learning platforms after the schools' shutdown marking the largest "online movement" in the history of education. According to the WEF, the challenges of limited staff training, insufficient bandwidth and little preparation may lead to poor user experience that is "unconducive to sustained growth". Yet there is a good chance that a new hybrid model of education will develop with significant benefits (World Economic Forum 2020). The challenges of accessibility to hardware and internet that exist between privileged and underprivileged communities (sometimes within the same nation) are hard to deny or overlook; still, studies have shown that the students' retention capacity jumps higher (25-60%) while taking online courses compared to classroom courses, according to the WEF. The datum might be justified by the fact that D-learning provides larger margins of autonomy and better customised learning pace (Andresen et al. 2002). These pedagogical and economic benefits, according to the WEF, imply that this new education model will be adopted for good and are not temporary.

To sum up, the review of D-learning literature suggests that the 2019 pandemic is but a trigger that released the process of inevitable radical change. It was just a matter of time before we witness a revolutionary change towards a more digitised model of education. Some countries have foreseen the inevitable need to invest in infrastructure, hence they acted and planned on a long run basis; others did not act until change has become urgent and forcible.

Methodology

The appraisal of distant learning in Morocco, at this point, imposed by the COVID-19 pandemic is important but may not yield a comprehensive ultimate verdict about the whole teaching model. The relevance resides in the fact that it pinpoints areas of weakness to rectify and areas of strength to capitalise on. The authors, thus, prefer to restrict the evaluation to Kirkpatrick's (2009) first two levels; reaction and learning. The reaction level takes into account the abundance of sufficient material, adequate learning environment, the students' interaction with peers and instructors and the students' impression about the experience. Positive feedback at this level does not necessarily mean that the learning process has been effective and successful. The next level (learning) gauges the students' performance and intake. The attainment of the objectives set forth by the teacher is detrimental to the potential sustainability of D-learning model post the pandemic.

Population of the Study

The population of the study consists of 136 first-year students from the Higher Institute of Technology. The students, whose majors are Business and Computer Science, descend from different parts of the country and divergent social milieus. They were surveyed by means of Google Forms during the first two weeks of May 2020 (7 weeks post the beginning of school shutdown). The survey observed the requirements of anonymity, randomness, representation and disclosure of the survey purpose. The authors notice that the answers were flowing at a high speed compared to other surveys conducted earlier for other purposes (Ismaili and Ouazzani Ibrahimi 2017). Over 85% of valid responses were generated in less than 4 hours, which may be explained by the students' alertness to updates and possession of gadgets to communicate with their school.

Rubrics of Survey

The survey incorporates 4 rubrics. Accessibility, Autonomy and Psychological impact would answer inquiries related to Kirkpatrick's level of Reaction, while the Retention rubric would provide answers relative to the next level that is Learning. Each rubric incorporates 5 items to answer.

- Accessibility: The rubric surveys the students' possession of ICT devices, access to the university's D-learning platform and frequency of use.
- Autonomy: The rubric surveys the students' ability to sustain self-regulated activities without direct interference from teachers.
- Psychological impact: the rubric examines the acceptance of the D-learning model as a constant component of future syllabi, in addition to its role in relieving levels of stress and tension.
- Retention: The rubric surveys the students' capability to retain information they receive online and their confidence in reproducing the inputs.

Data Analysis

The process of data analysis is based on quantitative and qualitative methodology and is carried out using IBM's Statistical Package for the Social Sciences V21. The analysis investigates areas of correlation between 20 variables; 19 of which are ordinal while 1 is nominal to help better explain the achieved results. Correlation of these variables would eventually lead to building connection(s) between the 4 rubrics of research and understand their mechanisms of interaction. The process will also help draft implications and recommendations for interested stakeholders. The 19 questionnaire items are to be answered on a scale from 1 to 5; 1 stands for highly disagree, while 5 translates into highly agree. The results are considered positive/satisfactory when the scale average is at least 4/5, and it is negative/unsatisfactory when it goes below 2/5. The analysis of each rubric is summed up with an index reference set at 3 based on the Mean. Failure to

achieve that number implies that immediate action by stakeholders is required to mend the gap.

Results

Accessibility

This rubric examines the abundance of the fundamental requirements to make the D-learning possible to take place. The items below (see Figure 1) depict the availability of gadgets, internet, engagement, and easiness of platform use.

Figure 1. *Accessibility*

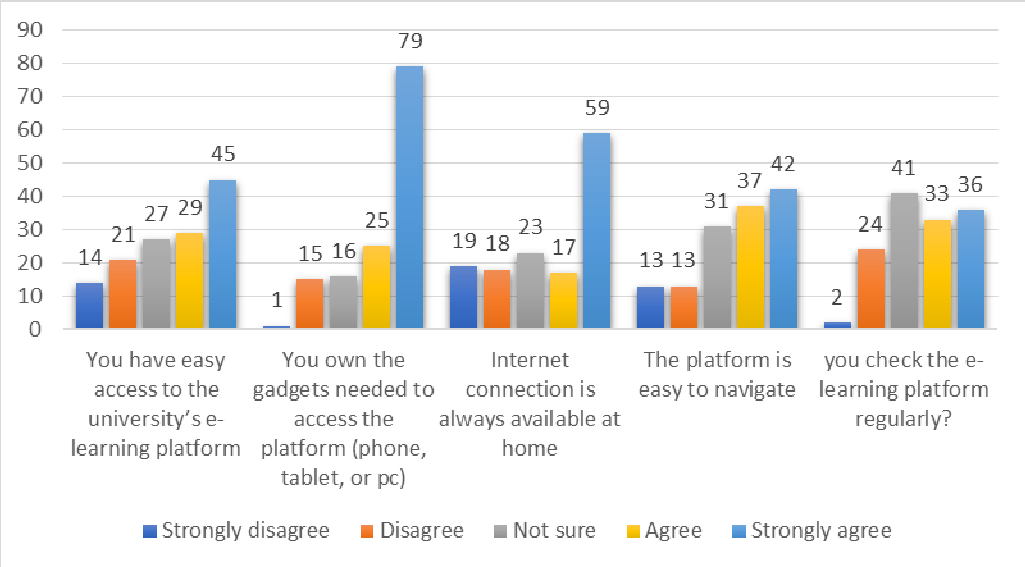

According to the survey (Figure 1), 54.5% of the sample students find accessibility to the university's D-learning platform (FAD) very easy while 25.7% find it a bit challenging. The observed affinity with figures related accessibility to internet access may correlate as 55.9% of students do have access to internet while 27.2% do not. Despite the fact that Moroccan internet operators have engaged in providing free access to the ministry of education's platforms "except YouTube"[1], the procedure remains of limited impact for higher institutes given that a big number of lectures are uploaded in video format on YouTube. By the same token, 51% of students may be described as regular visitors to the platform, 30% frequent visitors, while 19% are irregular users. The most satisfying results in this rubric are those related to ownership of smart gadgets given that 76.5% of students constantly possess a laptop, a smartphone or a tablet, while only 11.7% do not. The 11.8% who answered "not sure" may have to use a shared device at home.

[1]https://www.moroccoworldnews.com/2020/03/297143/moroccos-telecommunication-operators-offer-free-internet-access-to-education-websites/.

Table 1. *Accessibility Index Reference based on Mean*

	Easy access to the platform	Ownership of gadgets	Internet availability	Easy to navigate platform	Regularity of visits
Mean	3.5147	4.2206	3.5809	3.6029	3.5662
N	136	136	136	136	136
Std. Deviation	1.36075	1.07972	1.49347	1.27819	1.10690

As the five items have scored higher than the index reference 3, and given that the average mean is 3.69, it is concluded that the accessibility results are satisfactory and indicate the abundance of decent conditions for D-learning to operate (Table 1).

Autonomy

Autonomy rubric examines the participants' ability to sustain self-regulated activities, and how well they can do relying on their prerequisite skills and competencies. In the absence of peers and teachers "physically" around, it is important to know how the students handle learning challenges of obscurity, lack of understanding and lagging behind their peers.

Figure 2. *Autonomy*

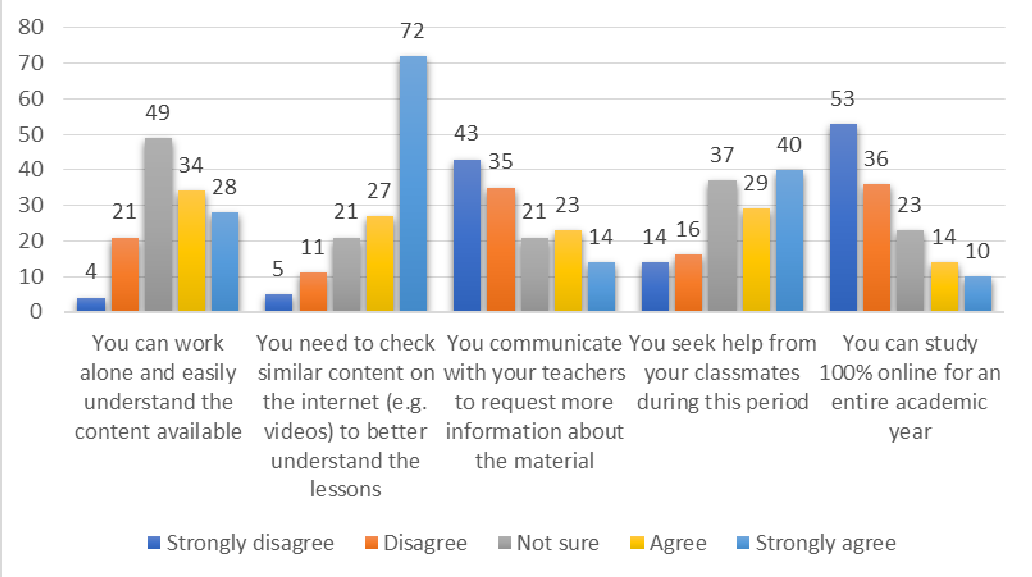

Figure 2 indicates that 45.6% of students can deal with the resources available online in full autonomy, while 18.3% encounter some challenges. 36.1% say they are not sure, and it is completely understandable since average students in the classroom need a bit of help before they can grasp the lessons and digest the difficulties. The study finds that the students deploy their intuitive autolearning mechanisms as 72.8% diversify their resources by consulting similar content on

the internet. Networking with peers is another mechanism used as 50.7% of students feel the need to stay connected with their classmates to seek help, coordinate and share material. 22.1%, however, do not feel like they need to. One striking finding about autonomy rubric is the modest level of direct communication with professors. It is true that the university, mainly the faculty, invested a huge effort setting up a D-learning strategy and compiling material in a short time[2], yet direct communication between students and teachers would result in a more significant outcome. The last question examines the participants' readiness to go 100% online for the upcoming year, and the idea is not welcomed by 65.5% of participants. The reactions suggest that the participants are not ready to trade the traditional classroom for a virtual one, at least for the time being. Only 17.7% do not mind the transition.

Table 2. *Autonomy Index Reference based on Mean*

	Full autonomy	**Checking other sources**	**Communicating with professors**	**Communicating with classmates**	**Going 100% online next year**
Mean	3.4485	4.1029	2.4853	3.4779	2.2059
N	136	136	136	136	136
Std. Deviation	1.07373	1.15649	1.36075	1.30507	1.26560

The index reference has been attained in 3 items and has not in 2 others (Table 2). Still, the average mean of the 5 variables is 3.13, which is satisfactory. The available content as well as the deployment of their autolearning strategies have scored satisfactory results, while direct communication with faculty is yet to be addressed by the university. Communication does not only help in the process of learning, but it is also a source of moral reassurance for students. Certainly, shifting to 100% online courses is an ominous proposition the authors do not endorse as it suggests the confinement will stay for a long time. Thus, the low mean recorded is not considered as negative or fit to be regarded as an index reference.

Psychological Impact

The psychological impact examines the students' emotional reaction to this experience in addition to identifying the affective filter if there is any. It also verifies whether any prior exposure to D-learning before the pandemic has made the full online transfer any easier.

[2]http://www.mapexpress.ma/actualite/societe-et-regions/covid-19-cinq-questions-au-president-luniversite-moulay-ismail-meknes/

Figure 3. *Psychological Impact*

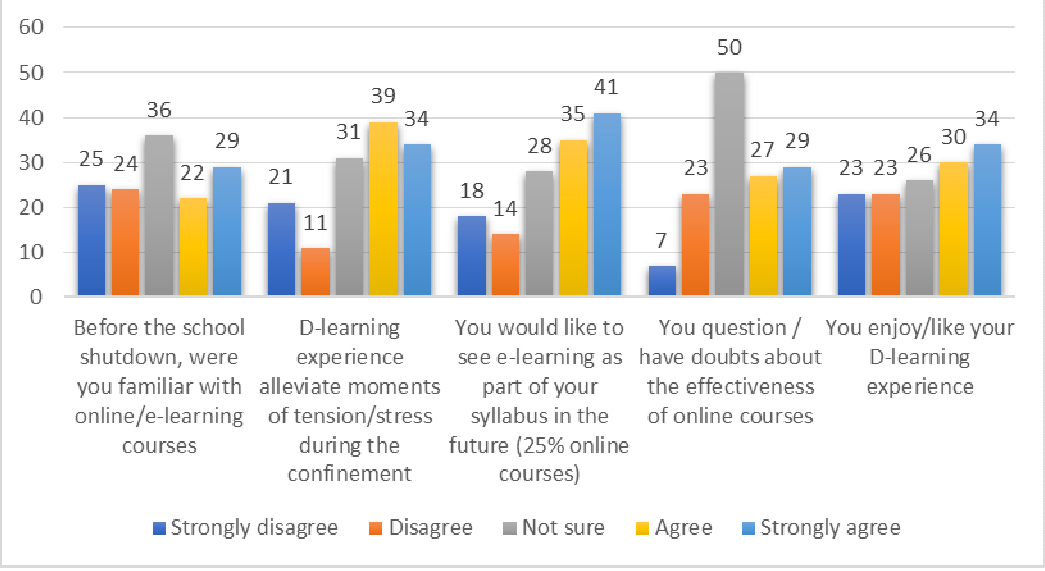

As Figure 3 illustrates, the first question of this rubric tries to detect whether students have been prepared to work online before the lockdown. Any preceding initiation would alleviate feelings of floundering and getting lost for novice students with nil D-learning experience. 37.5% of participants acknowledge having a previous e-learning experience, while 36% stated that they do not. The 20.5% left of the sample (undecided) suggests that some students have doubts about their technology skills and are not confident to call themselves experienced D-learners. 41.2% of surveyed students doubt the equivalence of D-learning to actual classroom learning, while 22% have high confidence in technology effectiveness. The good news for D-learning advocates is finding that it helps alleviate feelings of stress and tension during the confinement for 53.7% of surveyed students. 23.5% say it does not because they have accessibility issues on the first place, especially with internet as they explain. In addition, 47.1% think the D-learning experience is enjoyable at the personal level, opposite to 33.8% who do not. When asked if they want D-learning to be partially incorporated (25%) in next year's syllabus, almost 56% welcomed the idea. Only 23.5% categorically rejected the proposition as they will have to deal with the current challenges again; mainly those mentioned in the accessibility rubric.

Table 3. *Psychological Impact Index Reference based on Mean*

	Familiarity with D-learning	**D-learning alleviates Stress**	**Incorporating 25% D-learning Permanently**	**Enjoyment of the experience**
Mean	3.0441	3.3971	3.4926	3.2132
N	136	136	136	136
Std. Deviation	1.39240	1.35690	1.36624	1.42677

Since the item relative to doubts about D-learning is not applicable to index referencing and may not serve as an objective to target, it was omitted from Table 3. The four other items scored satisfactory results ranging between 3.04 and 3.49. The average mean of psychological impact (3.28) is likely to improve once the issues stated above are redressed.

Retention

In this rubric we study the effectiveness and return on investment of the D-learning model. The D-learning experience may be considered a success only when the students manage to acquire or at least internalise knowledge and skills they at home.

Figure 4. *Retention*

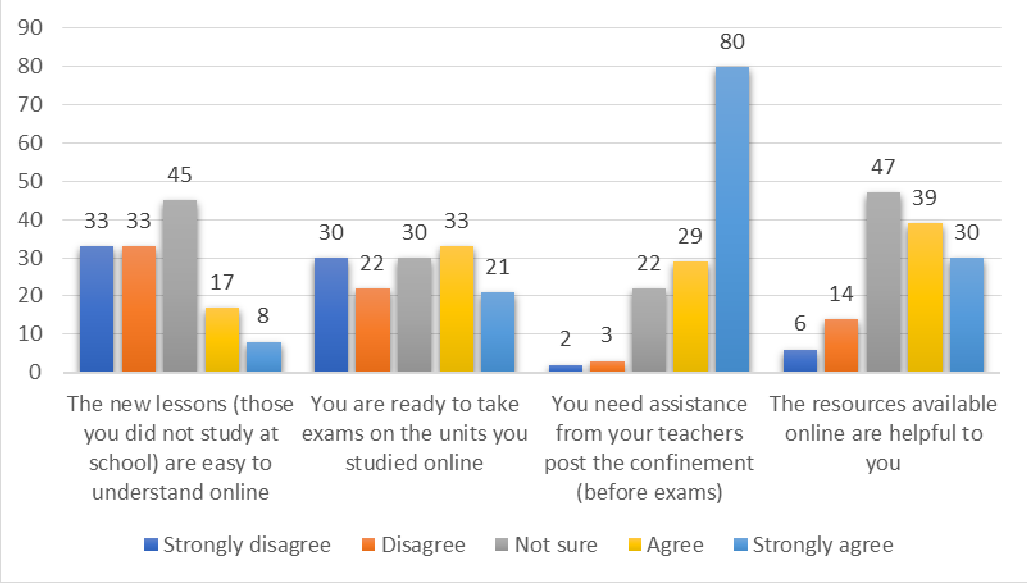

Figure 4 shows that the students encounter challenges with new lessons they are introduced to for the first time that only 18.4% find them within everyone's reach; 48.6% think they are hard to understand. It is worth mentioning that the students were only two or three weeks away from the end of modules and the remaining lessons make up only a small fraction of the syllabus. These results are consistent with those recorded by the ENSAM (see the related work section). When asked about the helpfulness of content available online, 85.3% left finds it either relatively or completely helpful, whereas only 14.7% think it is not. As for their readiness to take an exam without any review or make-up classes, around 40% said they are ready and 38.3% are not, while 34.6% remained undecided. Nonetheless, the vast majority do not mind the initiative of make-up classes and review before the exams with over 80%. A tiny proportion of 3.7% think they do not need it.

Table 4. *Retention Index Reference based on Mean*

	Content is easy	**Ready for exam**	**Assistance before exam is needed**	**Resources are helpful**
Mean	2.5147	2.9485	4.3382	3.5368
N	136	136	136	136
Std. Deviation	1.16100	1.38414	.92872	1.08121

Table 4 above shows that the index reference of success has been achieved in two rubrics. The average mean for the retention rubric is 3.32, which is satisfactory. Students, accordingly, demonstrate their appreciation of the human factor as indispensable to any successful D-learning scenario. The resources placed at the disposal of students by their professors are doubtlessly valued. On the other hand, the weak direct communication with professors apparently affects the students' retention capabilities and confidence in their competencies. Internalising the learners' newly acquired knowledge and skills, praising hard work and correcting mistakes reinforce the process of learning and self-efficacy.

Interpretations

Many of the above findings lead us to inspect the potential correlations between variables and subsequently rubrics. Understanding the relations between variables can help interested bodies to find adequate solutions that can elevate the index references. There is still room for the university to adapt and polish the D-learning strategy, but some solutions must be taken at a national level as they involve other parties. It is observed, for instance, that students who do not enjoy the D-learning experience are those who struggle with gadget and internet issues (see Table 5). So, if the ministry in collaboration with other ministries, donors, partners and stakeholders can fix this issue, many other issues would, hopefully, get fixed. Following are observed correlations with the authors' interpretation and personal recommendations

Table 5. *Positive Correlations*

Correlations

		Enjoyment of the experience	Full autonomy	Content is easy	Ownership of gadgets	Ready for exam
Enjoyment of the experience	Pearson Correlation	1	.406**	.497**	.325**	.358**
	Sig. (2-tailed)		.000	.000	.000	.000
	N	136	136	136	136	136
Full autonomy	Pearson Correlation	.406**	1	.384**	.291**	.255**
	Sig. (2-tailed)	.000		.000	.001	.003
	N	136	136	136	136	136
Content is easy	Pearson Correlation	.497**	.384**	1	.316**	.399**
	Sig. (2-tailed)	.000	.000		.000	.000
	N	136	136	136	136	136
Ownership of gadgets	Pearson Correlation	.325**	.291**	.316**	1	.112
	Sig. (2-tailed)	.000	.001	.000		.195
	N	136	136	136	136	136
Ready for exam	Pearson Correlation	.358**	.255**	.399**	.112	1
	Sig. (2-tailed)	.000	.003	.000	.195	
	N	136	136	136	136	136

**. Correlation is significant at the 0.01 level (2-tailed).

Table 6. *Negative Correlations*

Correlations

		Communicating with professors	D-learning alleviates Stress
unicating with sors	Pearson Correlation	1	-.209*
	Sig. (2-tailed)		.014
	N	136	136
ning alleviates	Pearson Correlation	-.209*	1
	Sig. (2-tailed)	.014	
	N	136	136

*correlation is significant at the 0.05 level (2-tailed).

1. There is a significant positive correlation between ownership of gadgets and enjoyment of the D-learning experience, $r(134)=0.32$, $p=0.000$.
2. There is a significant positive correlation between easiness of the content and enjoyment of the experience, $r(134)=0.49$, $p=0.000$.
3. There is a significant positive correlation between ownership of gadgets and easiness of the content, $r(134)=0.31$, $p=0.000$.
4. There is a significant positive correlation between the student's feeling of autonomy and enjoyment of the experience, $r(134)=0.40$, $p=0.000$.
5. There is a significant positive correlation between easiness of content and readiness to take exams, $r(134)=0.39$, $p=0.000$.
6. There is a significant negative correlation between communication with professors and levels of stress for D-learners, $r(134)=-0.20$, $p=0.014$.

Discussion

The study of D-learning experience in MIU concludes that 14 out of 19 surveyed items have scored satisfactory results (based on index reference) while 5 require redressing by the university and the ministry. The average mean for the 4 rubrics (accessibility, autonomy, retention and psychological impact) has scored 3.35, which is generally reassuring and subject to positive change post the confinement.

At the level of reaction, the surveyed items may have scored satisfactory levels, yet there is a lot to be done to improve the D-learning experience for students. Because the students did not benefit from any initiative that promotes accessibility to internet and laptop such as Nafida (launched in 2008), they were left to their own financial capacity to provide one. For many years, Nafida provided access to internet and multimedia resources for public schools and subsidised the purchase of laptops and internet connection for students and teachers. This initiative would have made a lot of difference had it been relaunched during the pandemic. The ministry claims that a newly signed agreement with three Moroccan phone and data operators should allow free access to the platforms created by schools and universities, still access to video content (uploaded on YouTube) is restricted and not covered by the pact.

The missing direct communication with some professors has contributed to magnifying the learning challenges for some students (see Table 6). Accessibility to apparatus and internet does not seem to be sufficient for the learning process to be effective. The D-learning model is a new for many professors and most of the students, so when challenges surface the blame is often put on the process as whole that is, then, seen not effective. Exploiting every communication medium, by both parties, helps to draw a much clearer idea about the ends that should be met. The challenges that go mishandled will eventually lead to losing confidence in the utility of D-learning and even in the students' self-efficacy.

As the study reveals a sense of fear by students, or at least aversion, of prolonging studies remotely, there is a good reason to believe that networking with professors and students would lead to maintaining social ties that alleviate tension. Once online communication with professors and peers is established, approaching learning difficulties would be more positive. The only rubric that did not attain index reference 4, or above, is that of psychological impact. It is perfectly logical to assert that the mounting learning difficulties prevent the enjoyment of D-learning experience. The widely recognised motivation that accompanies the use of ICT for learning (Ismaili 2020) is spoiled by the challenges that accumulate.

Finally, it is repeatedly reported in the survey that the students' household conditions do not help in the process of D-learning. Although the feedback of the sample population does not elaborate on the nature of nuisance they feel, the study recommends adopting a blended/hybrid scenario that reduces the time of physical interaction at school, yet it maintains a minimum of social ties that are essential for the students' psychological health.

Study Limitations

Although the study adopts a mixed method approach, the qualitative dimension remains limited. Direct interviews with the students at the time of lockdown when the disturbances (cognitive and emotional) were reaching their topmost could have drawn a much clearer and real-time image about the students' reactions. Despite the fact that the teachers' perspective is not focal in this study, it is of paramount importance for future related studies to investigate this axis in order to connect the dots and devise effective D-learning solutions.

Conclusions

This study comes to investigate areas of success and failure for the D-learning scenario proposed under the compelling conditions of COVID-19 lockdown. It is a real-time evaluation of a learning strategy that has long been considered complementary and optional for students whose particular professional or personal conditions do not allow attending in-person classes. Probably the lockdown will not last forever, but the D-learning model is being, certainly, reconsidered as a Plan A constituent by many governments and education departments around the

world that are now compulsorily invited to examine their ICT assets. Although Kirkpatrick (2009) asserts that the four levels of evaluation (reaction, learning, behaviour, results) may not necessarily be conducted consecutively, doing so is primordial to shaping a better understanding of a programme's effectiveness. The success or failure to deliver is conditioned by the abundance of investment in the infrastructure and learning environment. This study has examined interrelated and interdependent variables of the D-learning experience in MIU at the level of reaction and learning and concluded that:

- The MIU students' satisfaction with the D-learning experience is conditioned by their ownership of decent quality gadgets and internet connection. Failure to help underprivileged students in this regard would leave them lagging behind their peers. When technology is available, it contributes to making the best of one's autolearning skills (Voogt and Pelgrum 2005).
- Whenever the university's platform content is easily understood, by means of virtual chatrooms for instance, it is noted that the students' motivation to engage in the D-learning experience jumps higher.
- The student's enjoyment of the D-learning experience relies heavily on the student's feeling of autonomy and ability to solve problems on their own.
- The students can get their confidence back only when they have a good command of the syllabus and are permanently guided. Again, stronger and direct contact with teachers can help in the process.
- The more communication with professors, which is below satisfactory in our case, increases, the lower levels of anxiety and stress can get. Communication at this point is not only a scholarly catalyst but also a psychostimulant agent.

References

Andresen BB, Van den Brink K, Abbott C (2002*) Multimedia in education. Specialised training course*. IITE MOSCOW: UNESCO Publications.

Bouziane A (2019) ELT issues in Morocco: a research-based perspective. In *MATE ELT Series: Book 4*, 137–149. Moroccan Association of Teachers of English (MATE).

Elaasri, R., & Bouziane, A. (2019). Applying the Quality Matters (QM)™ Rubric to Analyze the Quality of ENT Platform Courses. *European Journal of Open Education and E-Learning Studies*, *4*(2), 12-22.

Ennda F (2010) *Programme GENIE premier bilan de la stratégie 2009-2013* (GENIE program first assessment of the 2009-2013 strategy). Retrieved from: https://www.maghress.com/fr/lesoir/10161. [Accessed 14 February 2021]

Gonzalez T, de la Rubia MA, Hincz KP, Comas-Lopez M, Subirats L, Fort S, et al. (2020) Influence of COVID-19 confinement on students' performance in higher education. *PLoS ONE* 15(10): e0239490.

Ismaili J (2020) Evaluation of information and communication technology in education programs for middle and high schools: GENIE program as a case study. *Education and Information Technologies* 25(2): 5067–5086.

Ismaili J, Ouazzani Ibrahimi E (2017) Mobile learning as alternative to assistive technology devices for special needs students. *Education and Information Technologies* 22(3): 883–899.

Kirkpatrick D (1996) Great ideas revisited. *Training & Development* 50(1): 54–60.

Kirkpatrick DL (2009) *Implementing the four levels: a practical guide for effective evaluation of training programs: easyread super large 24pt edition*. ReadHowYouWant.Com.

Kirkpatrick DL, Kirkpatrick J (2006) *Evaluating training programs: the four levels*. Williston: Berrett-Koehler.

MapNews (2021) *Distance learning has contributed to improvement of school and teacher image* (Minister). Retrieved from: https://www.mapnews.ma/en/actualites/social/distance-learning-has-contributed-improvement-school-and-teacher-image-minister. [Accessed 14 February 2021]

Minister of National Education (2021) *Morocco reacted 'very early' to COVID-19 pandemic*. Retrieved from: https://www.maroc.ma/en/news/morocco-reacted-very-early-covid-19-pandemic-minister-national-education. [Accessed 12 February 2021]

Moldovan L (2016) Training outcome evaluation model. *Procedia Technology* 22(Dec): 1184–1190.

Osman ME (2020) Global impact of COVID-19 on education systems: the emergency remote teaching at Sultan Qaboos University. *Journal of Education for Teaching* 46(4): 463–471.

Oubibi M, Wei PZ (2017) Chinese and Moroccan higher education MOOCs: rationale, implementation and challenges. *The International Journal of E-Learning and Educational Technologies in the Digital Media* 3(1): 31–34.

Riyami B, Mansouri K, Poirier F (2016) Towards integrating MOOC in the Moroccan higher educational system: economic pedagogical model based on ICT for on-going education and teacher motivation. In *ICERI 2016*, 6867–6873. November 2016, Seville, Spain.

Scull J, Phillips M, Sharma U, Garnier K (2020) Innovations in teacher education at the time of COVID-19: an Australian perspective. *Journal of Education for Teaching* 46(4): 497–506.

Tamkin P, Yarnall J, Kerrin M (2002) *Kirkpatrick and beyond: a review of models of training evaluation*. Brighton, England: Institute for Employment Studies.

Voogt J, Pelgrum H (2005) ICT and curriculum change. *Human Technology: An Interdisciplinary Journal on Humans in ICT Environments* 1(2): 157–175.

World Economic Forum (2020) *The COVID-19 pandemic has changed education forever. This is how*. Retrieved from: https://www.weforum.org/agenda/2020/04/coronavirus-education-global-covid19-online-digital-learning/. [Accessed 8 May 2020]